Università degli Studi di Milano-Bicocca

CONSULTAZIONE TESI DI DOTTORATO DI RICERCA

La sottoscritta ***TROMBIN FEDERICA*** n° matricola 033075
Nata a MONZA (MI) il 25.10.1981
Autrice della tesi di DOTTORATO dal titolo:

Mechanisms of ictogenesis in an experimental model of temporal lobe seizures

AUTORIZZA

la consultazione della tesi stessa, fatto divieto di riprodurre, in tutto o in parte, quanto in essa contenuto.

Data: 25 marzo 2010 Firma

Table of contents

Abstract

Epilepsy is not a single disorder, but presents with a surrounding of symptoms that are not always of immediate identification and classification. About 50 million people worldwide have epilepsy. Seizures are more likely to occur in young children, or people over the age of 65 years.

The mainstay of treatment of epilepsy is preventive anticonvulsant medication with anti epileptic drugs (AED). Despite the proven efficacy of most of these drugs, it is estimated that over 30% of people with epilepsy do not reach complete seizure control, and this category of patients is eligible for surgical therapy. Among them, people suffering from focal seizure and in particular temporal lobe epilepsy are candidates for surgery. In recent years, surgical ablation of the epileptogenic focus has been rewarded as the best way to cure seizures in patients with intractable focal epilepsy.

Diagnostic scalp and intracranial stereo-EEG recordings can provide direct information from the epileptogenic focus and surrounding areas in order to circumscribe the zone to be surgically removed. Data obtained from the analysis of the patients' EEG brought to the identification of specific ictal patterns which in turn helped to better classify the already clinically defined seizure types. These patterns can be reproduced in animal models of epilepsy and/or seizures.

Focal seizures in the temporal lobe of the isolated in vitro guinea pig brain can be induced by perfusion of proconvulsant drugs. The electrophysiological recordings from the limbic structures of this animal model inform about the mechanisms leading to seizure onset (ictogenesis) and their progression. These phenomena are being studied both from a neuro-physiological and functional point of view;

also histology and other anatomo-functional techniques give us a global idea of the activities occurring in different brain compartments during seizure-like events.
The ultimate goal of this research will be to further clarify the causes for which a focal seizure is generated and the regulatory mechanisms that govern the different patterns similar to those identified in humans.

Intracellular recordings from principal neurons in the superficial and deep layers of the entorhinal cortex showed a different involvement of these two regions in seizure initiation and development. We demonstrate that at seizure onset there is a strong activation of GABAergic interneuron (Gnatkovsky et al., 2008). This finding points to a primary role of GABAergic inhibition in seizure generation.
We further showed that slow potentials recorded during the first steps of ictal activity are a typical sign of modifications of ionic composition of the extracellular medium and describe very well the shape of low voltage shifts with fast activity (Trombin et al., in preparation).
Spikes shape identified by intracellular recordings during seizures was also analyzed to evaluate the epileptogenic network. The correlation of AP changes during seizures with the field potential and the increase in extracellular [K] clearly indicates both neuronal and non-neuronal processes, take place during the initiation and the termination of a seizure (Trombin et al, in preparation).

Taken together all these data point out a multi-factorial scenario in which inhibitory networks play a crucial role in seizure generation, in association with changes in glial function and extracellular homeostasis. The impairment of one of these elements can be a

triggering event in the development of seizures (ictogenesis), and can start in turn a cascade of permanent modifications that maintain an hyper-excitability condition, leading to epileptogenesis. The precise knowledge of each passage needed to transform a normal tissue into an epileptogenic one is a fundamental achievement in order to recognize and classify the different syndromic manifestations of epilepsy. Further, the possibility to interfere with one of the above mentioned processes is of evident relevance for the modulation of seizure beginning and establishment.

Chapter 1

1. Introduction

1a. General characteristics of epilepsy.

Epilepsy is one of the most common neurological disorders (Fig. 1) that has been considered in the past a sort of “sacred disease” because epileptic people were thought have religious experience if not demonic possession during seizures. The word epilepsy is derived from the Ancient Greek verb ἐπιλαμβάνειν [epilambánein] "to take hold of". In most cultures and societies, persons with epilepsy have been stigmatized: in ancient Rome, epilepsy was known as the *morbus comitialis* and was seen as a curse from the gods. It was not so uncommon, even in the last century, to find in hospitals people with epilepsy side-by-side with the mentally retarded, people with chronic syphilis, and the criminally insane.

In younger patients it is mostly associated with genetic, congenital, and developmental conditions; in people over the age of 40 there is a more likely association with brain lesions, such as tumours. Head trauma and central nervous system infections factor may be associated with any age.

Epilepsy's approximate annual incidence rate is 40–70 per 100,000 people in industrialized countries, with a rate decrease in children, and 100–190 per 100.000 in developing countries.

The prevalence of epilepsy is roughly in the range 5–10 per 1000 people. It is estimated that up to 5% of people experience a seizure at some point in life; epilepsy's lifetime prevalence is relatively high because most patients either have isolated seizures or (less commonly)

die of it. Not all epilepsy syndromes are life-long, some forms are confined to particular stages of childhood, for example in Childhood Absence Epilepsy (CAE) in the majority of case the seizures cease spontaneously during maturation.

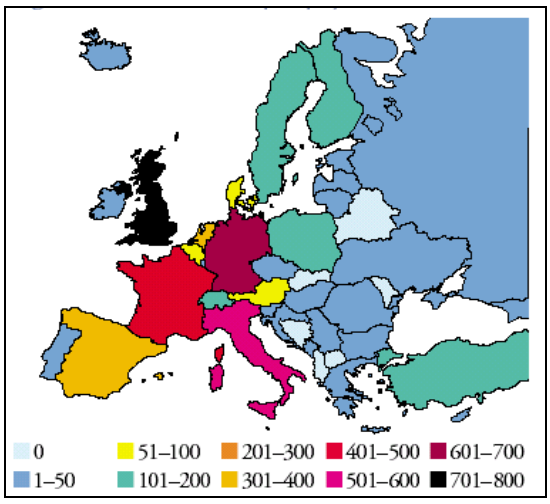

Fig. 1 Prevalence of epilepsy in Europe.

The overall prognosis for full seizure control is very good, with more than 70% of patients achieving long-term remission under pharmacological treatment, the majority within 5 years of diagnosis. (Sander JW, 2003)

People with epilepsy are at risk for death from four main problems: status epilepticus (most often associated with anticonvulsant noncompliance), suicide associated with depression, trauma from seizures, and sudden unexpected death in epilepsy (SUDEP). Those at highest risk for epilepsy-related deaths usually have underlying neurological impairment or poorly controlled seizures; those with more benign epilepsy syndromes have little risk for epilepsy-related death.

The International League Against Epilepsy (ILAE) in 1981 proposed a scheme to group and widely define the numerous types of epileptic seizures.

Partial or Focal onset
A. *Local:*
1. Neocortical
a. Without local spread 1) Focal clonic seizures
2) Focal myoclonic seizures
3) Inhibitory motor seizures
4) Focal sensory seizures with elementary symptoms
5) Aphasic seizures
b. With local spread
1) Jacksonian march seizures
2) Focal sensory seizures with experiential symptoms
2. Hippocampal and parahippocampal
B. *With ipsilateral propagation to:*
1. Neocortical areas (includes hemicortical seizures)
2. Limbic areas (includes gelastic seizures)
C. *With contralateral propagation to:*
1. Neocortical areas (hyperkinetic seizures)
2. Limbic areas (dyscognitive seizures with or without automatisms
D. *Secondarily Generalized:*
1. Tonic-clonic seizures
2. ? Absence
3. ? Epileptic spasms
Generalized Onset
A. Seizures with tonic and/or clonic manifestations
1. Tonic-clonic
2. Clonic
3. Tonic
B. Absence
1. Typical
2. Atypical absence
3. Myoclonic absence
C. 1. Myoclonic seizures
2. Myoclonic astatic seizures
3. Eyelid myoclonia
D. Epileptic spasms
E. Atonic seizures
Unclassified Epileptic seizures
Neonatal seizures

Table 1: 2006 updated seizure classification points out the differences between focal and generalized events. From *www.ilae-epilepsy.org*

This classification accounts for the different typologies of epilepsy on the basis of their causes. In 2006 the Classification Task Force of ILAE provided a much more detailed list of seizure types (see Table 1) than had been previously considered in common, daily use. The "common" list presented in the 1981 is still largely valid, though the new list of the 2006 report provides more details in some areas, particularly for the focal seizures.

For a long time the terms "focal" and "generalized" have been used to express a dichotomous classification to describe the site of seizure onset. In referring to the site of seizure onset, **focal** indicates that seizures originate primarily within a region of one cerebral hemisphere with propagation patterns which may involve the contralateral hemisphere. In some cases there can be more than one epileptogenic focus that involves distinct networks. Each focus has its characteristic seizure type and there can be different patterns originating from different foci.

Generalized epileptic seizures involve bilaterally distributed networks, can be asymmetric but do not necessarily include the entire cortex. Although individual seizure onset can apparently have a localized origin, the site of onset and lateralization are not consistent from one seizure to another.

Since there is not a unique cause that leads to seizure generation in a patient, it has been useful to describe epilepsy as a syndromic disease. According to the ILAE definition an epileptic syndrome is *an epileptic disorder characterized by a cluster of signs & symptoms customarily occurring together* (www.ilae-epilepsy.org). Given the variety of factors found to be implicated in the origin of the disease

Electro-clinical syndromes arranged by age at onset
Neonatal period Benign familial neonatal seizures (BFNS) Early myoclonic encephalopathy (EME) Ohtahara syndrome
Infancy Migrating partial seizures of infancy West syndrome Myoclonic epilepsy in infancy (MEI) Benign infantile seizures Benign familial infantile seizures Dravet syndrome Myoclonic encephalopathy in nonprogressive disorders
Childhood Febrile seizures plus (FS+) (can start in infancy) Early onset benign childhood occipital epilepsy (Panayiotopoulos type) Epilepsy with myoclonic atonic (previously astatic) seizures Benign epilepsy with centrotemporal spikes (BECTS) Autosomal-dominant nocturnal frontal lobe epilepsy (ADNFLE) Late onset childhood occipital epilepsy (Gastaut type) Epilepsy with myoclonic absences Lennox-Gastaut syndrome Epileptic encephalopathy with continuous spike-and-wave during sleep (CSWS) Childhood absence epilepsy (CAE)
Adolescence – Adult Juvenile absence epilepsy (JAE) Juvenile myoclonic epilepsy (JME) Epilepsy with generalized tonic-clonic seizures alone Progressive myoclonus epilepsies (PME) Autosomal dominant partial epilepsy with auditory features (ADPEAF) Other familial temporal lobe epilepsies
Less Specific Age Relationship Familial focal epilepsy with variable foci (childhood to adult) Reflex epilepsies
Distinctive Constellations Mesial temporal lobe epilepsy with hippocampal sclerosis (MTLE with HS) Rasmussen syndrome Gelastic seizures with hypothalamic hamartoma
Epilepsies attributed to and organized by structural-metabolic causes
Malformations of Cortical development (hemimeganencephaly, hetertopias etc) Neurocutaneous syndromes (Tuberous sclerosis complex, Sturge-Weber, etc)
Tumor
Infection
Trauma
Angioma
Peri-natal insults
Stroke, etc.
Epilepsies of unknown cause
Benign neonatal seizures (BNS) and Febrile seizures (FS)

Table 2. Classification of epileptic syndromes on the basis of EEG features and etiology.

From *www.ilae-epilepsy.org*

and the heterogeneity of clinical manifestations, a "syndromic" approach to the study of epileptogenesis has helped in recognizing different mechanisms that are involved in this process. An electroclinical syndrome is a complex of clinical features, signs and symptoms that together define a distinctive, recognizable clinical disorder.

Epilepsies that do not fit into any of these diagnostic categories can be distinguished on the basis of a known structural or metabolic alteration (presumed cause) and then on the basis of the primary mode of seizure onset (generalized versus focal).

On the basis of this definition epileptic syndromes have been sub-classified into categories depending on the localization of seizure onset (localized or generalized) and on their cause, when known (idiopathic or symptomatic or presumed symptomatic, previously called "cryptogenic"; Beghi E, 2009).

In idiopathic epilepsies, genetic factors, for example channelopathies, are presumed to have a major causative role in the development of seizures. Shorovon (2009) classified the epilepsies of unknown origin as follows: autoimmune and inflammatory disorders (Hashimoto disease or Rasmussen encephalitis), mitochondrial disease (MELAS - mitochondrial encephalopathy with lactic acidosis and stroke-like episodes, MERRF – Myoclonus epilepsy with ragged red fibers, NARP - neuropathy, ataxia, retinitis pigmentosa), infections (Herpes simplex virus infection is the most common or Creutzfeldt-Jakob disease). Chromosomal disorders, such as ring 20 (a chromosome 20 malformation that produce prolonged nonconvulsive SE associated with long runs of EEG theta activity) and several genetic causes and inborn errors are frequent in many epileptic syndromes.

There are some examples of syndromes characterized by specific seizures patterns. Benign partial epilepsy with centrotemporal spikes (BECTS) is the most common childhood idiopathic partial epilepsy and is often associated with a continuous spike–wave syndrome reinforced by sleep. Juvenile myoclonic epilepsy (JME) is a common epilepsy syndrome characterized by onset in the early teenage years with a strong genetic component. Mesial temporal lobe epilepsy (MTLE) is a syndrome characterized by mesial temporal sclerosis of the hippocampus and the parahippocampal region, it is a surgically remediable epilepsy syndrome.

In symptomatic epilepsies there is an identifiable lesion in the brain that triggers seizures. The lesion can be, for example, a genetically programmed cellular alteration, like cortical dyslamination, or an acquired lesion, like TBI. Symptomatic epilepsies typically develop in three phases: a brain-damaging insult (e.g., TBI, ischemia, cortical malformation, etc.) then a latency period during which there are no seizures, but starts the process of epileptogenesis and last the appearance of recurrent seizures or epilepsy. (Pitkanen A, 2006) The process is best understood in animal models, where all the passages from one stage to the next are controlled and several parameters can be evaluated, even with invasive techniques that cannot be easily feasible on humans.

The remaining part of seizure manifestations are still unexplained and is said to be idiopathic or criptogenic. It is evident that a more detailed knowledge about the steps that lead from an initial event to seizures and epilepsy will have a clear impact in improving therapies that can be used in different epilepsy forms.

1b. Focal epilepsy and epileptogenesis

The progression of events that lead to the generation of spontaneous and recurrent seizures in a brain area is defined as the process of epileptogenesis. The acquisition of epileptogenic properties by a normal brain area takes time to develop and can follow different paths. It is necessary an initial insult that is likely to be the cause of the first seizure attack. After that there can be a variable period of latency (*latency period)* during which pathogenic changes occur and give rise to a condition that promotes spontaneous seizures generation (Fig. 2).

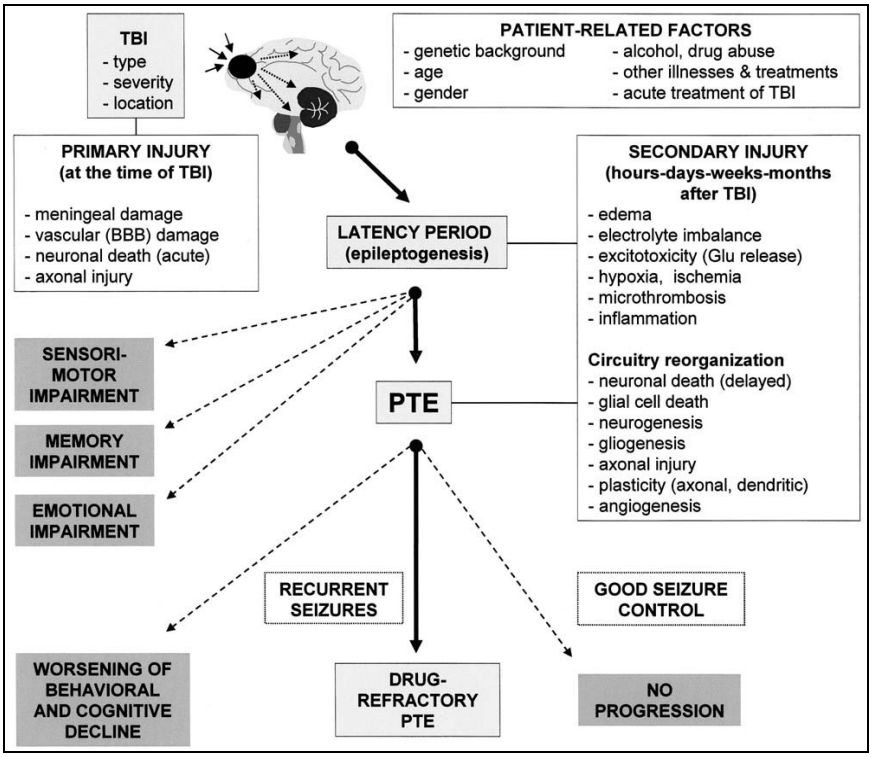

Figure 2. Summary of the factors contributing to the course of epileptic process leading to post-traumatic epilepsy (PTE) after traumatic brain injury (TBI). (from Pitkanen A, 2006)

The study of epileptogenesis in human relied on the help coming from epidemiological surveys, clinical reports and statistical analysis of

population studies. Modern techniques like stereo-EEG, advanced imaging as fMRI or genotypization of familial forms of epilepsy, gave a new deeper insight into the origin of the disorder. The most common causes from which epilepsy can originate are brain injury, both mechanical or ischemic (e.g. stroke), CNS infections, brain malformation, as focal cortical dysplasia (FCD) or genetic defects for example in channelopathies.

In mesial temporal lobe epilepsy (MTLE) a generating insult can be hippocampal sclerosis (HS). Whether this is congenital or secondary to perinatal sufferance and/or prolonged febrile seizures is still a matter of discussion. It is a characteristic lesion involving the regions of CA3 and CA1 and presents with neuronal loss and gliosis of the affected areas. In specimens collected from operated MTLE patients the hippocampal tissue presented with aberrant neuronal network and uncommon connections (Gabriel S., 2004). Metabolic dysfunction and ion homeostasis dysregulation in the hippocampus of both rat models and of human TLE patients have been demonstrated to play a role in the induction and maintenance of seizures. (Kann O., 2005)

Mechanical causes such as head trauma can be another example of an epileptogenic lesion. In the animal model of traumatic brain injury (TBI) immediate and early seizures can develop after the lesion have been induced. (Pitkanen A 2006) Two potential "prime movers" have been identified: disinhibition of cortical circuitry and development of new functional excitatory connectivity, which occur in a number of animal models and some forms of epilepsy in humans. There are several important unknowns between the latent period from injury to onset of epilepsy. In humans the latent period may be as long as years (Prince DA, 2009).

CNS infections represent a high risk for the development of epilepsy. Although the risk for epilepsy after CNS infections is high, the fairly low population incidence of these infections makes them secondary players in the mechanisms of epilpetogenesis.

Post-stroke seizures account for 11% of all epilepsy. The risk for late seizures and epilepsy evolution is correlated with the volume of tissue affected and stroke severity. Patients with large (total MCA or ICA) infarcts have a consistent substantial risk of developing seizures (at least 15% at 5 years).

Epilepsy resulting as a consequence of focal cortical dysplasia (FCD) and related malformations of cortical development (MCDs) represent an increasingly recognized cause of medically intractable epilepsy. These patients are optimal candidates for surgery.

Lastly, the genetic background is a weighty player in the development of epilepsy. According to the *two hits hypotheses* a genetic mutation in one gene involved in neuronal development, or in membrane polarization is a strong predisposing factor that can become explicit after a second hit has disclosed its pathogenicity. It is demonstrated that seizures can induce the expression of many genes. (Pernot, 2010)

There are many evidences both from clinical studies on patients and from data obtained in animal models of focal epilepsy that progressive rearrangements in the injured area take place during the process of seizure development. The process of neuronal loss following one of the possible types of insults described above give rise to a series of repairing mechanisms that withdraw from the physiologic status and in the end flow into a pathological condition such as epilepsy.

In many animal models of chronic epilepsy it is observed a massive neuronal loss after the induction of status epilepticus. Kindling is a heavy inducer of neurogenesis (from 75 to 140% of neuronal growth)

and involves bilaterally the granular layers of the hippocampi. (Scott BW, 1998) Axonal sprouting is a secondary phenomenon related to neuronal growth: mossy fiber sprouting can be induced by recurrent seizures in animal models. The functional outcome of axonal reorganization is a restoration of synaptic connections, but it implies an augmentation in neuronal excitability so a increased risk to develop seizures.

Glial proliferation is another hallmark of tissue damage and is prominent in the sclerotic hippocampus. Even though glia do not have a direct role in promoting hyper-excitability, it is fundamental in the maintenance of ionic homeostasis, in the buffering of potassium and pH regulation. All these aspects concur to the dysregulation of extracellular composition and in turn can increase the predisposition of neurons to pathological synchronization.

From the examination of epileptic tissue collected from patients it is clear that all the aspects listed above are present. Histological observation of brain tissue resection from intractable epilepsy showed an important neuronal loss in particular in hippocampal district but also in the para-hippocampal region. The damage requires time to become evident (even years) both in terms of neuronal loss and neuronal replacement following a massive neurogenesis, rearrangement of axonal fibers (mossy fiber sprouting also seen in animal models). All these data point out a series of changes that are undoubtedly progressive and cumulative.

1c. Defining pharmacoresistant forms of epilepsy

It is of recent publication the list of consensus definition for refractory epilepsy, that comprise all that forms that do not respond to the usual pharmacological treatments. The continuous development of new

AEDs is widening more and more the therapeutic opportunities for a patient, and that this is a bit complicating the evaluation of intractable epilepsy.

It is estimated that 30% of patients with epilepsy are refractory to medical therapy and should be considered for surgical treatment. The progress of the disease in response to treatment does not enable the clinicians to reliably predict the outcome towards any form of pharmacoresistance in individual persons. Patients should be considered for surgery after failure of at least two appropriate AEDs (Kwan & Brodie, 2010; Kwan & Sperling 2009).

Of all the patient suggested for surgery, the majority are for seizures arising in the antero-medial temporal lobe, a minor part about 30–40% comprise a heterogeneous group of patients with extra-temporal lobe (or neocortical) epilepsy. (Williamson et al., 1993)

1d. Preoperative preparation of the patient

The first goal of preoperative work-up is to determine where is precisely located the epileptogenic region in a patient with focal epilepsy. History, semeiology, EEG and imaging studies can be very helpful in differentiating different forms of "lobe" epilepsy.

Once clinical features of seizures are established, next step is to discriminate the region of abnormal physiology from the areas of normal function. Different techniques can be set to localize the epileptogenic zone in temporal lobe, but no single method is completely sensitive or specific. Interictal and ictal scalp EEG is critical in localizing the site of seizure onset. Magnetoencephalography can also be used for the identification of epileptogenic areas in focal cortical dysplasia (FCD; Ishii R et al., 2008). Magnetic resonance imaging (MRI) is one of the most

efficacious diagnostic imaging tools for detecting even small structural abnormalities. Because subtle lesions that generate a focal drug-resistant epilepsy may be invisible at MRI, these cases usually require invasive monitoring using subdural electrodes in the form of grids and/or strips, sometimes with the addition of depth electrodes. Intraoperative stereotactic localization is often utilized to ensure proper placement of the electrodes. The advantages for using invasive monitoring are to accurately localize the site of seizure onset.

Despite the application of all the best available diagnostic methods not all the patients (about 40% in one large study by Wetjen et al., 2008) who had undergone invasive EEG and MRIs studies are diagnosed for surgery and they had ultimately the electrodes removed without a resection.

1e. The epileptogenic focus/circuit.

In 1982 Engel localized the epileptic foci in 50 patients using PCT (Positron Computed Tomography) and EEG techniques. He recorded ictal and interictal epileptiform activity and found that there was good correlation between the site of focal hypometabolism from PCT and the epileptic focus identified as a EEG abnormalities (i.e., slow waves and attenuation of fast rhythms) and that their localization agreed completely. (Engel J Jr. et al., 1982).

In a subsequent histopathological study he found a zone of hypomethabolism, already identified by PCT that correlated well with the severity of the pathological lesion, but the size of the hypometabolic zone was generally much larger than the area resected for pathological involvement. In a third study he recognized 3 distinct anatomico-functional regions: the **epileptic focus** (the area of maximal electrophysiological interictal activity), the **epileptogenic**

lesion (usually a structural lesion responsible for the epileptic state), and the **epileptogenic region**. This region is a dynamic spatiotemporal zone because interictal activity often shifts from one location to another. The epileptogenic region can be defined as the area that is necessary and sufficient for producing recurrent ictal events, or seizures. This concept is important during epilepsy surgery because removal of this region should lead to cessation of seizures (Engel J Jr, 1993).

MTLE is one of the most common forms of focal epilepsy often treated by surgery resection of the mesial part of the temporal lobe. According to the focal model previously described, one damaged region (i.e. hippocampal sclerosis and/or atrophy) would be sufficient to generate epileptic seizures. In contrast, the "network" model holds that limbic seizures may result from a more extensive alteration of limbic networks within the temporal lobe (Bartolomei F., 2001; 2004). Recent studies demonstrated a reduction in the volume of the entorhinal cortex, besides hippocampal sclerosis. Moreover, depth electrodes recordings from patients with MTLE showed an involvement of the entorhinal cortex and other limbic regions, but the situation still remains controversial in humans (Bartolomei F., 2001). The relative contribution of amygdala, hippocampus, entorhinal cortex and other structures has been studied in animal models. Especially an abnormal interaction between the entorhinal cortex and the hippocampus has been proposed as the basic mechanism of seizure generation.

Based on the analysis of interactions between the regions involved at the onset of seizures recorded intracerebrally, Bartolomei and colleagues (Bartolomei F., 2001) state the **epileptogenic network** hypothesis. The epileptogenic network is defined as the region in

which synchronized oscillations among spatially distributed limbic structures are generated in the interictal and the ictal periods.

1f. Intracranial recordings: new windows on seizure generation (ictogenesis) in humans.

The use of intracranial recordings from patients with medically refractory partial epilepsy is giving clinicians a unique opportunity to explore the ictal zone and the correlated brain regions activated during a seizure. Unlike in evidence derived from experiments with animals, these findings have shown that a discrete epileptic focus does not exist in the human condition. Delineation of an epileptogenic region is confounded by the fact that epileptic and non-epileptic brain tissue can expand beyond the interested area and may even involve the contralateral hemisphere.

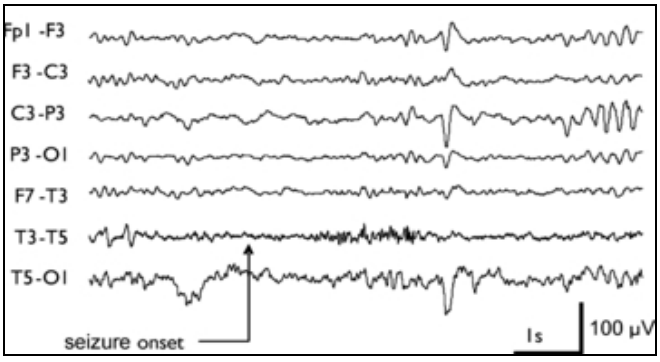

Figure 3 Seizure pattern recorded during scalp EEG recording in a patient with focal epilepsy of the posterior left hemisphere. EEG flattening and low-voltage fast activity was observed in the area of seizure onset.

The signals recorded from the epileptogenic zone revealed that one of the most common pattern of seizure onset was characterized by a low voltage fast activity (25-30Hz) superimposed to a slow potential shift. This phenomenon lasted several seconds and involved the contacts

near the focus with a general de-synchronization of the signals. On the scalp EEG the same activity can be seen as a low voltage fast rhythm and the abolition of background activity components, called “ictal flattening” (Figure 3; de Curtis and Gnatkovsky, 2009).

Activity of low amplitude in the beta-gamma range (15-40Hz) has been characterized during the onset of seizure in limbic and neocortical epileptogenic zones, in cryptogenic focal epilepsies and in focal neocortical dysplasias (Figure 4). For these reasons low voltage fast activity can be proposed as the hallmark of seizure onset.

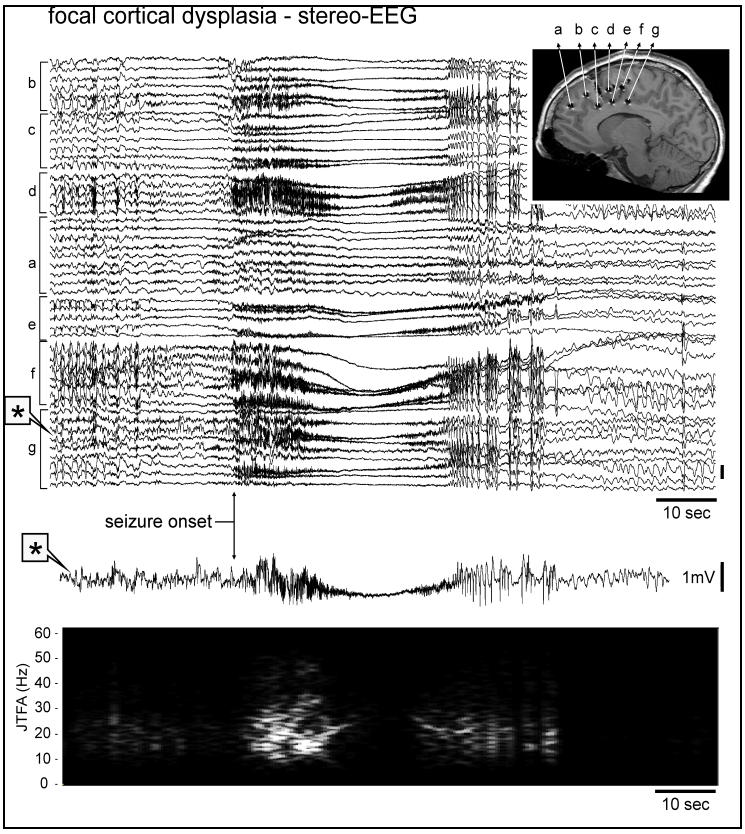

Figure 4. Stereo EEG recordings in a patient with CFD. The position of the intracranial recording electrodes is illustrated in the MRI. The spectrogram of the activity recorded shows the typical fast activity at seizure onset.

1g. Temporal lobe epilepsy

More than a century ago, Jackson associated the clinical features of complex partial seizures to a structural lesion of the hippocampus and the temporal lobe area (Jackson 1880). Postmortem examination of brain tissue from a patient revealed the presence of sclerotic tissue; moreover surgical removal of the temporal lobe confirmed the hipothesis of a causative role for **hippocampal sclerosis** and **mesial temporal lobe epilepsy**.

Partial or complex seizures are the main characteristic of temporal lobe epilepsy (TLE) and have been related to important hippocampal damage, involving mainly the hilus, CA1 and DG area with selective neuronal loss. Axonal sprouting form granule cells make recurrent excitatory monosynaptic circuits and abnormal network reorganization that increase the susceptibility to excitation. The surviving hippocampal neurons fire with synchronous discharges, producing the clinical features of complex partial seizures.

Different authors have demonstrated that in TLE and in animal models of TLE long-lasting seizures start a complex chemical cascade, triggering neurochemical alterations in neurons and glial cells. These immediate or long-lasting events can modify the cellular environment through changes of ionic gradient across the cell membrane, alteration of gene expression such as receptors, trophic factors, enzymes, proteins from cytoskeleton, protein from matrix and the phosphorylation of macromolecules. Furthermore, seizures can induce reactive gliosis generated by cell death. These modifications concur in synaptic remodeling, which can orient the excitability of neurons in temporal structures to a permanent hyperexcitability.

1h. Animal models of epilepsy and seizures.

The study of many diseases is largely facilitated by the use of animal models because they can be customized to reproduce the exact pathophysiology of the disease. Current advances in the development of modern molecular biology and genetic research tools had an impact on the generation of new and more suitable animal models. Best qualities for a good model are: a relatively simplicity of realization to achieve a good degree of reproducibility and reliability compared to the kind of modeled disease.

The development of an animal model is helpful to study the physiological mechanisms (basic science) that underlies the generation of aberrant pathways leading to the development of diseases (translational approach). Animal models have been developed and used for this purpose to study neuronal connections and brain networking under different conditions. Also models of brain development or neuronal damage and repair are very useful to study the changes in cortex organization during the early stages of life or after brain insult. Animal models were also relevant in explaining many of the structural transformations that occur during the process known as epileptogenesis that involves the rearrangement of different brain areas.

The different types of animal models of epilepsies can replicate a high variety of clinical manifestations. Animal **models for epilepsy** are used to answer two major questions: how do seizure initiate (study of *ictogenesis*) and what are the mechanisms that lead to the permanent condition of epilepsy (study of *epileptogenesis*). There are two different models to do that. They are **acute seizure models**, used to reproduce a transient ictal event, and **chronic seizure models** that bring long lasting changes and require all the functional and

anatomical changes described in the previous paragraphs to acheive recurrent epileptic condition.

There are different ways to induce seizures in an animal, using different techniques: mechanical, biochemical or genetic.

1h.i. Models of seizures.

The electrical stimulation-induced model of seizures

Seizures are induced through an electric stimulation that can be generalized to the whole brain (*electroshock*) or a single area can be stimulated (*epileptic afterdischarge*). The clear advantage of this model is the restricted action of the pro-convulsive agent only during the time of its application.

A series of 0,2s pulses of AC at 60Hz frequency are given through corneal electrodes to the rat or the mouse. This technique is called MES test: maximal electroshock seizure test and it induces generalized tonic-clonic seizures. The intensity that induces tonic extension seizures in 50% of animals (CD50) is measured. To screen drugs, the effective dose of anticonvulsant that blocks these seizures (ED50) is evaluated. Epileptic afterdischarges (AD) are a model of partial seizures, they can be achieved by local stimulation both with high frequency (50-60Hz) or low frequency (3-12Hz) currents. This technique can be used to measure the threshold intensity for stimulation to induce AD and also to induce acute seizures, but to avoid kindling. The phenotypic outcome of this type of seizure models depends on which area is being stimulated (usually the neocortex, hippocampus, amygdala and other limbic structures).

Chemically induced acute seizures

Generalized seizures can be induced by systemic or focal application of pro-convulsive drugs to the animal. The systemic injection sites can

be of three types: sub-cutaneous (sub-Q), intraperitoneal (IP) and intravenous IV. The action of drugs administered through sub-Q is slower than IP or IV because the ADME kinetics of the drug requires more time. The IP and IV methods give faster responses, even within sec.

The γ-aminobutyric acid (GABA) related drugs are probably one of the most common used pro-convulsive drugs. They can act both on the Cl^- channel and on the GABA receptor.

Pentylenetetrazol (PTZ) has significant convulsant properties in mice, rats, monkeys and also humans. After about 20min from the application, PTZ induces all of the signs of tonic-clonic seizures in the animal. Repetitive low doses administration of PTZ can induce SE in immature rats; the EEG shows a rhythmic, spindle shaped discharges and are associated with a freezing behavior.

A similar pattern can be obtained by the injection of IP **bicuculline** in rats. BMI administration produces all the phenomena previously described, but the dose to reach the effect is high because it requires the "first-pass effect". (A phenomenon in which the concentration of a drug is greatly reduced before it reaches the systemic circulation, because of drug metabolism) The mechanism of action of bicuculline is well known, it is a competitive antagonist fro the GABA-A binding site.

EAA drugs are very effective in inducing SE in experimental animals with the advantage that a low dose is required. A systemical administration of EAA in adult or infant rats produces various automatisms, clonic and/or tonic-clonic seizures, with already described EEG patterns: spike, spike and wave complexes, polyspikes and wave complexes. In general all these drugs can induce a neuronal

damage that can produce SE (prolonged seizure for more than 30min) with the related cellular damage.

Kainic Acid (KA), a specific agonist for the ionotropic glutamate receptor, is the most common used neurotoxin to induce SE and related neuropathological changes. Systemic administration of KA in rats induces a series of behavioral changes that end up in seizures in about 60min from the injection. A specific cell loss is seen in rats hippocampi after the injection of KA, associated with the synaptic remodeling. Other zones that are affected are the piriform cortex, the entorhinal cortex, the amygdala and the thalamic nuclei (Araki T., 2002; Ben-Ari Y., 2001). NMDA is another specific antagonist for the ionotropic glutamate receptor. Injection of 100mg/kg of NMDA can induce seizures in adult rats beginning with a phase of locomotor hyper-activity, flexion of the head, tail flicking. NMDA induces tonic-clonic but not clonic seizures during development. The EEG patten is non specific and various behavior can be observed: often it is chaotic activity. To a cellular point of view, intracerebral administered NMDA induces severe neuronal damage with apoptotic cells found in the piriform cortex and dentate gyrus of the hippocampus.

Here is a list of substances that do not fit the previous categories, but do have a convulsive action on animals and men.

The injection IP of **insulin** 5-30IU/kg is enough to induce epileptic seizure within 4 hours in rats. The hypoglycemic effect of massive dose of insulin mimic the neurologic consequences of diabetes mellitus type I. Metabolic studies on rats demonstrated a significant impairment of hypothalamic nuclei, but also the midbrain and brainstem structures.

Inhalation of **Fluorothyl** (bis-2,2,2-trifluoroethyl ether) provokes seizures in mice, rats, gerbils and humans. The animal is placed inside a sealed chamber to the exposure of ether vapors. The exact maechanisms of action of fluoroethyl ether are uncertain. The sequence and seizure phenomena after fluorothyl ether are very similar to those obtained with GABA-A related drugs, expecially PTZ and bicuculline. EEG shows rythmic dyscharges; also individual spikes or sharp waves are recorded.

The potency of antibiotic drugs to induce seizures has been extensively studied both in vivo and in vitro models. The application of **penicillin** to the cortex induces an epileptogenic focus. Systemic application of high doses of penicillin or cephalosporins induces seizures.

Transgenes and gene replacement

The production of transgenic animals through modern techniques of recombinant DNA microinjection in mouse embryos or in utero electroporation is now highly utilized. The most common genes targeted are genes encoding for ion channels and proteins involved in the neurotransmission pathways. They can be inserted through DNA recombination, or koncked out by mechanisms of DNA excision and repair (e.g. the CRE loxP recombination).

1h.ii. Models of epilepsy

The hallmark of epilepsy is the occurrence of chronic unprovoked spontaneous seizures. Several of the available **traumatic brain injury (TBI)** models mimic well the clinical aspects of the human counterpart. Postraumatic epilepsy (PTE) was originally modeled by the application of metals to the cortex (aluminum, or iron) because hemosiderin deposits were seen to be associated with PTE.

Experimental seizures can be induced also after the application of lateral fluid-percussion brain injury (FPI) which is one of the most used TBI model for human head injury (D'Ambrosio R., 2004). TBI models display a complex assembly of acute and delayed molecular, cellular and network alterations. Some of them are directly caused by the traumatic agent, whereas others are developed secondary to the initial trauma (Pitkanen A., 2009). The latency period typically lasted several months before the animal develops spontaneous seizures.
Histological analysis of rats with PTE showed extensive damage to the hippocampal areas CA3 and CA1 with neuronal loss. Inhibitory neurons damage after TBI contributes to an increased susceptibility to seizure development. In response to neuronal death, structural and functional reorganizations of the damaged areas take place: for example it has been observed an increase in astrocytic compartment. Taken together all these changes contribute to the remodeling of the damaged areas with a modification in its structure and so also in its physiological functions. In rats PTE has demonstrated to have all the characteristics of the human counterpart.

IP injection (300-400mg/kg) of the non specific muscarinic receptor agonist **pilocarpine** in the rats and mice can induce seizures. Pilocarpine induces automatisms and clonic seizures developing into SE. In the EEG fast spikes can be observed, that spread from the hippocampus to the cortex. In adult rats the hippocampus is most damaged, but also dentate gyrus, globus pallidus, substantia nigra, ventrobasal and mediodorsal thalamus, pyriform and visual cortex.
In the **pilocarpine** rat model of epilepsy, repetitive administration of this potent muscarinic agonist induces sequential changes that state 3 distinct periods: (a) an acute period that lasts 24 h and built up

progressively into a limbic status epilepticus, (b) a silent period (up to one month) with a progressive normalization of EEG and behavior, (c) a chronic period with spontaneous recurrent seizures. The main features observed during the long-term period resemble those of human complex partial seizures and recurs 2-3 times per week per animal. The induction of status epilepticus by pilocarpine leads to severe and widespread cell loss in several brain areas. The primary insult occurring during pilocarpine induced SE produce an immediate cell damage, while the protracted process of neurodegeneration may take weeks to become evident. The most damaged neuronal types are the principal cells in the hippocampus. The progressive injury takes more time to become evident and involve other neighbor areas like the entorhinal cortex and the amygdala (Scorza FA., 2009)

Drug family	Drug	Dose in vitro	Dose in vivo
$GABA_A$ receptor antagonists	bicuculline picrotoxin penicillin	10-50 µM 50-200 µM 2 mM	6-8 mg/kg IP 3-6 mg/kg IP 25-175mmol/l
Glutamate receptor agonists	kainic acid(KA) low-Mg^{2++}	0.1-1 µM	10-14mg/kg --
Muscarine recepor agonists	Carbachol Pilocarpine	50-100 µM 1-10 mM	273pmol (local inj) 300-400 mg/kg IP
K^+ channel blockers	4-aminopyridine Tetraethylammonium	<100 µM 5-10 mM	

Table 3. Summary of the principal types of drug-induced seizures (de Curtis et al, 2010)

Chemical kindling can be induced by administration of low doses of excitatory agents or more routinely by repeated administration of convulsants agents, such as PTZ, NMDA, GABAA receptor antagonists, either systemically or directly into the brain at subthreshold concentrations (de Curtis M. 2010 in press).

GABA-A receptor antagonists release principal neurons from fast inhibitory neurotransmission and induce interictal-like bursts that depends on fast glutamatergic neurotransmission (Williamson and Wheal, 1992). Ictal discharges are observed in immature tissue only (Swann and Brady, 1984). Glutamate receptor agonist KA induces interictal-like epileptiform discharges that depend on the convergence of several mechanisms mainly attributable to a decrease in synaptic inhibition (Fisher and Alger, 1984). KA also influences inhibitory activity by indirect enhancement of tonic inhibition of pyramidal cells and by modulating mutual interneuron inhibition . To date, the mechanisms underlying the generation of epileptiform discharges in hippocampal slices challenged with KA are unclear. The removal of extracellular magnesium, which leads to the release of the NMDA ionophore also induces interictal and ictal-like discharges. This activity is blocked by NMDA receptor antagonists, but not by AMPA receptor blockers . Muscarinic agonists can also induce epileptiform discharges consisting of recurrent population bursts or more complex patterns that include both interictal events and ictal-like components that require NMDA receptor activation. K+ channel blockers, such as 4-aminopyridine (4AP, Avoli et al., 2002) or tetraethylammonium increase the release of neurotransmitters from both excitatory and inhibitory terminals, therefore enhancing overall network excitability where inhibitory activity is preserved. In combined hippocampus-entorhinal slices 4AP and other K+ channels blockers induce both interictal and ictal discharges.

Aim of the project

The cellular changes that sustain epileptic activity in the brain and network remodeling during the process of epileptogenesis are largely unknown.

The development of local seizures in the temporal lobe after application of pro-convulsive drugs has long been used to reproduce ictal patterns coherent with the human pathological situation. The acute model of the isolated brain can be used to study the mechanisms operating during the process of ictogenesis. There are also different types of chronic epilepsy models that can reproduce the pathological modifications occurring in the brain during the process of epileptogenesis.

Principal aim of this project is to study the mechanisms of ictogenesis after induction of local seizures in the temporal lobe of the isolated guinea pig brain by the application of bicuculline, a GABA-A antagonist. With this model we reproduce the typical ictal pattern observed in human EEG recordings. The field potential activity is recorded by classical electrophysiology glass capillary electrodes. The extracellular ionic modifications are monitored through potassium-sensitive and pH-sensitive electrodes. The peculiar activity of pyramidal neurons in the EC is analyzed with sharp electrodes for intracellular recordings and the cell position among the cortex layers is located after biocytine labeling

The basic circuitry operating in the olfactory cortex and the limbic areas of the guinea pig brain have been extensively characterized with

electrophysiological studies. Mapping of the paths of neuronal activation in the EC following LOT fibers stimulation and the study of connections between olfactory cortex and the adjacent structures of hippocampus and para-hippocampal region settled the basis to better understand the altered mechanisms acting in epilepsy.The pathological modifications of the basic circuitry during a seizure reflect a network reorganization that is necessary to start the epileptic activity itself.

Secondary to the characterization of network remodeling during the priming events that lead the transition from an interictal to ictal activity, there is the study of the local modifications in the extracellular environment using ion-sensitive and pH-sensitive electrodes. The increase in potassium concentration can both be seen as an effect of the paroxysmal neuronal activation and as a cause of long acting, slow wave activities. These long acting phenomena involve also non-neuronal cell types, such as astroglia. It has been demonstrated to have a role in circuit synchronization, after massive activation under calcium waves, and maybe in seizure ending. We identified three progressive phases characterized by an initial slow wave that correlates with low voltage fast activity at seizure onset; an inverting phase that we hypothesize to astrocytes activation and potassium ions pumping from the extracellular space. A third delayed slow wave delineate the bursting activity and field potential recovery until seizure termination.

A deeper knowledge of the cellular mechanisms and the network processing that take place during the different phases is pivotal to clarify the role of cellular categories (principal neurons, GABAergic interneurons and astro-glia) in promoting the advance from one phase

to the next one. The action of modulation on the slow waves by the application of drugs specific for ion-channels is giving insights to the ionic equilibrium that is initially broken during epileptic activity and then recovered by homeostatic mechanisms.

The possibility to modulate seizure progression opens huge perspectives on a targeted therapy, for example for ion-channels related forms of epilepsy, in which the etiology is known.

Although the application of AED is largely of common use, their specificity is not suited for all the variety of epileptic syndromes classified. The perfect matching of basic science research and clinical information from stereoEEG recordings and MRI imaging will shape a specific therapy for different pathological situations.

Chapter 2

2a. The isolated guinea pig brain *in vitro.*

The procedure if the isolated in vitro guinea pig brain was developed originally by Llinas and colleagues (Llinàs R., 1981, 1988) to obtain a viable preparation in vitro. “This new technique offers potential for the study of ionic mechanisms underlying electrical activity as well as neurochemistry, neuroanatomy, neuropharmacology, and neuroendocrinology.” (Llinàs R., 1981) The recordings of field potential activity but also intracellular potentials are applicable to this kind of preparation.

The model was further characterized and improved by de Curtis and collaborators at Istituto Neurologico “C. Besta” to obtain a high-performing model to describe the anatomical structure and physiological properties of brain cortices, to study the mechanisms of ictogenesis in the temporal lobe or the effects of ischemia in different brain areas (de Curtis M., 1991; 1998; Pastori C., 2007).

The procedure to maintain and perfuse in vitro the isolated brain has been exhaustively described by de Curtis and coworkers in methodological papers (see de Curtis M., 1991, 1998). Briefly, young adult guinea pigs were anesthetized by i.p. injection of a lethal dose of barbiturate (pentothal sodium Abbott, Italy; 20 mg/kg). The animal blood is substituted with cold oxygenated ACSF (pH 7.2) by intracardiac perfusion through the left ventricle. This prevents clotting activation and preserve brain cellular functions during the surgery. The brain is carefully dissected out of the head and placed in the recording chamber and cannulated by the basilar artery. All these

operations are performed at a temperature of 15°C, the temperature is slowly (0,2°C/min) raised to 32°C.

The isolated brain set-up is composed of the following parts (Fig. 5).

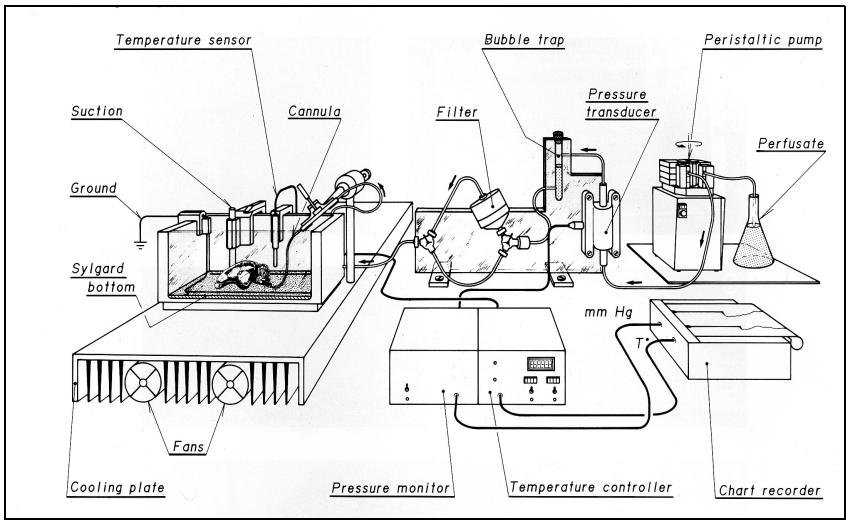

Figure 5. Set up for the isolate in vitro guinea pig brain (from de Curtis et al., 1991).

Solution is perfused from a reservoir, along Tygon tubing system via a peristaltic pump (Raining-Gilson Minipulse 3) at a constant flow of about 6.5/7 ml/min. A custom-made Plexiglas bubble-trapping air chamber blocks air bubbles to flow through the tubes to the brain. One Nalgene holder for 47mm diameter cellulose–acetate filtering membranes (0.22 mm pores, Millipore) connected via a Luer-lock three-ways plastic stopcock that allows to switch between the filter and the unfiltered pathway. The saline solution reaches the brain through a polyethylene tubing (PE 60 and 90). The composition of the saline solution is126 mM NaCl, 3 mM KCl, 1.2 mM KH_2PO_4, 1.3 mM $MgSO_4$, 2.4 mM $CaCl_2$, 26 mM $NaHCO_3$, 15m M glucose and 3%

dextran molecular weight 70,000), oxygenated with a 95%O_2 5%CO_2 gas mixture (pH7.3; ;).

A custom-made incubation chamber (Biomedical Engineering, Thornwood, USA) internally coated with a silicon elastomer (Sylgard, Dow-Corning; 0.5–1 mm thick) film on the side walls and the bottom of the chamber. The temperature of both the chamber and the solution is controlled by a thermostatic system (Biomedical Engineering, Thornwood, USA). A polyethylene cannula 0.3–0.5 mm internal diameter tip fire-pulled from a PE 60 is inserted in the basilar artery to supply the brain with the ACSF solution.

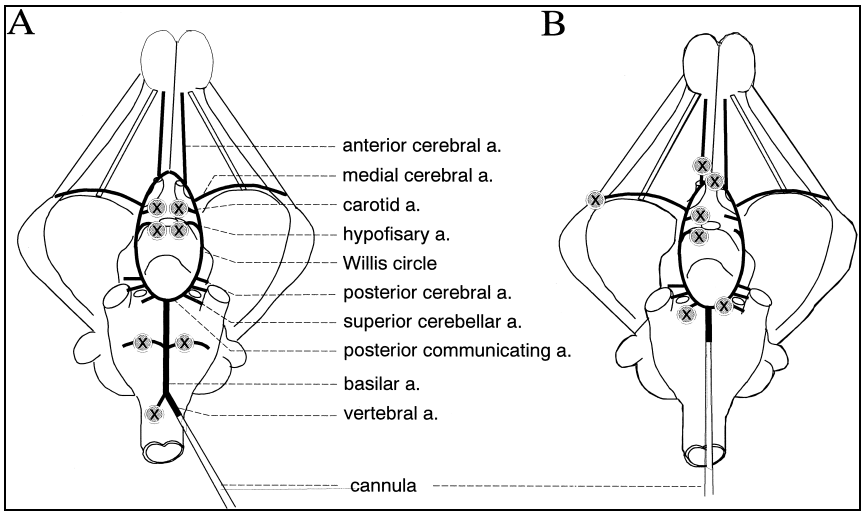

Figure 6. Schematic drawing of the arterial system in a ventral view of the isolated guinea pig brain. (from de Curtis M., 1998)

The procedure for isolating the guinea pig brain has been published (;). Anaesthesia of 150–250 g guinea pigs is induced with penthotal sodium 80 mg/kg, i.p. When the trigeminal reflex cannot be elicited, start the surgical procedure. After exposing the heart, intracardiac perfusion with the cold solution is performed to reduce brain metabolism and preserve the brain tissue during the dissection. After 3

min of intracardiac perfusion, the brain is isolated and transferred it to the perfusion chamber. The olfactory bulbs and the cervical spinal cord are positioned under the silk string pinned to the Sylgard-coated bottom of the chamber, to stabilize the brain. Under a stereomicroscope, gently remove the dura that enfolds the basilar artery and insert the tip of the PE cannula into one of the vertebral arteries_Fig. 6. The cannula is inserted in the basilar artery, 3–4 mm caudal to its bifurcation. Incubation temperature of the chamber is raised to 308C_0.1–0.28Crmin. The warming up of the system will determine a dilation of the PE tubing and a drop in pressure.

To restrict the vascular perfusion to the piriform cortex _PC. and entorhinal cortex _EC. of one hemisphere, the following arteries were tied with silk knots: the contralateral posterior communicating artery, the ipsilateral superior cerebellar, hypophyseal, carotid, anterior cerebral arteries and the anterior communicating artery _see schematic drawing in Fig. 6. The more distal branch of the median cerebral artery was also ligated 1 mm dorsal to the rhinal sulcus.

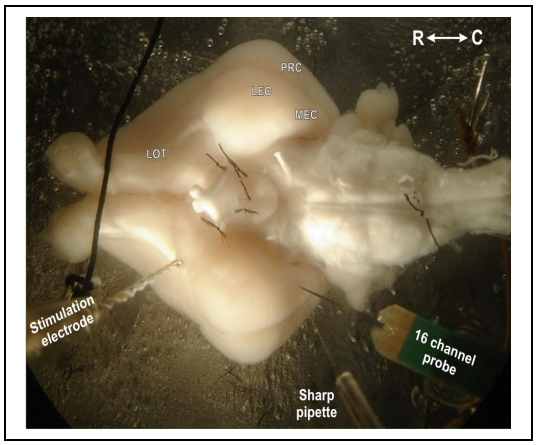

Figure 6. Microphotograph of the ventral view of the isolated guinea pig brain. Different types of electrodes are illustrated.

Electrophysiological recordings were performed with 0.9% NaCl-filled micropipettes positioned in the PC and EC lateral and medial. To see the slow components of the signal no filtering was performed. Evoked field responses were obtained by stimulating the lateral olfactory tract LOT with a bipolar electrode made of twisted silver wires (Figure 7). Drugs were applied by arterial perfusion.

A complete set up (see Fig. 8) for electrophysiological recordings that includes an anti-vibration table (TMC, Peabody, MA.), a temperature controller (Biomedical Engineering, Thornwood, NY.), an extracellular recording amplifier (Biomedical Engineering, Thornwood, NY.), an oscilloscope (Tektronix, Italy.), a pulse generator (Biomedical Engineering, Thornwood, NY.), a stimulus isolation unit, an A/D board recording system (National Instruments, TX) and a personal computer. The ELPHO® tool is used to record electrophysiological signals and is used to perform off-line analysis of the acquired data. It was developed in our laboratory by dr. Vadym Gnatkovsky from the NI software provided with the A/D board system.

Glass calpillaries (Harvard Apparatus OD 1,5mm; ID 0,86mm) are pulled with a Sutter electrodes puller (Sutter Instruments, USA) using a custom programmed ramp to obtain an electrode with a sharp edge that is cut at about 15-20um for extracellular recordings. Electrodes are then filled with NaCl 0,9% and an Ag/AgCl wire is inserted into the capillary and used as the anode for the electrical recordings. Signals are acquired with a low impedance amplifier (Biomedical Engineering, Thornwood, USA) with no incoming filtering and digitized with a NI A/D board provided with the LabVIEW ® software analysis.

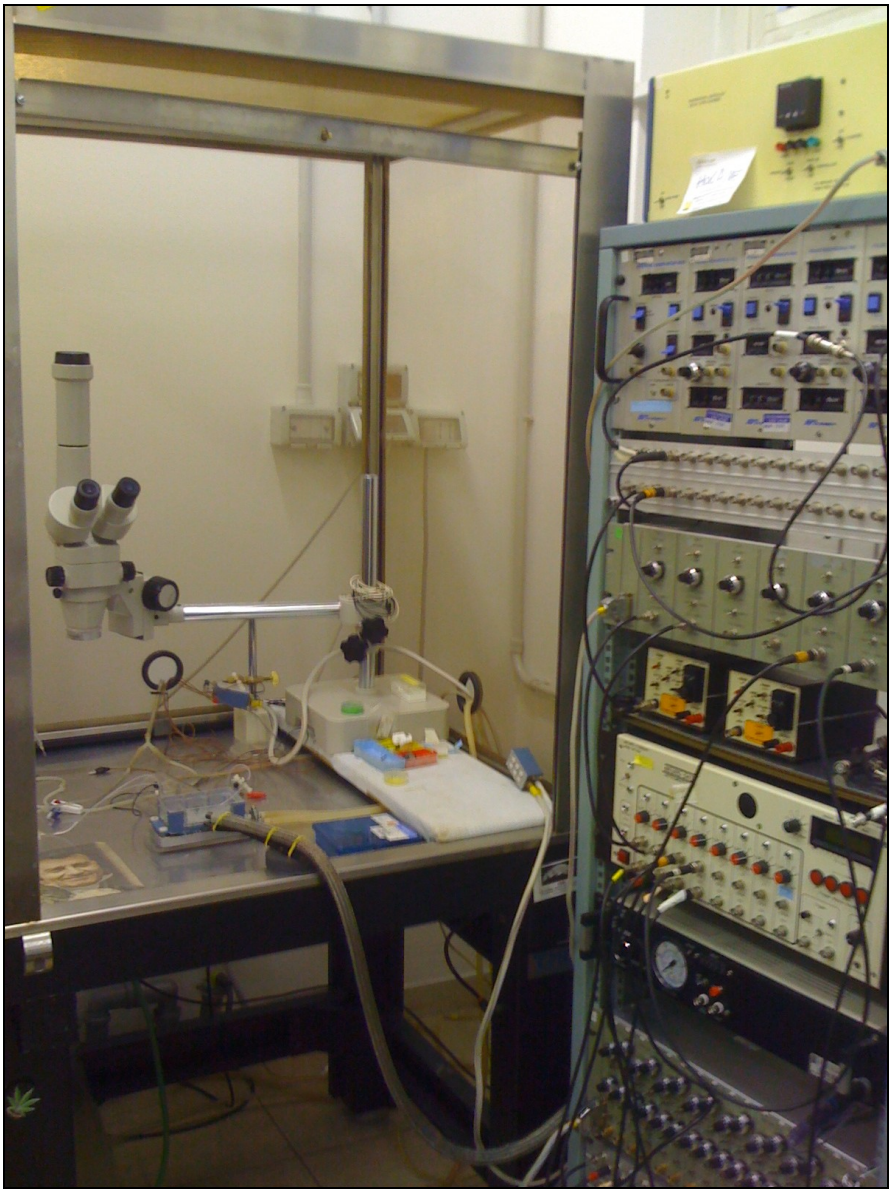

Figure 8. A set-up for electrophysiology recordings. On the left top, the temperature controller, the oscilloscope, the stimulus with isolation unit, the multichannel extracelluar amplifier. On the right, the perfusing system with a peristaltic pump, the tubing system to the chamber and, on the floor the waste collector. The stereomicroscope inside the cage for brain cannulation and artery ligation.

For ion-sensitive electrodes preparation, double barreled glass capillaries are pulled and the tip broken under a light-microscope to obtain a tip of 5μm. One capillary is sealed with dental cement and the other one is exposed to sylane vapors and fixed at high temperature (120°C for 90min).This procedure makes the electrode internal walls electrostatic so that the the ionophore resin can be easily places into the small tip of the capillary. The reference electrode is filled with KCl 0,1M and the sylanized ion-sensitive capillary is filled with a ionophore resin (Fluka 60031,Germany) in the tip and KCl 0,1M for the rest of the capillary. The electrodes are then calibrated using standard known solutions with increasing [K]. The voltage measured for each step is assigned to a specific concentration using a linear regressive curve. The equation of the curve is $Y = a + b\text{Log}X$ where Y is the change in voltage (mV), X is the change in K concentration expressed as the logarithm of [K], and *a* and *b* are the coefficients of the curve. During experimental recording in the tissue one channel gives the extracellular field potential while the other one is the differential between the FP and the ion-sensitive signal. So the net ionic changes in time and at the electrode recording site are measured through the whole experiment.

Sharp electrodes filled with K-acetate 2M were used for intracellular recordings (input resistance, 70–100 MΩ). An oscilloscope is used to measure the changes in voltage potential across the membrane and to calculate the resting membrane potential (rmp). The recordings are performed in current clamp, the cell is maintained in a depolarized/hyperpolarized or resting status by the injection of positive/negative or no current. The cell is then labeled with biocytine 1,5% injected through the recording electrode by current pulses.

After the experiment has ended, the brains are fixed in a 4% paraformaldehyde solution and then cut with a vibratome into 70 μm slices. The sections of tissue around the site of injection are processed with a histochemical reaction (ABC kit – streptavidine-biocytine commercial kit) to reveal the labeled cell(s). The slices that positively react to the histochemical processing are then carefully selected to reconstruct the exact order of slice cut and to localize the labeled cells.

2b. The guinea pig model of temporal lobe seizures

Systemic perfusion of the isolated brain with bicuculline 50μM for 3min induces epileptic seizures in the temporal lobe. The epileptic model has been accurately characterized by Uva L. and colleagues in a paper describing the ictal patterns observed in different portions of the cortex after the induction of epileptic seizures with bicuculline. (Uva L., 2005)

Previous studies on complex slices saving hippocampal and entorhinal cortex connections, demonstrated that the induction of ictal events by the application of pro-convulsive drugs (4AP, low Mg) is first circumscribed to the EC and then from here the epileptiform activity spreads to the hippocampus. It is necessary for the layer II/III fibers along the temporo-ammonic pathway from the EC to overcome the inhibitory gate of the DG and activate the CA3/CA1 region. (For details on hippocampal/entorhinal cortex circuitry see next paragraph). The interictal pattern induced by arterial bicuculline perfusion in the isolated guinea pig brain is typically characterized by interictal spikes (ISs) that originate in the PC and propagate to the lateral entorhinal cortex (l-EC), but never spread to the peri-rhinal cortex (PRC). A change in interictal pattern during the preictal transition represents a

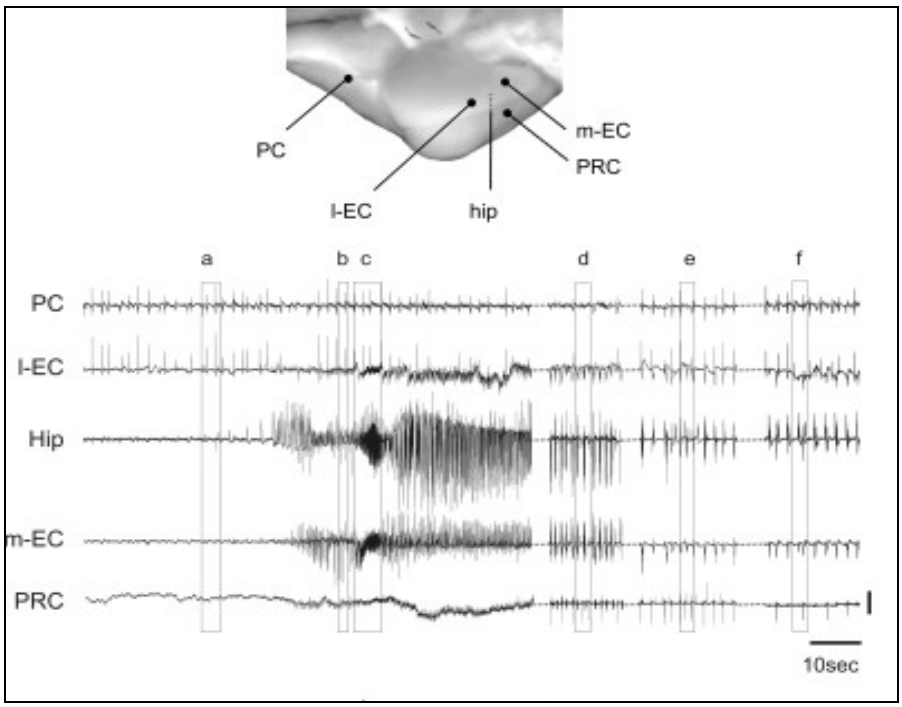

Figure 9. Typical pattern of interictal to ictal transition induced by a 3-min arterial perfusion of 50 μm bicuculline in the isolated guinea pig brain. Simultaneous extracellular recordings performed in the piriform cortex (PC), in the medial and lateral entorhinal cortex (m-EC and l-EC), in area CA1 of the hippocampus, and in the perirhinal cortex (PRC). The position of the recording electrodes is illustrated in the upper panel. As already said in the text, bicuculline application induces interictal spikes in the PC that propagate to the l-EC (**a** and **b**), but not the hippocampus and m-EC. Just before ictal discharge onset, independent preictal spikes are generated in the hippocampus and m-EC (**b**). Ictal onset (**c**) is characterized by fast activity at circa 25Hz originating in the hippocampus, EC. During the late phase epileptic activity is propagated to the PRC (**d** and **e**). At the end of the ictal discharge, the PC resumes its leading interictal spiking role (**f**). (modified from Uva L., 2005)

predictive condition for the development of the ictal discharge. Just before the ictal discharge onset, the interictal focus, shifted from the PC/l-EC region to the medial entorhinal cortex (m-EC) and the hippocampus.

Ictal discharges are characterized by fast oscillatory activity at about 25 Hz. They showed an onset in the same structures that generated

preictal ISs, namely the m-EC and the CA1 region of the hippocampus. (see Fig 7.) Correlation analysis demonstrated that the fast ictal discharge originated within the m-EC and in the hippocampus. The l-EC and the PC were not involved. The PRC may be secondarily entrained within seconds by ictal afterdischarges.

Current source density analysis of laminar field potential profiles was performed with multichannel silicon probes positioned in different parahippocampal subfields. Multichannel silicon probes were positioned in different cortical areas and the sinks and sources of locally generated currents were located. CSD analysis demonstrated that ISs are generated in the PC and spread to the l-EC; CSD also confirmed the preictal change of focus from the PC to the m-EC, already observed with field potential recordings. ISs generated in the olfactory cortex propagate neither to the PRC nor to the medial EC, unless a priming ictal event is generated in the hippocampus or in the m-EC. After seizure induction by systemic application of bicuculline, fast activity at 25-30Hz is generated between the m-EC and the hippocampus CA1 area and it does not recruit the l-EC and the PC.

Fast rhythmic activity at seizure onset has been typically observed during stereo-EEG recordings performed with depth electrodes in human subjects, in chronic models of temporal lobe epilepsy, and in studies performed in combined PHR–hippocampal slices exposed to different epileptogenic drugs (bicuculline, 4-aminopyridine, pilocarpine).

Wendling proposed that an impairment of GABAergic interneuron system is at the basis of fast activity at seizure onset. (Wendling F., 2002) The parameters used to explain the changes in signal frequency in one hypothetical hippocampal neuronal population are: (i) the behavior of inhibitory interneurons in the generation of gamma

frequency oscillations; (ii) the impairment of dendritic GABAergic inhibition in experimental epilepsy; and (iii) the depression of $GABA_A$ fast circuit activity by slow inhibitory $GABA_A$ currents. The model includes two main features: a fast inhibitory feedback loop that represents somatic projections from the subset of fast-$GABA_A$ interneurons onto the subset of pyramidal cells and a slow inhibitory control on the former subset by the subset of dendritic slow-$GABA_A$ interneurons.

Acute slice studies demonstrated that CA subfields, the EC, and the PRC have the intrinsic property to sustain prolonged (>30 s) ictal discharges characterized by fast activity in the frequency range of that observed in our experiments (Avoli M., 2002). Intracellular recordings performed in the superficial and deep layers of the m-EC of the guinea pig brain demonstrated a strong inhibition of principal neurons during the first seconds of seizure onset by the GABAergic action of layer II/III interneurons. The appearance of low voltage fast activity well correlated with a strong interneurons activation exactly during this phase of seizure onset. It can be postulated that the 25-30Hz activity is locally generated by interneuronal firing.

Referring to a human pathophysiological situation, low-voltage rapid discharges are characteristic patterns observed at seizure onset in human partial epilepsy. As in the animal model, these processes are linked to a reduction of GABAergic dendritic inhibition that would paradoxically allow somatic inhibitory interneurons to abnormally and continuously generate fast IPSP's on pyramidal cells. (see Wendling F., 2002, 2004 and Gnatkovsky V., 2006). Intraoperative stereoEEG observations in MTLE patients sustain the theory that the EC is involved in mesial temporal lobe seizures. Magnetic resonance imaging of extrahippocampal temporal cortices in patients suffering of

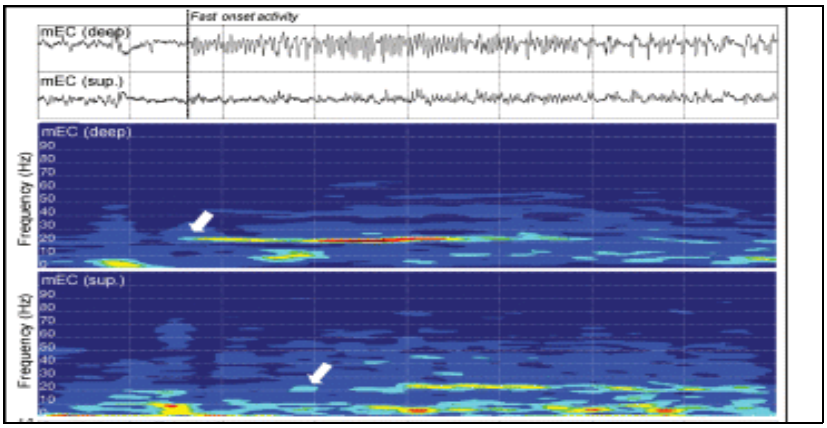

Figure 10. The figure illustrates the local field potential recordings from the medial EC (left) superficial layers (upper trace) and deep layers (lower trace). The two spectrograms represent the changes in frequency content of the signal along time. The white arrows indicate the onset of fast activity. Hot and cold colors, respectively, denote high- and low-energy values at a given time-frequency point.

MTLE (with or without demonstrable MTS) demonstrated that the EC is markedly reduced in volume. These findings suggest that changes in EC excitability and network interactions may act as trigger elements in the development of MTLE and may precede the direct involvement of the hippocampus proper

2c. The olfactory and limbic area

The olfactory area comprises the piriform cortex, the olfactory tubercle, and the lateral EC. They are strongly interconnected with the limbic structures of the medial entorhinal cortex and the hippocampus. This circuitry is involved in the processes of memory and learning. Given the high plasticity of the network connections that form these structures they are continuously rearranged during the early stages of growth and under particular repetitive inputs. The process of learning and the related consolidation of memory involves the activation of hippocampal-entorhinal loop circuits that elaborate and store the

information. The anatomical correlate of the learning process is an increase of the synaptic connections along that way producing a reinforcement of that pathway following network activation.

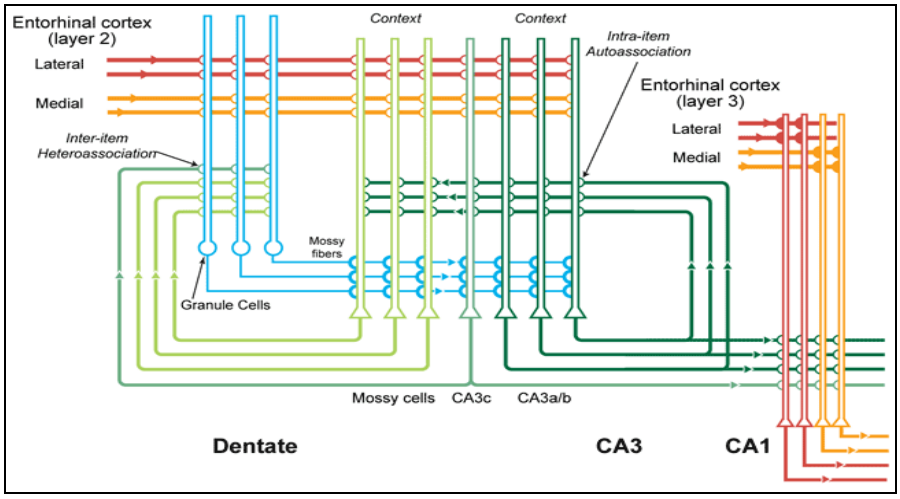

Figure 11. Schematic drawing of the two different types of pathways activating entorhinal-hippocampal circuit. EC layer II sends inputs to granule cells in the dentate girus that follow the classical pathway of CA3/CA1 activation. Pyramidal CA3 neurons can send feed-back inputs to Granule cells (heteroassociation), or make connections with other CA3 pyramidal cells (autoassociation). EC layer III principal neurons make connections directly with CA3/CA1.

The organization of the layers of the cortex has been studied in different animal species. The cytoarchitecture of the piriform cortex is organized as a three layered cortex in which we can distinguish a superficial part (layers Ia/b and IIa/b) and a deeper zone (layer III). Layer I receives the projections from the LOT and contains principally the dendrites of the neurons that form the superficial layer. Layer II is a compact layer of cell bodies for the vast majority pyramidal neurons. Layer III displays a higher variability in cellular composition: the superficial part contains a discrete number of pyramidal cells that declines in depth along the cortex and the neuronal axons become the principal components of the layers.

The entorhinal cortex has the peculiar organization in a 6-layered cortex. The layers from I to III are the same as seen in the piriform cortex, then a *lamina dissecans* (also called layer IV) divide the further two layers (layer V and VI) from the previous.

The olfactory bulb is the main source of afferent inputs to the olfactory cortex even if many olfactory areas are inter-connected with each other. Output pathways from the olfactory area have been described to the neocortex, thalamus, hypothalamus, hippocampus and limbic system.

The hippocampus forms a principally uni-directional network with inputs from the EC. The *perforant pathway* (PP) originates from layer II/III of the EC that make connections with the dentate gyrus (DG) and CA3/CA1 areas. CA3 neurons receive inputs from the DG via mossy fibers, and send axons to CA1 pyramidal cells via Schaffer collaterals (SC). There have been documented also connections from one hippocampus to the contralateral via the Associative Commissural pathway (AC) that originates from CA3. Another possible way of

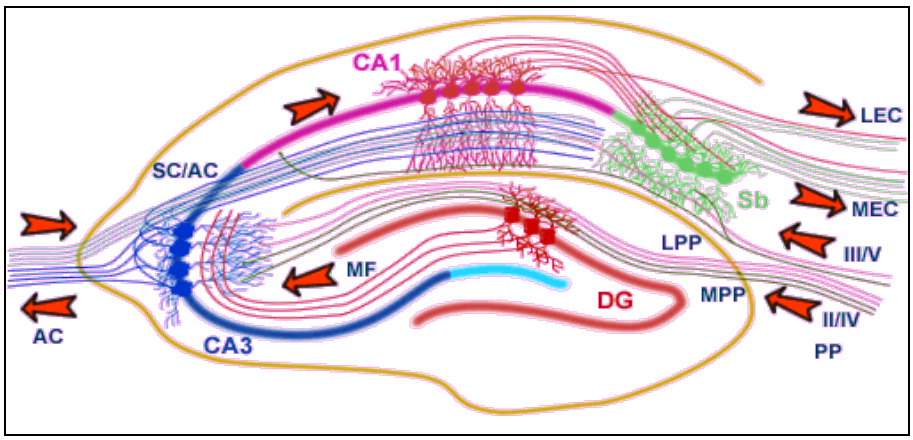

Fig. 10. Schematic representation of the hippocampus circuits with its input connections and internal connections. The arrows indicate the direction of the signas coming from and returning to the EC.

activation of the contralateral hippocampus may derive from commissural fibers originating from the EC to the contralateral DG, or even directly from the olfactory area. (Uva and de Curtis, 2005).

The stimulation by electrical pulses with a bipolar twisted-wire electrode of the lateral olfactory tract (LOT) gives rise to the activation of the limbic pathway from the piriform cortex, the lateral and medial entorhinal cortex in its superficial layers and the hippocampus which loops back with the deep layers of the mEC again.

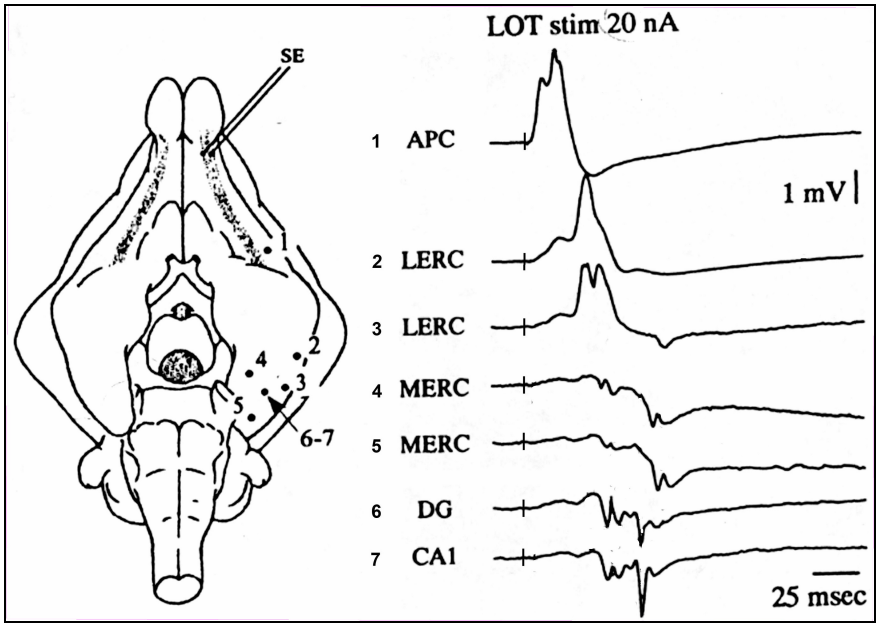

Fig. 11. Evoked responses (right) obtained after stimulation of the LOT and recorded in the positions indicated by the points on the brain scheme (left).

LOT is a bundle of fibers which in turns receives inputs from the olfactory bulbs (OB) and give rise to a series of collaterals. LOT fibers spread across the entire surface of the tubercle (Carriero G., 2009), the piriform cortex, the entorhinal cortex itself and other areas associated with amygdala. Due to the GABAergic inhibitory system

previously described, it was not possible to elicit any response from the PRC area 36 after LOT stimulation. The electrophysiological study of different patterns of propagation from the neocortex to the EC is explained by analyzing the associative cortico-cortical interactions between the rhinal/peri-rhinal cortices of the guinea pig.

The field potential response elicited in the anterior PC (1.APC in Fig. 11) is mediated by a large monosynaptic response appearing with a 8/10 sec delay followed by a polysynaptic population spike activation. The monosynaptic connections are maintained also in the l-EC (LERC 2 and 3 in Fig.11). It is of immediate notice that the hippocampus activation (DG and CA1 number 6 and 7 in Fig.11) precedes the m-EC (MERC number 4 and 5 in Fig.11) field potential response. Electrophysiology experiments performed both with either optical imaging (Biella et al., 2003) or multielectrode techniques (Gnatkovsky et al., 2004), demonstrated that the delayed hippocampus-mediated response was restricted to the caudal and medial part of the EC and was not observed in the lateral/rostral EC.

To demonstrate that delayed responses are not mediated by intra-EC associative fibers a cut was made in the cortex to interrupt the connections between the two EC subfields. Simultaneous extracellular recording in m-EC and intracellular recording in a superficial m-EC neuron confirmed the persistence of the delayed responses after the disconnection between l-EC and m-EC. (see Fig. 12). Experimental findings suggest that, in conditions of normal excitability, the PRC-EC pathway is under the control of a powerful feedforward inhibition that regulates excitability within the PHR. It has been hypothesized that a breakdown of the inhibition that characterizes the interactions between the PRC and the EC, for example after the administration of GABAergic antagonists, may initiate hyperexcitability phenomena

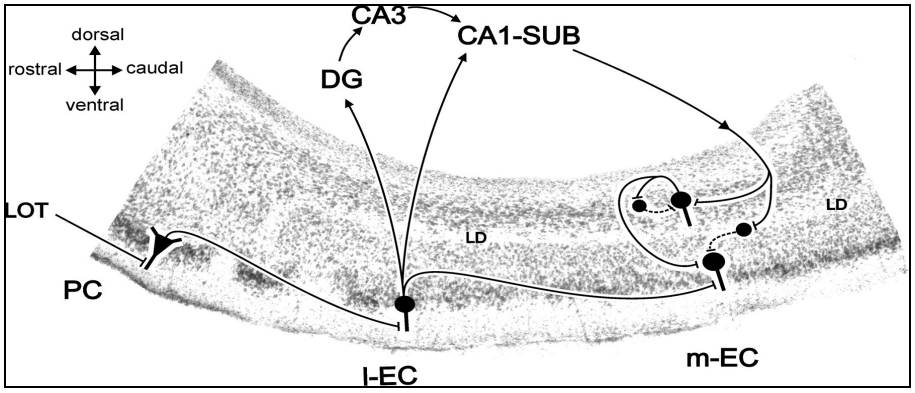

Fig. 12. Hypothetical networks activated by the LOT-evoked hippocampal input into the m-EC. Excitatory and inhibitory pathways are illustrated by continuous and dotted lines. (form Gnatkovsky V., 2006)

that promote limbic epileptogenesis. After these experimental indications, the focus of the clinical studies on human TLE shifted from the hippocampus proper to the EC-PRC interactions.

Intracellular recordings performed on the superficial neurons of layer II in the EC together with LOT stimulation of the afferent fibers, dmeonstrated an absolute wall of inhibition between the EC and the PRC, that do no receive any connection with this brain area. This findings were also confirmed by the fact that there was no depth reversal in field potential when reocrded with 16-channel silicon probes. CSD analysis of the same laminar profile did not show local sinks–sources, confirming that the potential is not generated locally.

Application of local bicuculline transiently abolished the GABA inhibitory network, so that after stimulation the EC-PRC connections can be activated.

References of Chapter 1 and 2

Annegers JF. The risk of unprovoked seizures after encephalitis and meningitis. Neurology. 1988; 38: 1407–1410

Avoli M, D'antuono M, Louvel J, et al. Network and pharmacological mechanisms leading to epileptiform synchronization in the limbic system in vitro. Prog Neurobiol 2002;68:167–207.

Bartolomei F, Wendling F, Regis J, Gavareta M, Guye M, Chauvel P. Pre-ictal synchronicity in limbic networks of mesial temporal lobe epilepsy Epilepsy Research 61 (2004) 89–104.

Beghi E. The concept of the epilepsy syndrome: How useful is it in clinical practice? Epilepsia, 2009 50(Suppl. 5): 4–10.

Biella G, Forti M and de Curtis M. Propagation of epileptiform potentials in the guinea-pig piriform cortex is sustained by associative fibres Epilepsy Research 24 (1996) 137-146.

Biella G, Uva L and de Curtis M. Propagation of Neuronal Activity along the Neocortical–Perirhinal–Entorhinal Pathway in the guinea Pig The Journal of Neuroscience, November 15, 2002, 22(22):9972–9979

Biella G, Uva L, Hofmann UG and De Curtis M. Associative Interactions Within the Superficial Layers of the entorhinal Cortex of the Guinea Pig J Neurophysiol 88:1159-1165, 2002.

Biella GR, Gnatkovsky V,Takashima I, Kajiwara R,Iijima T and de Curtis M. Olfactory input to the parahippocampal region of the isolated guinea pig brain reveals weak entorhinal-to-perirhinal interactions European Journal of Neuroscience, Vol. 18, pp. 95–101, 2003

Carriero G, Uva L, Gnatkovsky V, Avoli M, de Curtis M. Independent epileptiform discharge patterns in the olfactory and limbic areas of the in vitro isolated guinea pig brain during 4-aminopyridine treatment. J Neurophysiol. 2010

Carriero G, Uva L, Gnatkovsky V, de Curtis M. Distribution of the olfactory fiber input into the olfactory tubercle of the in vitro isolated guinea pig brain. J Neurophysiol. 2009 Mar;101(3):1613-9.

D'Ambrosio R and Perucca E. Epilepsy after head injury Current Opinion in Neurology 2004, 17:731–735.

de Curtis M, Gnatkovsky V. Reevaluating the mechanisms of focal ictogenesis:The

role of low-voltage fast activity. Epilepsia. 2009 Dec;50(12):2514-25.

de Curtis M, Murashima Y, Sankar R. 9th Workshop on the Neurobiology of Epilepsy (WONOEP IX): the transition from the interictal to the ictal state (Teluk Nibong, Langkawi Island, Malaysia, July 4-7, 2007). Epilepsia. 2008 Aug;49(8):1475-9.

de Curtis M, Parè D. The rhinal cortices: a wall of inhibition between the neocortex and the hippocampus. Prog Neurobiol 2004;74:101–10.

de Curtis M. Induced and acquired epileptogenicity in animal models Chapter 81, in press

de Curtis M. Simultaneous investigation of the neuronal and vascular compartments in the guinea pig brain isolated in vitro. Brain Res Protoc 1998;3:221–8.

de Curtis M. The electrophysiology of the olfactory-hippocampal circuit in the isolated and perfused adult mammalian brain in vitro. Hippocampus 1991;1:341–54.

de Guzman P, Inaba Y, Baldelli E, de Curtis M, Biagini G, Avoli M. Network hyperexcitability within the deep layers of the pilocarpine-treated rat entorhinal cortex. J Physiol. 2008 Apr 1;586(7):1867-83.

Dugladze T. Impaired hippocampal rhythmogenesis in a mouse model of mesial temporal lobe epilepsy. Proc Natl Acad Sci U S A. 2007 Oct 30;104(44):17530-5

Engel J Jr. Intracerebral recordings: organization of the human epileptogenic region. J Clin Neurophysiol. 1993 Jan;10(1):90-8

Engel J Jr. Pathological findings underlying focal temporal lobe hypometabolism in partial epilepsy. Ann Neurol. 1982 Dec;12(6):518-28

Engel J Jr.Comparative localization of epileptic foci in partial epilepsy by PCT and EEG. Ann Neurol. 1982 Dec;12(6):529-37

Engel JJr Research on the human brain in an epilepsy surgery setting Epilepsy Research 32 (1998) 1–11

Gabriel S. Stimulus and potassium-induced epileptiform activity in the human dentate gyrus from patients with and without hippocampal sclerosis. J Neurosci. 2004 Nov 17;24(46):10416-30

Gnatkovsky V, Librizzi L, Trombin F, de Curtis M. Fast activity at seizure onset is mediated by inhibitory circuits in the entorhinal cortex in vitro. AnnNeurol. 2008 Dec;64(6):674-86.

Gnatkovsky V, Wendling F, de Curtis M. Cellular correlates of spontaneous periodic

events in the medial entorhinal cortex of the in vitro isolated guinea pig brain. Eur J Neurosci. 2007 Jul;26(2):302-11.

Gnatkovsky V. Topographic distribution of direct and hippocampus mediated entorhinal cortex activity evoked by olfactory tract stimulation. European Journal of Neuroscience, Vol. 20, pp. 1897–1905, 2004

ILAE Commission Report. Mesial Temporal Lobe Epilepsy with hippocampal sclerosis Epilepsia 45(6) 695-714, 2004

Jauch R. Effects of barium, furosemide, ouabaine and 4,4'-diisothiocyanatostilbene-2,2'-disulfonic acid (DIDS) on ionophoretically-induced changes in extracellular potassium concentration in hippocampal slices from rats and from patients with epilepsy. Brain Res. 2002 Jan 18;925(1):18-27

Kwan P. Refractory seizures: Try additional antiepileptic drugs (after two have failed) or go directly to early surgery evaluation? Epilepsia, 50(Suppl. 8):57–62, 2009

Kwan P., Definition of refractory epilepsy: defining the indefinable? Lancet Neurol. 2010 Jan;9(1):27-9

Kwan P., Early identification of refractory epilepsy. N Engl J Med 2000;342:314-9.

Librizzi L. Epileptiform ictal discharges are prevented by periodic interictal spiking in the olfactory cortex. Ann Neurol 2003;53:382–9.

Linàs R. An electrophysiological study of the in vitro, perfused brain stem-cerebellum of adult guinea-pig. Journal of Physiology (1988), 404, pp. 215-240

Llinás R. Isolated mammalian brain in vitro: new technique for analysis of electrical activity of neuronal circuit function. Fed Proc. 1981 Jun;40(8):2240-5.

Muhlethaler M, de Curtis M, et al. The isolated and perfused brain of the guinea-pig in vitro. Eur J Neurosci 1993;5:915–26.

Pitkänen A. Animal Models of Post-Traumatic Epilepsy Journal of Neurotrauma 2006 Vol 23, Num 2.

Sander JW. The epidemiology of epilepsy revisited. Curr Opin Neurol. 2003 Apr;16(2):165-70.

Scorza FA. The pilocarpine model of epilepsy: what have we learned? An Acad Bras Cienc. 2009 Sep;81(3):345-65.

Shorovon S. Uncommon causes of status epilepticus Epilepsia, 2009; 50(Suppl. 12):61–63

Uva L, Avoli M, de Curtis M. Synchronous GABA-receptor-dependent potentials in

limbic areas of the in-vitro isolated adult guinea pig brain. Eur J Neurosci.2009 Mar;29(5):911-20.

Uva L. Propagation dynamics of epileptiform activity acutely induced by bicuculline in the hippocampal–parahippocampal region of the isolated guinea pig brain Epilepsia, 46(12):1914–1925, 2005

Uva L.and de Curtis M. Polysynaptic olfactory pathway to the ipsi and contralateral entorhinal cortex mediated via the hippocampus. Neuroscience 2005;130:249–58.

Wendling F, Bartolomei F, Bellanger JJ and Chauvel P Epileptic fast activity can be explained by a model of impaired GABAergic dendritic inhibition. European Journal of Neuroscience, Vol. 15, pp. 1499±1508, 2002

Chapter 3

Research Article **Annals of Neurology** 2008 Dec;64(6):674-86

Inhibitory networks support fast activity at seizure onset in the entorhinal cortex of the in vitro isolated guinea pig brain

Vadym Gnatkovsky, MD PhD, Laura Librizzi, PhD, Federica Trombin and Marco de Curtis, MD

Abstract

Objective. The cellular and network mechanisms responsible for the initiation of focal seizures are still largely unknown. Intracranial neurophysiological data from epileptic patients demonstrated that distinctive discharge patterns are generated at seizure onset in specific cortical areas. One of the prevalent seizure pattern observed in mesial temporal lobe epilepsy is characterized by fast activity at 20-30 Hz. We reproduced 20-30 Hz activity at seizure onset in the temporal lobe of the in vitro isolated guinea pig brain, to study cellular and network mechanisms involved in its generation.

Methods. Seizure-like activity was induced in the in vitro isolated guinea pig brain by brief (3 minutes) arterial perfusion of 50 μM bicuculline. Intra, extracellular and ion-selective electrophysiological recordings were performed simultaneously in the entorhinal cortex (EC) during interictal-ictal transition.

Results. Principal neurons in deep and superficial layers of the EC did not generate APs during fast activity at ictal onset, whereas sustained firing was observed in putative interneurons. Within 5-10 seconds from seizure onset principal neurons generated a prominent

firing, that correlated with the appearance of extracellular hypersynchronous bursting discharges. In superficial EC neurons, fast activity correlated with rhythmic inhibitory potentials superimposed to a slow depolarization that developed concurrently with an increase in extracellular potassium, [K]o. The gradual amplitude decrease of rhythmic inhibitory potentials during the [K]o rise suggest that the furtherance of the ictal discharge is promoted by a potassium-dependent change in reversal potential of inhibitory activity.

Interpretation. In an acute model of temporal lobe ictogenesis, sustained inhibition without firing of principal neurons correlates with the onset of a focal seizure. These findings contribute to understand the mechanisms of seizure onset in human temporal lobe epilepsy.

The treatment of epilepsies depends on how effectively drugs control seizure onset and propagation. New strategies to cure epilepsy will benefit directly from the identification of the mechanisms involved in the transition from the interictal to the ictal state, which, despite many studies, remains elusive. The most common surface EEG correlate of seizure onset in human focal epilepsies originating from the temporal lobe is the occurrence of small amplitude fast activity (EEG flattening) in the temporal region1;2. Such activity may evolve into large amplitude, rhythmic discharges that secondarely diffuse to adjacent cortical areas. Invasive pre-surgical studies with intracranial depth electrodes have been utilized to circumscribe the epileptogenic zone in patients suffering from mesial temporal lobe epilepsy (TLE) resistant to pharmacological treatment 3;4. Such invasive diagnostic procedure demonstrated that the ictal discharge associated to a temporal lobe seizure most often initiates with a sequence of fast activity at 20-30 Hz in the hippocampus and in the parahippocampal region 1;5-12. Even though alternative ictal onset patterns were

described 8;13;14, it has been proposed that fast 20-30 Hz activity has the highest localizing value for the identification of the temporal epileptogenic region 6;11;15.

Network and cellular mechanisms associated with the generation of fast, small amplitude cortical activity in the beta-gamma range that initiates a seizure in the mesial temporal lobe are not clearly identified yet. Seizure-like fast ictal discharges in mesial temporal lobe structures can be experimentally reproduced in animal models of seizures 16. Ictogenesis was reliably induced in the temporal lobe of the in vitro isolated guinea pig brain preparation 17;18 by acute and transient disinhibition with the GABAa receptor antagonist, bicuculline 19;20. We utilize this procedure to study network mechanisms that regulate the generation of 20-30 Hz activity at seizure onset in the EC of the in vitro isolated guinea pig brain. We focused on the EC, since this temporal lobe region is primarely involved in seizure generation in humans 9;10 and in experimental models of temporal lobe epilepsy and seizures 19;21-24. The study demonstrates for the first time that seizure onset in the EC is associated to a complete interruption of neuronal firing in principal neurons and is supported by the activation of inhibitory network.

Methods

guinea pig brains were isolated in vitro according to the previously described procedure 17;18. Following barbiturate anesthesia (80 mg/kg sodium thiopental, i.p.), intracardiac perfusion with cold (15°C) saline solution (see below) was performed for 3 minutes to reduce brain temperature during dissection. The entire brain was isolated and transferred to a perfusion chamber. A poliethylene cannula was inserted in the basilar artery to restore brain perfusion with a solution

composed by NaCl, 126 mM, KCl, 3 mM, KH2PO4, 1.2 mM, MgSO4, 1.3 mM, CaCl2, 2.4 mM, NaHCO3, 26 mM, glucose, 15 mM and 3% dextran M.W. 70.000, oxygenated with a 95% O2-5% CO2 gas mixture (pH 7.3). Experiments were performed at 32°C. The experimental protocol was reviewed and approved by the Committee on Animal Care and Use and by the Ethics Committee of the Istituto Nazionale Neurologico, in accordance with National and International guidelines on care and use of laboratory animals.

Extracellular recordings were performed with glass pipettes filled with 0.9M NaCl (2-5 MOhm resistance). Intracellular recordings were performed with sharp electrodes filled with 3M potassium acetate and 2% biocytine (60-120 MOhm input resistance). Electrophysiological signals were amplified via a multichannel differential amplifier (Biomedical Engineering, Thornwood, NY) and an intracellular amplifier (Neurodata. New York, NY). Data were acquired and analyzed utilizing software developed by Dr. Vadym Gnatkovsky in our laboratory (ELPHOTM).

Ictal discharges in the EC were induced by brief (3 minutes) arterial perfusions with 50 μm of the GABAa receptor antagonist, bicuculline methiodide 19;20;;26 (Sigma-Aldrich, St.Louis, MO).

Recordings of extracellular potassium concentration ([K+]o) in EC were carried out as previously described 27. Briefly, ion-selective electrodes (tip diameter 3-5 μm) were filled with the potassium ionophore I cocktail A (Fluka 60031,Germany). Absolute [K+]o values were calculated by solving the equation y= a + b logx, were x is the [K+]o, y is the measured voltage reading induced by the changes in [K+]o and a + b is the slope coefficient derived from the calibration curve performed for each K+-sensitive electrode (calibration solutions with K+ concentrations of 1, 1.5, 6, 12.5 and 48

mM). Only electrodes with a response of 30-40 mV for 10 mM of K+ were utilized. Ion-selective signals were amplified with a high-input impedance head-stage amplifier (Biomedical Engineering, Thornwood, NY) and field potential values were subtracted.

Principal neurons and putative interneurons in layers II-III (n=24) and in layers V-VI (n=6) were identified on the basis of their response to the hippocampal input driven by stimulation of the olfactory area 28. Thirteen out of 27 principal cells were further identified morphologically as stellate or pyramidal cells. At the end of the electrophysiological experiment, brains were fixed in 4% paraformaldheide and the standard protocol to reveal neurons injected with biocytine was utilized biocytin-horseradish peroxydase visualization (ABC kit, Vector Laboratories, Burlingame, CA). Sections were counterstained with thionine to identify cortical layers.

Results

Seizure-like activity correlates with transient and partial EC disinhibition. Seizure-like, ictal activity was reliably induced in the medial EC of the in vitro isolated guinea pig brain by a brief (3 minutes) arterial perfusion with bicuculline methiodide (50 μM). Only experiments in which ictal activity initiated with fast activity at 20-30 Hz (Figure 1a; 27 out of 32 tests) were selected for the present study. Five seconds (4,73 ± 0,85 sec; mean ±SD) after fast ictal onset, bursts of high-amplitude potentials appeared and progressively increased with time in amplitude, regularity and duration (Figure 1b and c). Seizure-like discharges lasted 8,4 ± 1,4 min (mean ±SD) and were followed by post-ictal depression, characterized by a decrease in the global activity content measured by signal frequency analysis (lower panel in Figure 1). As previously demonstrated 19, large amplitude

interictal spike could be observed ahead of an ictal discharge (see Figures 1 and 4). In the present study we focus on the characterization of intrinsic networks that generated fast 20-30 Hz activity by recordings different types of neurons in the seizure onset zone in the medial EC.

Three-minute perfusions of bicuculline induced transient and partial dysinhibition of the isolated brain, as demonstrated by paired-pulse test 29. The depression of the conditioned responses evoked by paired stimulation of the lateral olfactory tract (LOT) were analyzed in the piriform cortex (PC) and in the lateral EC, a region bordering the seizure onset area in the medial EC that receives a direct olfactory input 19 (see scheme in Figure 2A). In control solutions, pairing with 25 msec inter-stimulus interval determined a ~60-65 % inhibition of the conditioned disynaptic responses recorded in both PC and lateral EC (filled circles in Figure 2A and B; n=12), measured as the difference between the amplitude of the disynaptic response to a single stimulus (a) and the amplitude of the subtracted disynaptic paired response, b-a (Figure 2A and B). The pairing test was repeated every 10 seconds and the time course of the changes in inhibition efficacy were evaluated during bicuculline arterial perfusion (Figure 2C). At seizure onset in the medial EC (marked by arrows) measurements of inhibition efficacy were reduced by 8% and 34% in the PC and in the lateral EC, respectively (n=12). We conclude that the efficacy of inhibitory circuits is only partially reduced in the isolated brain preparation when EC seizure initiate. An abrupt and more robust reduction of inhibition efficacy was observed during the bursting phase of the ictal discharge and after the seizure.

Cellular correlates of fast activity at ictal onset: superfial EC neurons. Stellate and pyramidal neurons in the supeficial layers II and III of the medial EC were characterized by electrophysiological and morphological features, as previously reported 28;30. In correlation with the appearance of fast activity at seizure onset, superficial layers principal cells did not generate action potential firing. If the cell was depolarized above firing threshold, as show in Figure 3A, neuronal firing ceased and subthreshold rhythmic potentials appeared in correlation with the extracellular fast oscillation (thin arrows in Figure 3Aa). The frequency of the small amplitude intracellular potentials (left panel) and of the simultaneously recorded extracellular fast activity (right panel) are illustrated in Figure 3B. Average frequency power of fast activity in superficial neurons and the corresponding extracellular signals are respectively illustrated in the left and right panels in Figure 3C (n=17). Mean correlation values calculated between pairs of intracellular and extracellular recordings during fast activity was 0,63 ± 0,11 (n=17).

During fast activity, membrane potential showed an abrupt hyperpolarization (arrowhead) followed by a slow depolarization (see below). In coincidence with the frammentation of fast activity, erratic firing resumed in superficial neurons in parallel with the emergence of irregular bursting in the extracellular trace (Figure 3Ab). Within a few seconds, bursts of action potentials superimposed on paroxysmal depolarizing shift appeared in coincidence with the occurrence of regular bursts in the extracellular trace (Figure 3Ac). These bursts and their extracellular correlates became progressively more robust and less frequent (Figure 3Ad) and were followed by post-ictal depression. To better analyze the intracellular correlates of fast activity at seizure onset, seizures were induced when the membrane potential of neurons

was hyperpolarized/depolarized by injection of steady current via the intracellular recording electrode. When the membrane potential of the recorded neuron was hyperpolarized, no spontaneous firing was observed before bicuculline perfusion (Figure 4Ab). In these conditions, the fast rhythms observed at seizure onset correlated with depolarizing potentials and often triggered a potential similar to that observed during a pre-ictal spike (see below and Figure 7). The amplitude of the fast potentials progressively decreased, while membrane potential slowly depolarized (Figure 4Ab). When membrane potential was depolarized to values more positive than -55 mV, fast potentials at seizure onset were hyperpolarizing (Figure 4Bb); rebound spikes could be generated at the break of each fast hyperpolarizing potential. The polarity of the fast activity deflection matched the polarity of the inhibitory postsynaptic potential (IPSP) evoked by LOT stimulation 31 recorded just before seizure onset (n=20; Figure 4Aa and Ba); it was depolarizing for membrane potentials more negative than -65 mV (n=5) and hyporpolarizing when the membrane potential was depolarized to values positive to -60 mV (n=15). In all experiments the ictal discharge was preceeded by interictal spikes (arrows in Figures 4A and B). Pre-ictal spikes correlated with a membrane potential deflection that showed the same reversal of LOT-evoked IPSPs (Figure 4Ab; see also Figure 7). Based on these evidences, we conclude that the intracellular correlates of both pre-ictal spikes and repetitive small amplitude potentials coupled with the extracellular fast activity are IPSPs. These data also confirmed that synaptic inhibition is preserved at seizure onset induced by brief bicuculline perfusion (see Discussion).

Cellular correlates of fast activity at ictal onset: deep EC neurons. In principle, ictal fast activity could be generated by neurons located in deep layers of the medial EC. Intracellular recordings from layer V-VI principal cells identified on the basis of previously described electrophysiological features 28;30 demonstrated that these neurons do not generate neuronal firing at seizure onset. In correlation with the extracellular fast activity they showed an abrupt a step-like membrane hyperpolarization (Figure 5a), followed by a slow depolarization that lasted 5-10 seconds. To reveal the prevalent inhibitory correlate at ictal onset, the membrane potential of the deep neurons was depolarized by a steady positive current injected via the intracellular pipette, as shown in the representative neuron illustrated in Figure 5. Unlike superficial neurons, no fast inhibitory potentials were observed in deep principal cells (n=6). Neuronal firing re-appeared in deep neurons during the extracellular afterdischarges that developed later on during the seizure (Figure 5b and c; n=6).

We conclude that, as for superficial principal neurons, firing activity was dampened in deep layer EC principal cells in temporal correlation with the appearance of fast activity at seizure onset. Moreover, all recorded neurons were transiently hyperpolarized at during fast activity.

Cellular correlates of fast activity at ictal onset: putative EC interneurons. Finally, we recorded from 10 cells in supericial EC layers identified as putative interneurons on the basis of the previoulsy described electrophysiological criteria28: 1) generation of fast burst firing in response to LOT stimulation, 2) generation of non adapting firing at > 100 Hz both during spontaneous depolarizing events that occur in the up-state and in response to the intracellular injection of a

suprathreshold depolarizing current pulse. Three of these putative interneurons were recorded for 10 minutes before bicuculline application and during the initiation of a seizure. As illustrated in Figure 6, putative interneurons generated a barrage of high frequency action potentials at >150 Hz either at the onset (Figure 6A) or few milliseconds ahead of the ictal initiation (Figure 6A). Continuous firing gradually evolved into phasic bursting that gradually became time locked with the extracellular discharge pattern (Figure 6Ab).

Pre-ictal spikes in different types of EC neurons. Overall, the intracellular findings demonstrate that putative interneurons generate firing during fast activity at seizure onset, whereas principal neurons in all EC layers are silent. To further analyze the role of inhibitory EC circuits during the transition to the ictal state, we evaluated the intracellular correlates of the pre-ictal spikes that occur 30 second ahead of the initiation of the seizure-like discharge. Figure 7 shows representative examples of intracellular recordings from principal neurons in superficial and deep layers and from putative interneurons during the pre-ictal spikes (right traces) and during responses evoked by LOT stimulation in the pre-ictal state 30 (left traces). Superficial principal cells (n=17) generated a direct IPSP in response to LOT stimulation (upper panel in Figure 7) and a negative potential with time course and membrane reversal similar to the evoked IPSP in correspondence to a pre-ictal spike. Also deep principal neurons generated a pronounced hyperpolarizing potential both during the preictal spike and in response to LOT stimulation (middle panel in Figure 7). Unlike principal neurons, the correlate of pre-ictal spikes in the 3 putative interneurons was a marked bursting discharge (lower right traces in Figure 7). A similar bursting response was also

observed in response to LOT stimulation (lower left traces). These findings confirm that in the medial EC inhibition is preserved in the pre-ictal state, just ahead of seizure discharge.

Extracellular potassium changes during fast activity at ictal onset. Finally, we investigated the mechanisms that promote the gradual switch from fast activity to bursting discharges during the ictal event. Extracellular field recordings and intracellular recordings from superficial principal neurons were performed in close proximity to a two-barrel electrode that recorded extracellular potassium changes, [K+]o, during a seizure (Figure 8). [K+]o gradually increased with the appearance of fast 20-30 Hz activity, while the superficial cell was still silent. The elevation in [K+]o was closely paralleled by membrane potential depolarization of the neuron and correlated with the slow downward shift in the extracellular trace. When both [K+]o and slow membrane depolarization reached a plateau value, irregular firing initiated both in the intracellular and extracellular recordings (upper panel in Figure 8A). The time course of the membrane potential depolarization, the [K+]o increase and the gradual decrease in amplitude of the inhibitory potential associated to the fast activity are shown in the expanded traces in the lower panel of Figure 8A. The IPSPs associated to the fast activity progressively decreased in amplitude in parallel with membrane depolarization and [K+]o increase (traces a, b and c in the right panel). Correlation data obtained in 3 experiments performed with the same protocol are illustrated in the graphs in Figure 8B. Finally, the plot of the IPSP amplitude as a function of the changes in [K+]o is illustrated for the 3 neurons in Figure 8C.

Discussion

We demonstrate that transient and partial disinhibition of an in vitro isolated guinea pig brain induces in the medial EC seizure-like discharges that initiate with 20-30 Hz oscillations. Such fast activity correlated with i) no firing in principal neurons of superficial and deep layers, ii) sustained firing in putative interneurons, iii) fast IPSPs at 20-30 Hz in superficial principal neurons and iv) a slow [K+]o rise associated with a progressive decrease of fast IPSPs in superficial neurons. Few seconds after the onset of fast activity, the ictal discharge procedes with the appearance of erratic bursting that becomes more regular with time and gradually cease within 10 minutes. As expected after a seizure, post-ictal depression was consistently demonstrated by signal frequency analysis. The mechanisms of ictal onset generation is the main focus of the present study.

Simulation studies based on intracranial recordings from human hippocampus and EC proposed that epileptic fast activity at 20-30 Hz can be explained by a transient and partial GABAergic impairment 15;32. This hypothesis was recently confirmed by reproducing in a computer model of the EC the seizure patterns observed in the isolated guinea pig brain with the experimental protocol utilized in the present study 33. We demonstrate now that in this model, indeed, 3-minutes arterial perfusion of bicuculline induced a moderate reduction of GABAergic transmission that result in a paradox transitory reinforcement of inhibitory netwoks. By evaluating paired-pulse depression of polisynaptic activity we observed a reduction of 8% and 34% in the efficacy of inhibition at the time of seizure onset in the EC and in the PC, respectively, where depression of disynaptic inhibitory recurrent circuits could be accurately analyzed 34.

Intracellular recordings demonstrated that inhibition prevail when seizures initiate and in the pre-ictal state. In principal neurons of the EC seizures start out with an abrupt membrane potential hyperpolarization that coincided with robust firing in putative interneurons. Moreover, we observed that interictal spikes recorded during the 30 seconds that precede a seizure (pre-ictal spikes) correlated with an inhibitory potential in superficial neurons and a burst discharge in putative interneurons. Since these responses were similar to those responsible for the generation of GABAa receptor dependent IPSPs evoked in normal excitability conditions by LOT stimulation 30, we propose that the intracellular correlates of the pre-ictal spikes and the abrupt hyperpolarization at seizure onset are mediated by GABAergic inhibition. We conclude that the transition from interictal to ictal in EC is promoted by synchronous inhibitory events. Avoli and coworkers demonstrated that in hippocampal and EC slices in vitro 35-37 the initiation of an ictal discharge induced by either 4-aminopyridine or low-magnesium solution correlates with the generation of a large amplitude depolarizing GABAa-receptor mediated potential that lasts circa 1 second 38. The inhibitory responses observed in our experiments retain the classical features of an IPSP (short duration and hyperpolarizing in nature), suggesting that the mechanisms of ictal generation in the 4-AP and low-Mg2+ slice models and in the isolated brain preparation may be different. Moreover, unlike EC slice studies, principal EC neurons in our experiments do not generate firing in the early phases of the ictal discharge and, therefore, cannot be responsible for seizure onset. The sustained firing was observed in the imminence of a seizure in the limited number of putative interneurons recorded in our close-to-in-vivo condition suggest that a paradox reinforcement of inhibition

associated to seizure initiation may be enforced by a prevalent reciprocal release of inhibition between inhibitory neurons induced by bicuculline.

Long sequences (circa 5 sec) of fast activity at 20-30 Hz was consistently observed in superficial EC neurons (but not in deep neurons) during the initial phase of the ictal discharge. These oscillations showed a membrane potential reversal similar to the LOT-evoked IPSP (see also 30 and should therefore be considered as fast inhibitory synaptic potentials. What is the source of such activity? We recently demonstrated that the hippocampal output generates direct IPSPs into the superfical neurons of the medial EC, via a feedforward inhibition mediated by EC interneurons located in superficial layers 30. According to this hypothesis, we propose that the 20-30 Hz oscillations in superficial neurons are generated by feedforward inhibition derived from fast activity that originates in the hippocampus, possibly in CA1 and subiculum. A more detailed simultaneous intracellular analysis of hippocampal and superficial medial EC neurons will allow to test this hypothesis. If this will prove to be the case, seizure activity in the medial EC may be considered to be secondary to hippocampal activation. Yet, the mechanisms by which seizures are generated within the medial EC rely on the reinforcement of activity in local inhibitory circuits.

Fast activities at 20-80 Hz recorded in vivo 39;40 or in vitro either by tetanic stimulation 41;42 or by pharmacological manipulation in the hippocampus 43-45 and in the EC 46;47 are sustained by reciprocal interactions between inhibitory and excitatory networks, with a prevalent role played by the synchronous activation of networks of interconnected interneurons 43. Fast oscillations in the beta-gamma band were also observed during seizure-like activities induced in the

hippocampus in vitro by either tetanic stimulation 48;49 and by double pulse stimulation in EC slices of chronic epileptic rats 50. It has been proposed that these oscillations may arise from excitatory GABAergic depolarizing potentials 48 mediated by hyper-synchronization of GABAergic interneuronal networks 49;51. Brief runs of ultra-fast activity (200-600 Hz), denominated fast ripples, were observed in the hippocampus and in the parahippocampal cortex of patients affected by TLE either in coincidence with an interictal spike or in isolation 52;53, but were never observed during a seizure. Fast ripples can be reproduced in chronic animal models of TLE 54 and were proposed to be generated by the synchronous activation of clusters of highly interconnected neurons capable of overcoming interneuron feedback inhibition. No direct relationship between fast ripples and the 20-30 Hz epileptiform activity has been reported. Therefore, these two patterns of fast activity associated with temporal lobe epileptic conditions are probably mediated by different mechanisms.

If interneuron activation is the prevalent event at seizure onset, what are the mechanisms that promote the transition from seizure onset into the massive and highly synchronous bursting typically observed during the advanced phase of an ictal event? Gradual inactivation of inhibitory potentials mediated by extracellular ion changes may be the main factor. In our experimental conditions, interneurons may contribute to ictal transition by generating pronounced bursting just ahead of and at the onset of seizures. This interneuronal hyperactivity occurs in the absence of principal neuron activation, and is probably responsible for the large extracellular potassium changes observed in our experiments 36. At the onset of a seizure-like event, the increase in [K+]o correlated with membrane potential depolarization and a

gradual decrease in fast IPSP amplitude in layer II-III principal neurons. This suggests the possibility that the reversal potential for the fast IPSPs may gradually change because of the potassium changes. A depolarizing shift in the reversal potential of the GABAa-receptor mediated chloride current is expected, indeed, when [K+]o increases 55. When GABAa reversal depolarizes above resting membrane potential, the inhibitory efficacy diminishes, chloride conductance becomes inward and GABAa receptor activation may turn into excitatory 31. This sequence of events could restore neuronal firing in principal neurons and may favour neuronal hypersynchronization, therefore promoting synchronous bursting discharges and the progression of seizure activity.

Acknowledgements

MdC supervised the research project and, in collaboration with VG, designed the experiments that were performed by VG and FT (simultaneous intra-extracellular recordings) and LL (ion-selective recordings). Data analysis was carried out by VG, LL and FT. All authors discussed the results and commented on the manuscript. MdC and VG co-wrote the paper. The study was supported by the Italian Health Ministry (Ricerca Corrente e Ricerca Finalizzata RF 64) and by the Mariani Foundation (grant n. R06-50).

References

1. Lieb JP, Walsh GO, Babb TL. A comparison of EEG seizure patterns recorded with surface and depth eleectrodes in patients with temporal lobe epilepsy. Epilepsia 1976; 17: 137-160.
2. Quesney LF, Gloor P. Localization of epileptic foci. Electroencephalogr Clin Neurophysiol Suppl 1985; 37: 165-200.

3. Engel JJ, Rausch R, Lieb JP, Kuhl DE, Crandall PH. Correlation of criteria used for localizing epileptic foci in patients considered for surgical therapy of epilepsy. Ann Neurol 1981; 9: 215-24.
4. Bancaud J, Angelergues R, Bernouilli C et al. [Functional stereotaxic exploration (stereo-electroencephalography) in epilepsies]. Rev Neurol (Paris) 1969; 120: 448.
5. Fisher RS, Webber WR, Lesser RP, Arroyo S, Uematsu S. High-frequency EEG activity at the start of seizures. J Clin Neurophysiol 1992; 9: 441-8.
6. Gotman J, Levtova V, Olivier A. Frequency of the electroencephalographic discharge in seizures of focal and widespread onset in intracerebral recordings. Epilepsia 1995; 36: 697-703.
7. Cendes F, Dubeau F, Andermann F et al. Significance of mesial temporal atrophy in relation to intracranial ictal and interictal stereo EEG abnormalities. Brain 1996; 119: 1317-26.
8. Pacia SV, Ebersole JS. Intracranial EEG in temporal lobe epilepsy. J Clin Neurophysiol 1999; 16: 399-407.
9. Spencer SS, Spencer DD. Entorhinal-hippocampal interactions in medial temporal lobe epilepsy. Epilepsia 1994; 35: 721-7.
10. Bartolomei F, Khalil M, Wendling F et al. Entorhinal cortex involvement in human mesial temporal lobe epilepsy: an electrophysiologic and volumetric study. Epilepsia 2005; 46: 677-87.
11. Bartolomei F, Wendling F, Vignal JP et al. Seizures of temporal lobe epilepsy: identification of subtypes by coherence analysis using stereo-electro-encephalography. Clin Neurophysiol 1999; 110: 1741-54.
12. Kahane P, Chabardes S, Minotti L, Hoffmann D, Benabid AL, Munari C. The role of the temporal pole in the genesis of temporal lobe seizures. Epileptic Disord 2002; 4 Suppl 1: S51-8.
13. Mintzer S, Cendes F, Soss J et al. Unilateral hippocampal sclerosis with contralateral temporal scalp ictal onset. Epilepsia 2004; 45: 792-802.
14. Spencer SS, Kim J, Spencer DD. Ictal spikes: a marker of specific hippocampal cell loss. Electroencephalogr Clin Neurophysiol 1992; 83: 104-11.
15. Wendling F, Bartolomei F, Bellanger JJ, Chauvel P. Epileptic fast activity can be explained by a model of impaired GABAergic dendritic inhibition. Eur J Neurosci 2002; 15: 1499-508.

16. Avoli M, D'Antuono M, Louvel J et al. Network pharmachological mechanisms leading to epileptiform synchronization in the limbic system in vitro. Progr Neurobiol 2002; 68: 167-207.
17. Muhlethaler M, de Curtis M, Walton K, Llinas R. The isolated and perfused brain of the guinea-pig in vitro. Eur J Neurosci 1993; 5: 915-26.
18. de Curtis M, Biella G, Buccellati C, Folco G. Simultaneous investigation of the neuronal and vascular compartments in the guinea pig brain isolated in vitro. Brain Res Protoc 1998; 3: 221-8.
19. Uva L, Librizzi L, Wendling F, de Curtis M. Propagation dynamics of epileptiform activity acutely induced by bicuculline in the hippocampal-parahippocampal region of the isolated guinea pig brain. Epilepsia 2005; 46: 1914-25.
20. Librizzi L, de Curtis M. Epileptiform ictal discharges are prevented by periodic interictal spiking in the olfactory cortex. Ann Neurol 2003; 53: 382-9.
21. Avoli M, D'Antuono M, Louvel J et al. Network and pharmacological mechanisms leading to epileptiform synchronization in the limbic system in vitro. Prog Neurobiol 2002; 68: 167-207.
22. Bragin A, Csicsvari J, Penttonen M, Buzsaki G. Epileptic afterdischarge in the hippocampal-entorhinal system: Current source density and unit studies. Neurosci 1997; 76: 1187-1203.
23. Pare D, deCurtis M, Llinas R. Role of the hippocampal-entorhinal loop in temporal lobe epilepsy: extra- and intracellular study in the isolated guinea pig brain in vitro. J Neurosci 1992; 12: 1867-81.
24. Wozny C, Gabriel S, Jandova K, Schulze K, Heinemann U, Behr J. Entorhinal cortex entrains epileptiform activity in CA1 in pilocarpine-treated rats. Neurobiol Dis 2005; 19: 451-60.
25. Forti M, Biella G, Caccia S, de Curtis M. Persistent excitability changes in the piriform cortex of the isolated guinea-pig brain after transient exposure to bicuculline. European J Neurosci 1997; 9: 435-51.
26. de Curtis M, Manfridi A, Biella G. Activity-dependent pH shifts and periodic recurrence of spontaneous interictal spikes in a model of focal epileptogenesis. J Neurosci 1998; 18: 7543-51.
27. Librizzi L, Janigro D, De Biasi S, de Curtis M. Blood-brain barrier preservation in the in vitro isolated guinea pig brain preparation. J Neurosci Res 2001; 66: 289-97.

28. Gnatkovsky V, Wendling F, de Curtis M. Cellular correlates of spontaneous periodic events in the medial entorhinal cortex of the in vitro isolated guinea pig brain. Eur J Neurosci 2007; 26: 302-311.
29. Dunwiddie TV, Worth TS, Olsen RW. Facilitation of recurrent inhibition in rat hippocampus by barbiturate and related nonbarbiturate depressant drugs. J Pharmacol Exp Ther 1986; 238: 564-75.
30. Gnatkovsky V, de Curtis M. Hippocampus-mediated activation of superficial and deep layer neurons in the medial entorhinal cortex of the isolated guinea pig brain. J Neurosci 2006; 26: 873-81.
31. Farrant M, Kaila K. The cellular, molecular and ionic basis of GABA(A) receptor signalling. Prog Brain Res 2007; 160: 59-87.
32. Wendling F, Hernandez A, Bellanger JJ, Chauvel P, Bartolomei F. Interictal to ictal transition in human temporal lobe epilepsy: insights from a computational model of intracerebral EEG. J Clin Neurophysiol 2005; 22: 343-56.
33. Labyt E, Uva L, de Curtis M, Wendling F. Realistic modeling of entorhinal cortex field potentials and interpretation of epileptic activity in the guinea pig isolated brain preparation. J Neurophysiol 2006; 96: 363-77.
34. Biella G, Panzica F, de Curtis M. Interactions between associative synaptic potentials in the piriform cortex of the in vitro isolated guinea pig brain. Eur J Neurosci 1996; 8: 1350-7.
35. Perrault P, Avoli M. 4-Aminopyridine-induced activity in hilar neurons in the guinea pig hippocampal slice. J Neurosci 1992; 12: 104-115.
36. Avoli M, Barbarosie M, Lücke A, Nagao T, Lopantsev V, Köhling R. Synchronous GABA-mediated potentials and epileptiform discharges in the rat limbic system in vitro. J Neurosci 1996; 16: 3912-24.
37. Lopantsev V, Avoli M. Laminar organization of epileptiform discharges in the rat entorhinal cortex in vitro. J Physiol 1998; 509: 785-96.
38. Lopantsev V, Avoli M. Participation of GABAA-mediated inhibition in ictallike discharges in the rat entorhinal cortex. J Neurophysiol 1998; 79: 352-60.
39. Chrobak JJ, Buzsáki G. Gamma oscillations in the entorhinal cortex of the freely behaving rat. J Neurosci 1998; 18: 388-98.
40. Csicsvari J, Jamieson B, Wise KD, Buzsaki G. Mechanisms of gamma oscillations in the hippocampus of the behaving rat. Neuron 2003; 37: 311-22.

41. Traub RD, Whittington MA, Buhl EH, Jefferys JG, Faulkner HJ. On the mechanism of the gamma --> beta frequency shift in neuronal oscillations induced in rat hippocampal slices by tetanic stimulation. J Neurosci 1999; 19: 1088-105.

42. Bracci E, Vreugdenhil M, Hack SP, Jefferys JGR. On the synchronizing mechanisms of tetanically induced hippocampal oscillations. J. Neurosci. 1999; 19: 8104-8113.

43. Traub RD, Jefferys JGR, Whittington MA. Fast Oscillations in Cortical Circuits. Cambridge: MIT Press, 1999.

44. Fisahn A, Pike FG, Buhl EH, Paulsen O. Cholinergic induction of network oscillations at 40 Hz in the hippocampus in vitro. Nature 1998; 394: 186-189.

45. Williams JH, Kauer JA. Properties of carcachol-induced oscillatory activity in the rat hippocampus. J Neurophysiol 1997; 78: 2631-2640.

46. van der Linden S, de Curtis M, Panzica F. Carbachol induces fast oscillations in the medial but not in the later entorhinal cortex of the isolated guinea pig brain. J Neurophysiol 1999; 82: 2441-2450.

47. Dickson CT, Biella G, de Curtis M. Evidence for spatial modules mediated by temporal synchronisation of carbachol induced gamma rhythm in medial entorhinal cortex. J Neurosci 2000; 20: 7846-7854.

48. Köhling R, Vreugdenhl M, Bracci E, Jefferys JGR. Ictal epileptiform activity is facilitated by hippocampal GABAA receptor-mediated oscillations. J Neurosci 2000; 20: 6820-6829.

49. Velazquez JLP, Carlen PL. Synchronization of GABAergic interneuronal networks during seizure-like actvity in the rat horizontal hippocampal slice. Eur J Neurosci 1999; 11: 4110-4118.

50. Tolner EA, Kloosterman F, Kalitzin SN, da Silva FH, Gorter JA. Physiological changes in chronic epileptic rats are prominent in superficial layers of the medial entorhinal area. Epilepsia 2005; 46 Suppl 5: 72-81.

51. Fujiwara-Tsukamoto Y, Isomura Y, Kaneda K, Takada M. Synaptic interactions between pyramidal cells and interneurone subtypes during seizure-like activity in the rat hippocampus. J Physiol 2004; 557: 961-79.

52. Bragin A, Wilson CL, Staba RJ, Reddick M, Fried I, Engel J Jr. Interictal high-frequency oscillations (80-500 Hz) in the human epileptic brain: entorhinal cortex. Ann Neurol 2002; 52: 407-15.

53. Staba RJ, Wilson CL, Bragin A, Fried I, Engel J Jr. Quantitative analysis of high-frequency oscillations (80-500 Hz) recorded in human epileptic hippocampus and entorhinal cortex. J Neurophysiol 2002; 88: 1743-52.

54. Bragin A, Engel J, Wison CL. Hippocampal and entorhinal cortex high-frequency oscillationss in human epileptic brain and kainic acid treated rats. Epilepsia 1999; 40: 127-137.

55. Thompson SM, Gahwiler BH. Activity-dependent disinhibition. II. Effects of extracellular potassium, furosemide, and membrane potential on ECl- in hippocampal CA3 neurons. J Neurophysiol 1989; 61: 512-23.

Figure 1 Extracellular recording of a typical ictal discharge in the medial EC induced by 3-minutes systemic perfusion of the isolated guinea pig brain with the GABAa receptor antagonist, bicuculline (50 μM). The fast activity at the onset of the ictal discharge is illustrated in the expanded trace in a. Irregular spiking followed by more regular bursting recorded during the seizure-like discharge at th indicated time points are also illustrated in b and c, respectively. The lower plot demonstrated the post-seizure depression: a marked reduction of the activity in all frequency ranges was observed after the seizure (black shading) in comparison to pre-ictal activity (gray shading).

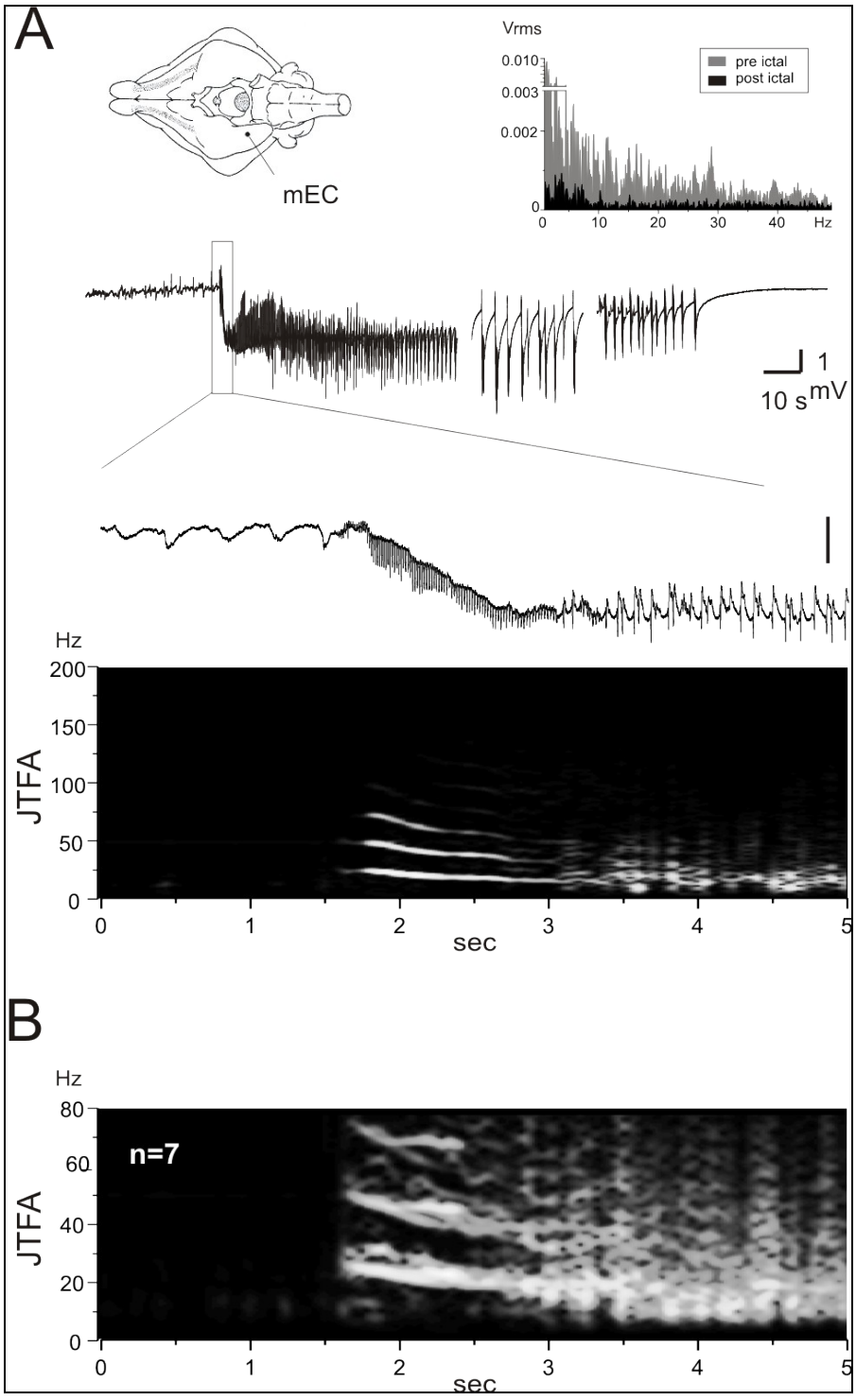
A
mEC
Vrms
0.010
0.003
0.002
0
pre ictal
post ictal
0
10
20
30
40
Hz
1
10 s
mV
Hz
200
150
100
50
0
JTFA
0
1
2
3
4
5
sec
B
Hz
80
60
40
20
0
n=7
JTFA
0
1
2
3
4
5
sec

Figure 2 Inhibition is partially preserved at the time of seizure onset in the limbic region of the isolated brain during 3-minutes arterial perfusion with 50 μM bicuculline methiodide. In the left panel in A, the position of the recording electrodes in the piriform cortex (PC) and in the medial and lateral entorhinal cortex (EC) and the position of the stimulating electrode on the lateral olfactory tract (LOT) are shown. Electrophysiological recordings were performed simultaneously at the three sites. Seizures recorded in the medial EC (but not in the lateral EC; Uva et al., 2006) was utilized to monitor ictal onset. On the right panel in A, the pairing test in the PC is shown: a) PC response to a single stimulus, characterized by a monosynaptic (asterisk) and a disynaptic potential (filled circle); b) PC response to a paired test with a 25 msec inter-stimulus interval. The reduction of the disynaptic component in the second response is evident in the subtracted trace b-a. B: The efficacy of inhibition was calculated by measuring the percentage reduction of the peak amplitude of the disynaptic component between the response evoked by a single stimulus (a) and the subtracted trace (b-a). Sample traces are illustrated for the PC (left) and the lateral EC(right). C: time course of average inhibition efficacy in the PC (left) and in the lateral EC (right) during the arterial perfusion of bicuculline (shaded area) in 12 experiments. Pairing tests were performed every 10 seconds. Seizure onset (recorded with the recording electrode in the medial EC) is marked by the arrow. Time values were normalized between experiments with reference to the time of seizure onset.

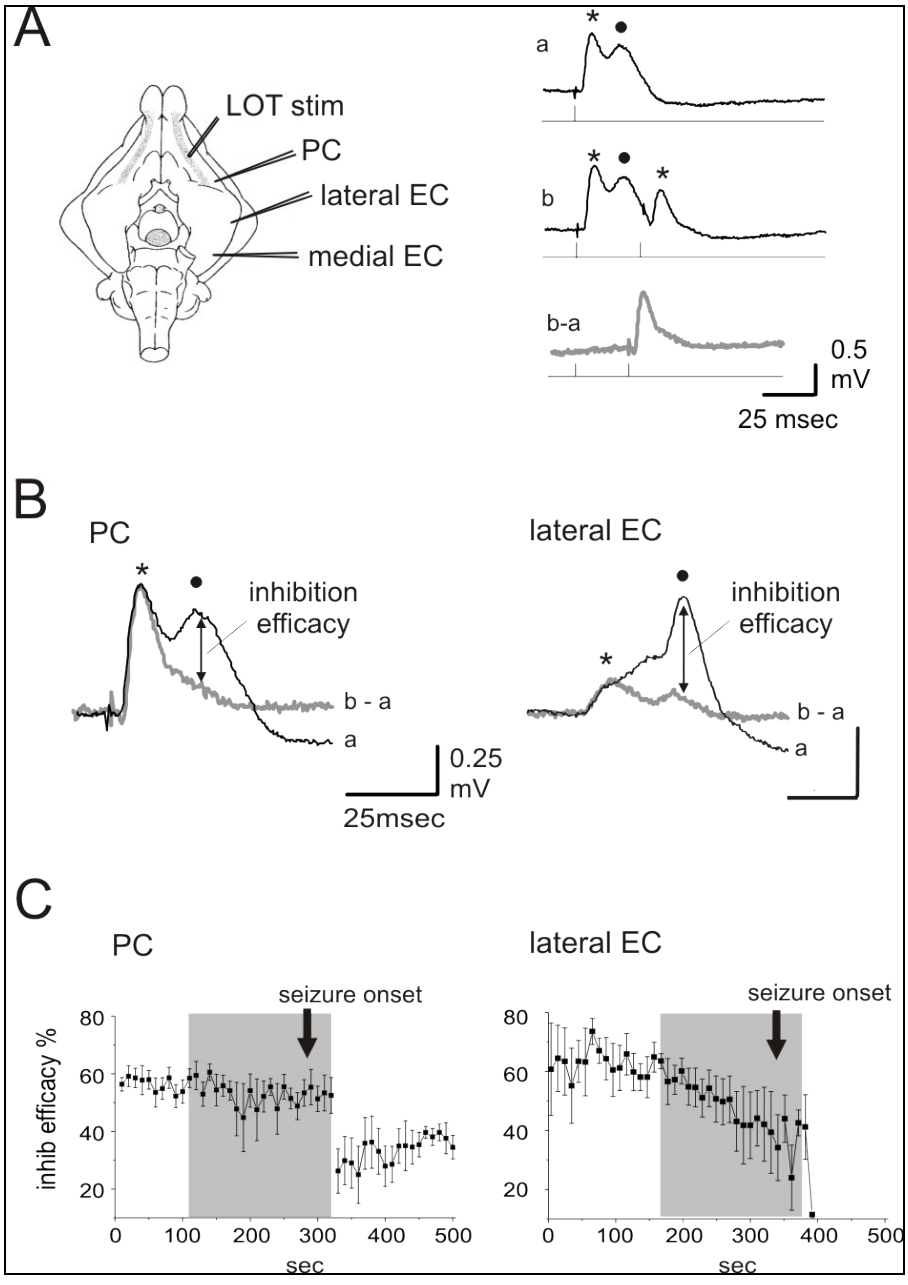
A
LOT stim
PC
lateral EC
medial EC
a
b
b-a
0.5
mV
25 msec
B
PC
inhibition
efficacy
b - a
a
0.25
mV
25msec
lateral EC
inhibition
efficacy
b - a
a
C
PC
seizure onset
inhib efficacy %
80
60
40
20
0
100
200
300
400
500
sec
lateral EC
seizure onset
80
60
40
20
0
100
200
300
400
500
sec

Figure 3 Intracellular correlate of seizure activity in a principal neuron of the superficial layers of the medial EC. A: Simultaneous extracellular recording (lower trace, extra) and intracellular recording from a principal neuron of the superficial layers of the medial EC (upper trace) during the transition into seizure-like discharge. Recording segments outlined by the boxes a, b, c and d are expanded in the lower part of the panel. Resting membrane potential (rmp; dotted line) was -64 mV. At the onset of the seizure, the membrane potential of the neuron was depolarized by 5 mV, via injection of a positive current through the intracellular recording electrode. The arrowhead marks the abrupt hyperpolarization that correlates with seizure onset. Thin arrows point to fast activity in the intracellular trace expansion in a. The thick arrow indicates the reappearance of rebound neuronal firing during fast activity. B: Power content of the intracellular (left) and extracellular (right) signals illustrated in A during the fast activity at seizure onset. High-pass filter was set at 10 Hz. A clear peak of activity centered around 25 HZ is shown. C: Average power content of the intracellular (left) and extracellular (right) signals during fast activity at seizure onset recorded in 17 superficial layer neurons.

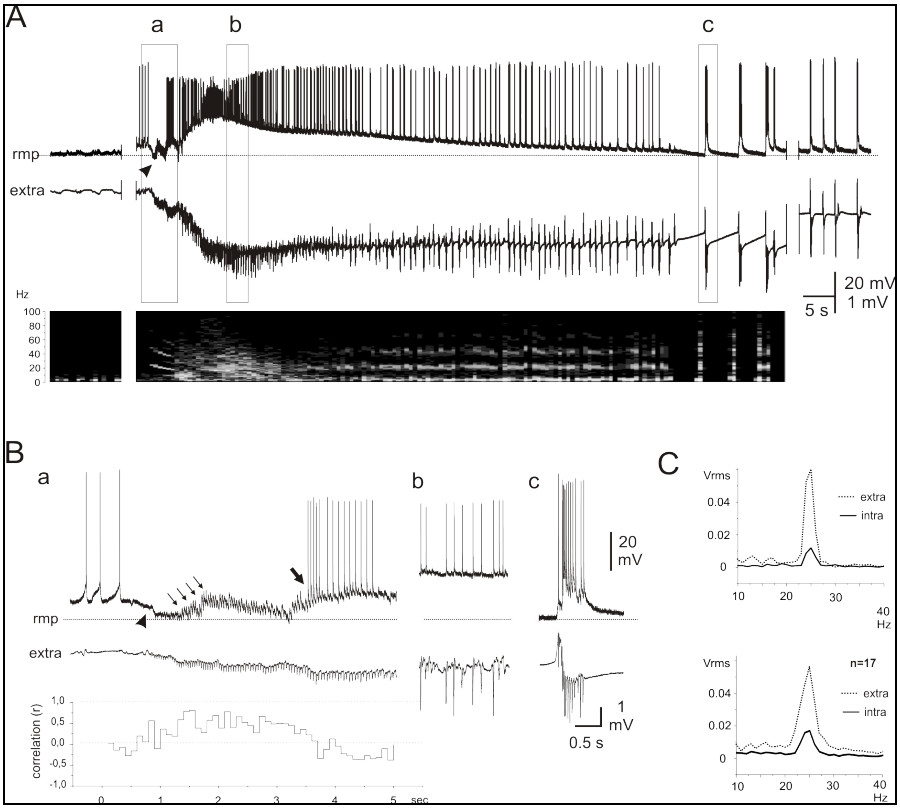
A
a
b
c
rmp
extra
Hz
100
80
60
40
20
0
20 mV
1 mV
5 s
B
a
b
c
rmp
extra
correlation (r)
1,0
0,5
0,0
-0,5
-1,0
0
1
2
3
4
5
sec
20
mV
1
mV
0.5 s
C
Vrms
0.04
0.02
0
extra
intra
10
20
30
40
Hz
n=17

Figure 4 Reversals of potentials evoked by lateral olfactory tract (LOT) stimulation (a; arrowhead) and fast activity (b) in superficial EC neurons. Simultaneous extracellular potentials are shown for each recording (extra). A: the membrane of the neuron was hyperpolarized from resting membrane potential (-63 mV, dotted line) by injection of a steady negative current via the intracellular recording pipette. The reversal potential of the LOT-evoked IPSP (a) and the intracellular correlate of the fast activity (b) are illustrated; the arrow points at the intracellular correlate of the spike that initiates the seizure. In the left part of the panel, two different traces recorded at -47 mV and -80 mV are illustrated, to show the membrane reversal potential of the LOT-evoked responses. In a different neuron in B, a positive current was injected to depolarize the membrane potential during the LOT-evoked response (a) and during the ictal onset discharge (b). In this neuron the rmp was -61 mV (dotted line). The arrowheads in a mark the LOT stimulation. The arrows point to the onset of the seizure-like discharge; note the abrupt hyperpolarization of the membrane potential that initiates the fast activity.

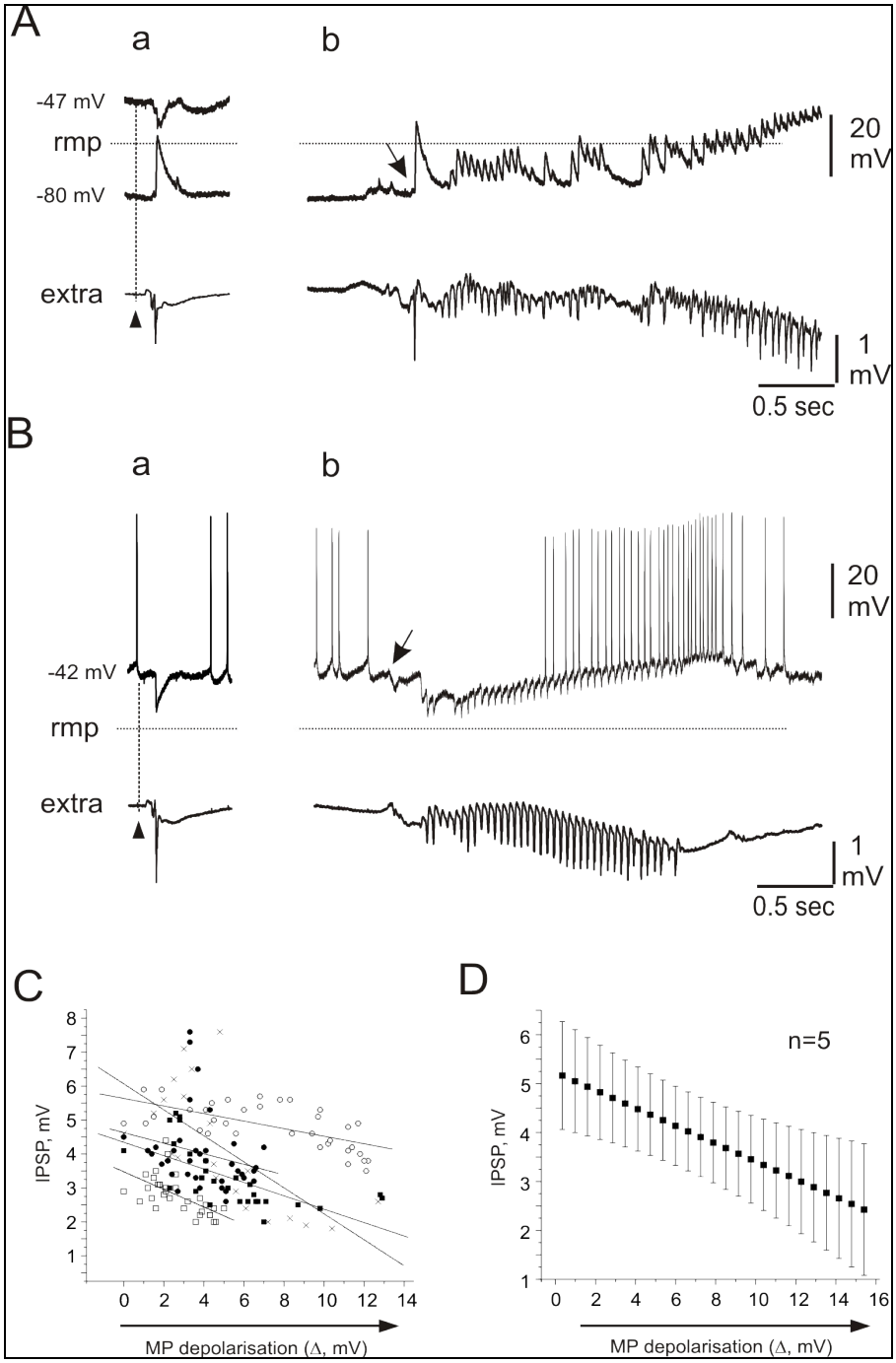
A
a
b
-47 mV
rmp
-80 mV
extra
20
mV
1
mV
0.5 sec
B
a
b
-42 mV
rmp
extra
20
mV
1
mV
0.5 sec
C
IPSP, mV
MP depolarisation (Δ, mV)
D
n=5
IPSP, mV
MP depolarisation (Δ, mV)

Figure 5 Intracellular correlate of seizure activity in a principal neuron of the deep layers of the medial EC. Simultaneous extracellular recording (lower trace, extra) and intracellular recording from a principal neuron of the deep layers of the mEC (upper trace) during the transition into seizure-like discharge. Sections a, b and c, outlined by the squares are expanded in the lower part of the figure. Arrow marks the abrupt hyperpolarization at the onset of seizure, characterized by fast activity in the extracellular recording. The resting membrane potential of the neuron (-67 mV) is outlined by the dotted line.

Figure 6 Firing features of putative interneurons during seizure-like activity induced by bicuculline. A: simultaneous extracellular (lower traces, extra) and intracellular recording from a putative interneuron of the EC superficial layers (upper trace). Expansions of a and b are shown in the lower part of the panel. In B, the firing of another putative interneuron is illustrated. As shown in the expanded trace (a) on the right, the cell firing started before the onset of the fast oscillatory activity that initiates the seizu

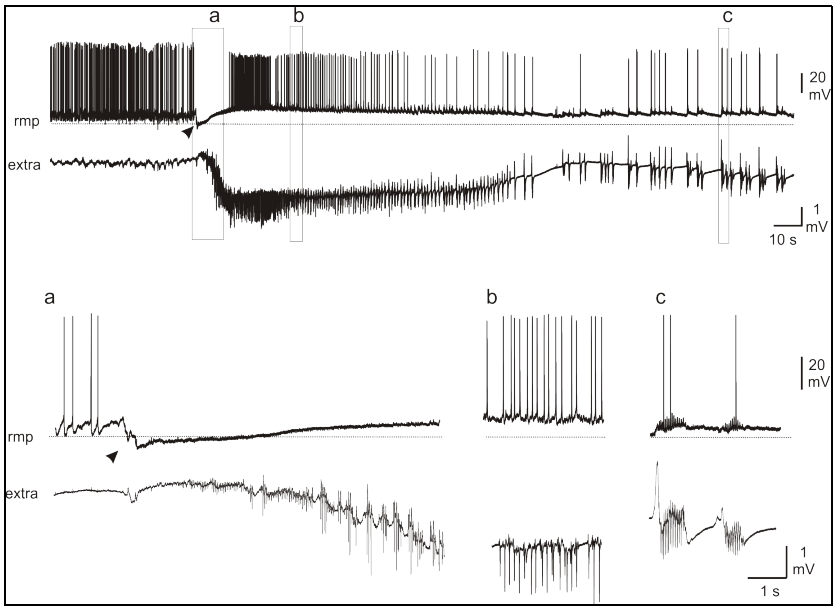
a
b
c
20
mV
rmp
extra
1
mV
10 s
a
b
c
20
mV
rmp
extra
1
mV
1 s

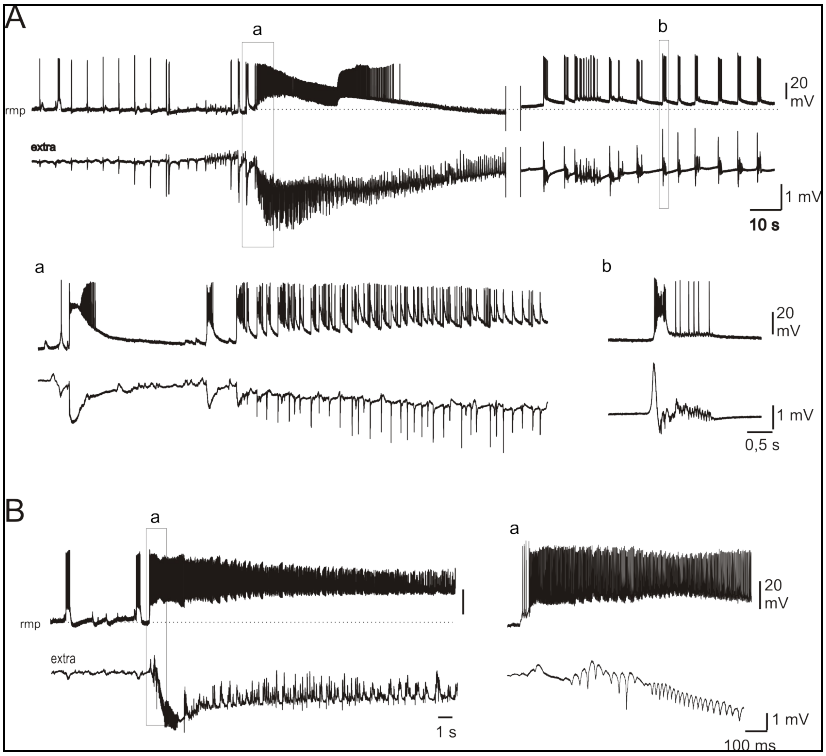
A
a
b
rmp
20
mV
extra
1 mV
10 s
a
b
20
mV
1 mV
0,5 s
B
a
a
rmp
20
mV
extra
1 s
1 mV
100 ms

Figure 7 Intracellular-extracellular correlates of pre-ictal spikes (right panels) compared to the potentials evoked by stimulation of the LOT (arrowheads in left panels) recorded in superficial (upper traces) and deep (middle traces) principal cells and in putative interneurons (lower traces) of the medial EC. Resting membrane potentials were -57 mV for the superficial neuron, -58 mV for the deep neuron and -56 mV for the putative interneuron. In the superficial cell the LOT-evoked intracellular traces were recorded at resting membrane potential (upper trace) and during steady membrane hyperpolarization to -82 mV. The inset on the right in the middle panel shows a longer extract of the deep neuron response during the pre-ictal spike.

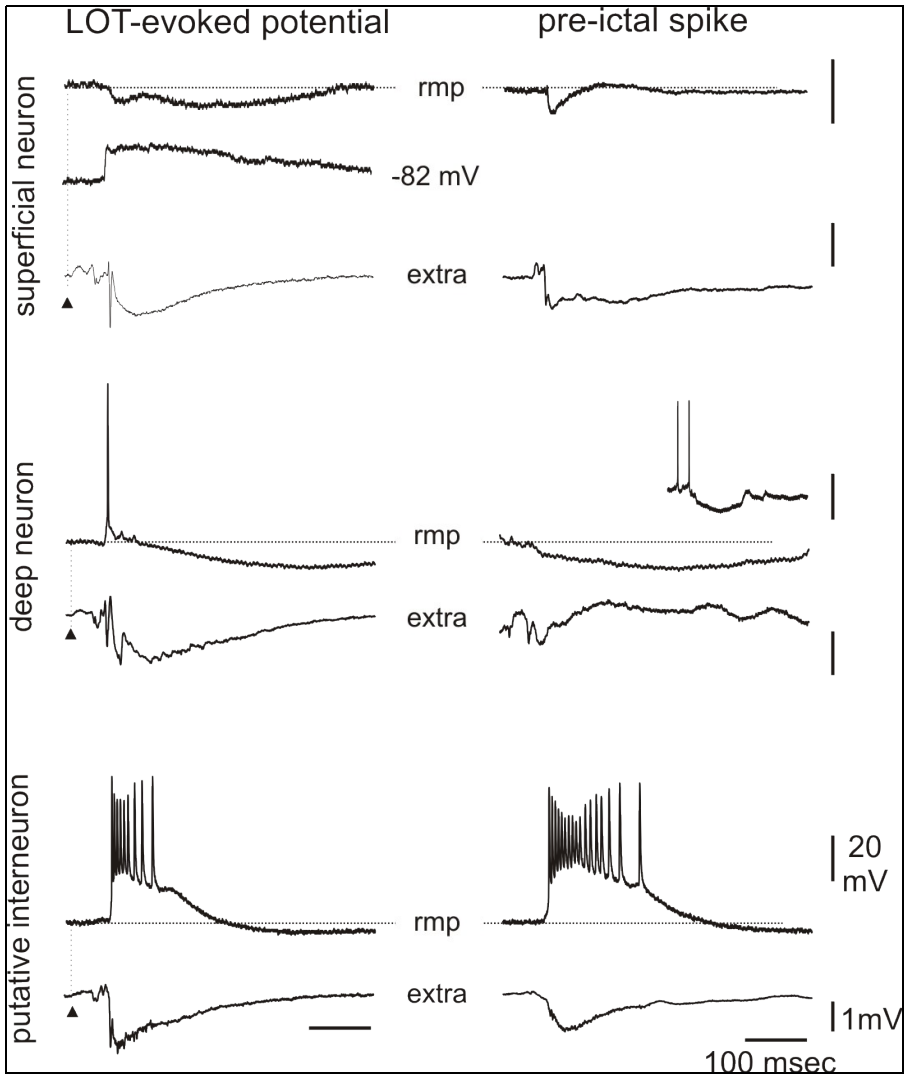
LOT-evoked potential
pre-ictal spike
superficial neuron
rmp
-82 mV
extra
deep neuron
rmp
extra
putative interneuron
rmp
extra
20 mV
1mV
100 msec

Figure 8 Changes in the extracellular potassium ([K+]o) during seizure onset in the medial EC. A: Simultaneous recordings of a principal neuron in superficial layers (upper trace), extracellular potential (middle trace) and changes in [K+]o (lower trace) during an ictal event induced by 3-minutes perfusion of bicuculline. The tract outlined by the box is expanded in the lower left part in A. Resting membrane potential (rmp) was -59 mV. Expanded sweeps of fast activity sequences marked by a, b and c are illustrated in the right panel. Values of potassium concentration are reported for each trace. B: Average values (± SE) of the changes in IPSP amplitude (marked by filled squares; left scale) and potassium concentration (filled circle; right scale) during seizure onsets recorded in 3 experiments. The time after the onset of the fast activity is reported in the abscissae. In C the dependence of the IPSP reduction on the changes in [K+]o are illustrated with different symbols for the 3 experiments.

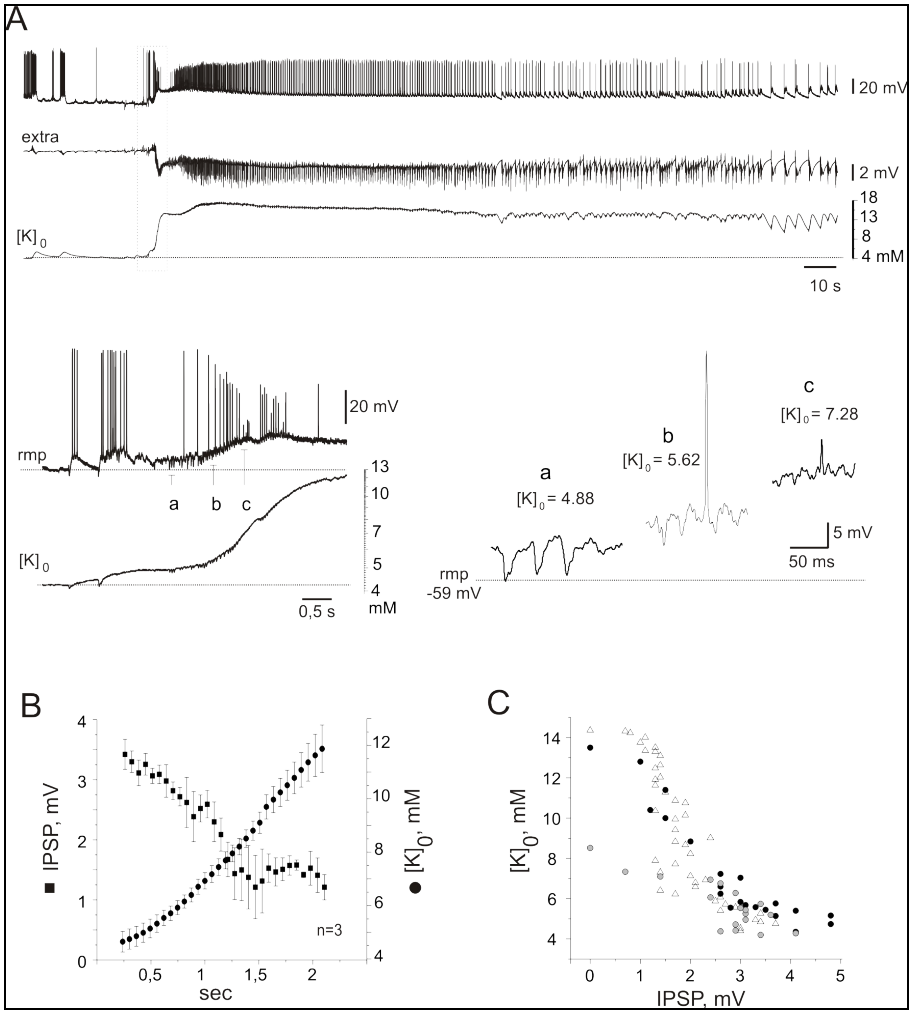
A
20 mV
extra
2 mV
[K]0
18
13
8
4 mM
10 s
20 mV
rmp
a b c
13
10
7
5
4
mM
[K]0
0,5 s
a
[K]0 = 4.88
b
[K]0 = 5.62
c
[K]0 = 7.28
5 mV
50 ms
rmp
-59 mV
B
■ IPSP, mV
● [K]0, mM
n=3
sec
C
[K]0, mM
IPSP, mV

CHAPTER 4

CORRELATES OF SLOW EXTRACELLULAR POTENTIALS DURING FOCAL ICTAL DISCHARGES IN THE ENTORHINAL CORTEX OF THE *IN VITRO* ISOLATED GUINEA PIG BRAIN

Federica Trombin, Vadym Gnatkovsky, Laura Librizzi and Marco de Curtis

ABSTRACT

Focal seizures recorded in humans and in animal models of partial epilepsy are associated with large slow potentials (<0.01 Hz) that are assumed to be generated by the ictal discharge itself. It is still not clear whether slow components are generated by extracellular ion changes or by potentials generated either in glial cells or across the blood-brain barrier. In the present study we analyzed the slow activities that accompany focal seizures in the entorhinal cortex of the *in vitro* isolated guinea pig brain transiently disinhibited by a 3-minute perfusion with the GABAa receptor antagonist, bicuculline (50 μM). Extracellular field responses and changes in potassium and proton concentrations were simultaneously measured. The slow potential did not show a clear depth reversal, suggesting that it is not due to local sinks/sources generated by fast transmembrane potentials. The onset and time course of slow potentials was closely coupled with the changes in extracellular K^+ concentration. An early inverting phase of the slow potential was abolished by local application of caesium chloride (100 mM), but not ouabaine (10 mM), both active in buffering extracellular K^+ increments due to hyperactivity of neurons.

Locally applied ouabaine blocked neuronal firing during seizures in a restricted area and allowed a direct correlation of slow potentials with the changes in extracellular K^+ propagating from adjacent active regions.

Our findings demonstrate that the slow potentials generated during seizure activity strictly follow extracellular K^+ changes. The early inverting component of the slow potentials is possibly due to glial buffering of raises in extracellular K^+. Since multi-phase slow potentials were described in diagnostic pre-surgical intracranial recordings performed in patients with drug-resistant epilepsy, the slow inverting potential could be used as marker of glial function in the human epileptic tissue.

INTRODUCTION

Focal seizures are characterized by the hypersynchronous activation of cortical neurons. Extracellular recordings performed with long time constants from both experimental models (O'Leary & Goldring, 1964) (Gumnit & Takahashi, 1965) and humans demonstrate that focal seizure activity is associated with slow voltage deflections. These very slow potentials are strictly coupled with the onset of the ictal epileptiform discharge and are not observed during interictal events. The nature of the slow signals is still not clearly defined. Negative slow shifts were proposed to be generated by transmembrane ions changes attributed to inward neuronal conductances that sustain neuronal depolarization. This hypothesis was questioned by the proposal that glia could be responsible for slow potential generation (O'Leary & Goldring, 1964). Neuronal activity during seizures induces accumulation of extracellular potassium (K^+) that is not removed by neuronal uptake (Heinemann & Lux, 1975) and is buffered by glial cells (Gardner-Medwin, 1986). Intake of K^+ via inward rectifier channels and sodium/potassium-ATPase induces a rapid membrane depolarization of astrocytes (Ransom & Goldring, 1973) (Somjen, 1973) (Amzica & Steriade, 2000). It has been suggested that glial uptake of K^+ released during a seizure and the associated glial membrane depolarization could contribute to the generation of slow potentials (Lothman & Somjen, 1975).

We recently demonstrated that slow potential shifts are generated in the entorhinal cortex (EC) of the isolated guinea pig brain preparation during seizures induced by several convulsants, such as bicuculline methiodide, 4-aminopyridine and pilocarpine. Slow potentials fluctuations during seizures in the EC showed a reproducible pattern characterized by an initial negative deflection, followed by a transient

positive wave that reverts to negativity within a few seconds (see figure 2A). This three-phase slow potential pattern during seizures was noticed in different experimental preparations of the EC (Avoli & Barbarosie, 1999) (Lopantsev & Avoli, 1998) and was also observed in other cortical structures. In the present study we investigate the mechanisms that sustain this peculiar pattern of slow shifts associated with a focal seizure. Since inward rectifier channels (Ransom & Sontheimer, 1995) and sodium/potassium-ATPase (Grisar, 1984) are the principal mechanisms that control K^+ buffering by glia, we focused on the effects of selective blockers of these channels, Cesium and ouabaine, to study slow potentials. The data were previously presented in abstract form (Trombin et al., 2009).

METHODS

Young adults Hartely guinea pigs (150-200gr weight) were anesthetized by i.p. administration of sodium thiopental (125 mg/kg). After extensive craniotomy performed in hypothermic conditions, the brain was isolated and was maintained *in vitro* by cannulation of the basilar artery followed by perfusion with a saline solution (composition: 126 mM NaCl, 3 mM KCl, 1.2 mM KH_2PO_4, 1.3 mM $MgSO_4$, 2.4 mM $CaCl_2$, 26 mM $NaHCO_3$, 15m M glucose and 3% dextran molecular weight 70,000), oxygenated with a 95%O_2 5%CO_2 gas mixture (pH7.3;)

Glass capillaries filled with 0.9% NaCl were used for extracellular recording, and ion-sensitive electrodes were used for extracellular K^+ and H^+ (pH) measurements. Double-barrel glass capillaries with tip of 3-5µm diameter were filled with either K^+ ionophore I cocktail A or H^+ ionophore II-cocktail A (Fluka 60031 and 95297,Germany). K^+ concentration expressed in mM was established from mV values using

a converting semi-logarithmic equation **Y = a + b Log X** where **Y** is the increase in mV, **X** is the increase in mM and **a** and **b** are the coefficients of the calibration curve based on electrode response to standard K^+ concentrations (1, 2.5, 6, 12.5 and 48 mM). For pH measurements, the tips of the ion-sensitive barrel were back-filled with a buffer solution (in mM: NaCl 100, HEPES, and NaOH 10, pH 7.5). pH-electrode calibration between 5.5 and 7.5 was performed and electrodes with a response of 50–55 mV per pH unit change were selected. Ion-selective signals were acquired with a high-input impedance head-stage amplifier (Biomedical Engineering, Thornwood, NY) and field potential values were subtracted to voltages measured through the ionophore-filled channel.

Caesium Chloride (CsCl; Sigma) was delivered at a concentration 100 mM in the medial EC close to the K^+-sensitive electrode using a Picospritzer II (Parker Instrumentation; US). CsCl is a cationic monovalent ion that transiently blocks the K^+ inward rectifying channels (K_{ir}; Constanti & Galvan, 1983). Ouabain 1 mM was also applied by local ejection. $GABA_A$ receptor antagonist bicuculline methiodide (BMI) was perfused through the arterial system for 3 minutes at a concentration of 50μM to induce seizures in the temporal lobe.

RESULTS

Experiments were performed in 15 isolated guinea pig brains. Epileptiform discharges were induced in the entorhinal cortex (EC) of the isolated guinea pig brain by application of the $GABA_A$ receptor antagonist, BMI (50 μM), perfused through the arterial system for 3 minutes. We included in the study only those experiments in which

comparable seizure patterns were observed, characterized by low-voltage fast activity at 25-30Hz at the onset superimposed on a slow deflection detected by recording the neurophysiological signals without filters for the low frequencies (DC recordings). We identified three different phases during the slow ictal events: i) an initial negative deflection (**a** in Figure1A) characterized by a 1.5±0.25 mV shift of the trace (n=15), superimposed to fast oscillatory activity, ii) a second delayed wave with inverting polarity (**b** in Figure 1A) and iii) a late negative-going, long-lasting wave (**c** in Figure 1A) that slowly returned to baseline values. The variability of slow potential duration correlated with the time course of the seizure.

To verify whether the different components of the slow potential were generated by voltage dipoles across EC layers mediated by synaptic transmembrane potentials, we performed simultaneous recordings from superficial and deep layers of the EC with double-barrel electrodes. As illustrated in the left panel of Figure 1B, the tips of the double-barrel electrode were separated by 400-500 μm and were positioned in the superficial part of layer I (100 μm depth) and in layer V (500-600 μm depth). A typical depth reversal between the two electrode tips was observed in the response evoked by electrical stimulation of the lateral olfactory tract (left pair of traces in Figure 1B). During BMI perfusion depth reversal of interictal spikes was also observed just ahead of a seizure (asterisk in Figure 1B). The slow field components associated with the seizure onset showed no depth reversal (Figure 1B; n=8), suggesting that slow potentials are not generated by a synaptically-driven depth dipole generated within the layers of the EC. Depth potential laminar profiles performed with 16-channels silicon probes arranged in a linear shaft, separated by either

50 or 100 μm, confirmed the absence of depth reversal within the EC (data not shown; n=8).

Next, the correlation between the slow potentials and the changes in extracellular ion concentration was verified with double barrel ion-sensitive electrodes. As previously reported, principal EC cells stop firing and interneurons become the only players in the generation of seizure onset. During this phase, corresponding to the inverting phase of the extracellular field potential (**b**), extracellular K^+ increased to values of about 7-8 mM (Figure 2); pH transiently alkalinized (n=4) and afterwards showed a large and prolonged extracellular acidification (Figure 2). The time course of the late slow component (phase **c**) closely replicated the extracellular K^+ changes (n=8). The tissue acidification outlasted by several tens of seconds the end of a seizure (n=4). We conclude that the slow potentials generated by EC seizures are mainly associated with extracellular K^+ changes. Since extracellular K^+ is regulated by glial buffering, we further investigated whether interference with the glial uptake of K^+ affected slow potentials.

Evaluation of the rise in K^+ concentration and the changes in field potential amplitudes were averaged between 13 experiments; values were expressed as mean ± se. Unpaired t-test was performed to compare control and CsCl-treated data. Paired t-test was performed between data from the same category.

In 13 experiments the blocker of astrocyte K^+ inward rectifier current, CsCl 100mM (Ransom & Sontheimer, 1995), was locally applied in the EC during simultaneous recording of field responses and K^+ signals in two positions, close to and remote from the local CsCl ejection. The dose of CsCl was selected on the basis of its ability to enhance excitability in the LOT-evoked field response. As illustrated

in Figures 3 and 4, CsCl modified the time course of both slow potentials and K^+ changes in the recording site close to its application (lower panels in Figures 3B and 4A), but not in the far site (upper panels in Figures 3B and 4A). The field potential amplitudes measured at 3 different time points (**a**, **b** and **c**, corresponding to the 3 wave components defined above) showed a clear smoothing of the reverting wave (phase **b**) at the CsCl ejection site (black column in Figure 3C) compared to the remote control site (empty columns; $p = 0.00007$). Values were expressed as percent of maximal amplitude variation at the steady state (peak amplitude at **c**). After application of CsCl an important reduction in the inverting wave amplitude (**b** in Figure 3) was observed.

Due to its action on inward rectifying K^+ channels, CsCl blocks the pore on glial membrane for K^+ uptake. The effect of CsCl was not immediately seen in the first slow wave, in which extracellular K^+ was not significantly different in CsCl-treated (8.5 ± 0.9 mM; n=6) and in control sites (10.2 ± 1.8 mM). The significant percent reduction between K^+ values measured in **a** and **b** ($p = 0.00501$) in control experiments was abolished at the site of CsCl action (Figure 4B; $p = 0.08960$, not significantly different). These findings demonstrate that CsCl enhances the K^+ changes (**a**) and reduces the correlated slow wave (**b)**.

Glial K^+ intake is also regulated by the sodium/potassium-ATPase (Grisar, 1984) sensitive to ouabaine. Therefore we tested the effect of local application of 1 mM ouabaine on the slow potentials and the K^+ shifts. Interestingly, ouabaine prevented seizure activity and the relative K^+ changes at the EC site where it was locally applied (Figure 5A). Seizure with the typical features and associated K^+ changes were simultaneously recorded >1 mm away from the ouabaine ejection site

(Figure 5). Juxta-cellular recordings performed with high impedance (30 MOhm) extracellular electrodes at the site of ouabaine ejection demonstrated that neuronal firing was blocked. (data not shown)

DISCUSSION

The present study investigates the mechanisms that underlie the generation of slow potential shifts during focal seizures, described in humans and in animal models. We observed that slow potentials during focal seizures are characterized by a large and prolonged bimodal negative wave: an early negative peak (wave ***a*** in Figure 1) is separated from the late negative wave (phase ***c***) by a positive notch lasting 3 seconds that we called the inverting wave (phase ***b***). This three-phase pattern was already described as an inverted saddle by Somjen (for review see Somjen, Ions in the brain. 2004), and is reported in studies performed in animal models as well as in humans during presurgical intracranial recordings (Ikeda et al., 1996). We show that i) the time course of slow potentials strictly correlates with changes in extracellular K^+ concentration associated to seizures and ii) the slow inverting component that develops after seizure onset is blocked by CsCl. We hypothesize that the inverting phase could be generated by the glial uptake of extracellular K^+ and could be utilized as biomarker of glial function.

Several mechanisms were proposed to explain slow potentials. One hypothesis is that slow waves are the consequence of transmembrane dipoles generated by the laminar arrangement of synaptic activity in the cortex, as for fast components of the field potentials. No depth reversal was reported in the neocortex (Lothman & Somjen, 1976). This could be due to the fact that synaptic potentials do not show a clear laminar distribution in the neocortex in comparison with the tight

laminar organization of the hippocampus. Several studies demonstrated that the superficial layers of the EC show a highly laminar organization of synaptic inputs generated during physiological activity and during seizures (Uva et al., 2005; Lopantsev & Avoli, 1998). We demonstrated that the slow potentials were not associated with a clear dipole generated within the EC. No depth reversal of any slow component was observed when activity was simultaneously recorded with electrodes positioned across superficial and deep EC layers. Depth potential profiles performed with 16-channels silicon probes confirmed the absence of depth reversal of slow potentials. Therefore, we can exclude that the large-amplitude voltage deflections associated with slow potentials are directly generated by the synchronous synaptic activity produced during seizures.

The most accredited hypothesis is that slow DC shifts are due to both K^+ ion changes in the extracellular space and astrocyte depolarization due to extracellular K^+ reuptake and buffering. The strict correlation between the DC shifts and the K^+ changes observed in our experiments seem to corroborate the hypothesis that K^+-related events generate the slow potentials. To evaluate if other ions largely modified during seizures, such as H^+ contribute to slow potentials, changes in pH were measured in our experiments. During seizures we observed an early and fast alkalinisation followed by a prolonged acidification that outlasted the termination of the seizure by several tenths of seconds. The early alkalinisation was not observed consistently and preceded the rise in potassium concentration and the onset of the fast activity. In principle it may contribute to the initiation of the slow potentials, though its reduced amplitude could not be directly related to an evident modification in the field potential shifts.

There is an evident relation between the extracellular field potential modifications and the K^+ increment. During the first tens of seconds of seizure onset the ISW and the inverting phase are well related. The excessive synchronous activation of neurons during seizures generates K^+ accumulation in the extracellular space. The plateau level to which extracellular K^+ rises during prolonged ictal seizures is established by the balance between the outflow from neurons and the uptake into neurons and glial cells. A light delay exists between the increase in extracellular K^+ and the onset of the K^+ uptake that correlates to cellular depolarization, especially in astrocytes. The more the membrane depolarizes, the greater the driving force pushes K^+ out; on the other side, the growth of the ratio $[K^+]o/[K^+]i$ slows the outward flow. When the K^+ concentration reaches a sufficient high value the polarization of the membrane is inverted again and action potentials can be evoked and so we have a second raise in potassium and a second slow wave. The first and second slow waves are separated by a inverting, depth-positive slow wave (phase, b in Fig1). During this phase the K^+ concentration is slowly lowered to physiological values indicating a continuous still efficacious astro-glial activity of K uptake.

As in Fig.2 the maximum deflection of the ISW (point a) corresponds to the maximum K extrusion from cells. The inverting phase represents the K-uptake from the extracellular fluid that is re-captured in part form neurons and in large part from the surrounding astrocytes. The mechanism by which astrocytes eliminate K^+ can be different. The primary modality of K ions clearance is the opening of K^+ inward rectifying channels. They are voltage sensitive pores that allow the passage of many positive ions, most of which are K^+ ions.

The other way potassium is taken away from the site of accumulation is a slower procedure, involving spatial buffering through the astrocitic body following an electrochemical gradient.

The precise mechanism of action of Cesium is doubtful, it acts on every cationic channels blocking its pore, but it has an especial affinity for potassium inward rectifying channels (Kir on astrocytes). The outcome of the blockade of cationic gates on the cell surface is an imbalance with positive charges accumulating in the extracellular space and leading to phenomena of over-excitability, glial metabolism shut down but also spreading depressive sinks in the field potential and strong and durable increments in [K].

This effect is even stronger after application of ouabain (1mM local injection) which is a poisoning glycoside, a selective inhibitor of Na/K ATPasic pump. The inactivation of the membrane enzyme disrupts the electrogenic gradient across the membrane of inward driving force for Na and outward gradient for K. So after neuronal activation and ionic gradients disruptions, the correct voltage membrane recovery is impaired. The action of ouabain perfusion through the artery system was already evaluated by Librizzi and colleagues (Librizzi, 2001). When the blocker of the Na/K pump ouabain (10 mM) was coperfused for 5 min with a high-K solution, a gradual increase in [K] in PC and EC was observed, which invariably determined a spreading depression (SD).

REFERENCES

Amzica F. and Steriade M. (2000) Neuronal and glial membrane potentials during sleep and paroxysmal oscillations in the neocortex. *Journal of Neuroscience* 20, 6648-65.

Avoli M. and Barbarosie M. (1999) Interictal-ictal interactions and limbic seizure generation. *Revue Neurologique* 155, 468-71.

Ballanyi K., Grafe P., and ten Bruggencate G. (1987) Ion activities and potassium uptake mechanisms of glial cells in guinea-pig olfactory cortex slices. *J Physiol* 382, 159-74.

Caspers H., Speckmann E.J., and Lehmenkuhler A. (1987) DC potentials of the cerebral cortex. Seizure activity and changes in gas pressures. *Rev Physiol Biochem Pharmacol* 106, 127-78.

Constanti A. and Galvan M. (1983) Fast inward-rectifying current accounts for anomalous rectification in olfactory cortex neurons. *J. Physiol. (Lond)* 335, 153-178.

D'Ambrosio R., Wenzel J., Schwartzkroin P.A., McKhann G.M.2., and Janigro D. (1998) Functional specialization and topographic segregation of hippocampal astrocytes. *Journal Of Neuroscience* 18, 4425-38.

de Curtis M., Biella G., Buccellati C., and Folco G. (1998) Simultaneous investigation of the neuronal and vascular compartments in the guinea pig brain isolated in vitro. *Brain Research Protocols* 3, 221-8.

de Curtis M., Biella G., Forti M., and Panzica F. (1994) Multifocal spontaneous epileptic activity induced by restricted bicuculline ejection in the piriform cortex of the isolated guinea pig brain. *Journal of Neurophysiology* 71, 2463-2475.

de Curtis M., Pare D., and Llinas R.R. (1991) The electrophysiology of the olfactory-hippocampal circuit in the isolated and perfused adult mammalian brain in vitro. *Hippocampus* 1, 341-54.

Dietzel I., Heinemann U., Hofmeier G., and Lux H.D. (1980) Transient changes in the size of the extracellular space in the sensorimotor cortex of cats in relation to stimulus-induced changes in potassium concentration. *Exp Brain Res* 40, 432-9.

Dietzel I., Heinemann U., and Lux H.D. (1989) Relations between slow extracellular potential changes, glial potassium buffering, and electrolyte and cellular

volume changes during neuronal hyperactivity in cat brain. *Glia* 2, 25-44.

Gardner-Medwin A.R. (1986) A new framework for assessment of potassium-buffering mechanisms. *Ann N Y Acad Sci* 481, 287-302.

Gnatkovsky V., Librizzi L., Trombin F., and de Curtis M. (2008) Fast activity at seizure onset is mediated by inhibitory circuits in the entorhinal cortex in vitro. *Ann Neurol* 64, 674-86.

Grisar T. (1984) Glial and neuronal Na+-K+ pump in epilepsy. *Ann Neurol* 16 Suppl, S128-34.

Grisar T., Guillaume D., and Delgado-Escueta A.V. (1992) Contribution of Na+,K(+)-ATPase to focal epilepsy: a brief review. *Epilepsy Res* 12, 141-9.

Gumnit R.J., Matsumoto H., and Vasconetto C. (1970) DC activity in the depth of an experimental epileptic focus. *Electroencephalogr Clin Neurophysiol* 28, 333-9.

Heinemann U. and Lux H.D. (1975) Undershoots following stimulus-induced rises of extracellular potassium concentration in cerebral cortex of cat. *Brain Res* 93, 63-76.

Ikeda A., Taki W., Kunieda T., Terada K., Mikuni N., Nagamine T., Yazawa S., Ohara S., Hori T., Kaji R., Kimura J., and Shibasaki H. (1999) Focal ictal direct current shifts in human epilepsy as studied by subdural and scalp recording. *Brain* 122 (Pt 5), 827-38.

Ikeda A., Terada K., Mikuni N., Burgess R.C., Comair Y., Taki W., Hamano T., Kimura J., Luders H.O., and Shibasaki H. (1996) Subdural recording of ictal DC shifts in neocortical seizures in humans. *Epilepsia* 37, 662-74.

Kivi A., Lehmann T.N., Kovacs R., Eilers A., Jauch R., Meencke H.J., von Deimling A., Heinemann U., and Gabriel S. (2000) Effects of barium on stimulus-induced rises of. *Eur J Neurosci* 12, 2039-48.

Librizzi L., Janigro D., De Biasi S., and de Curtis M. (2001) Blood brain barrier preservation in the *in vitro* isolated guinea -pig brain preparation . *Journal of Neuroscience Research* 66, 289-297.

Lopantsev V. and Avoli M. (1998) Laminar organization of epileptiform discharges in the rat entorhinal cortex in vitro. *Journal Of Physiology* 509 (Pt 3), 785-96.

Lothman E., Lamanna J., Cordingley G., Rosenthal M., and Somjen G. (1975) Responses of electrical potential, potassium levels, and oxidative metabolic activity of the cerebral neocortex of cats. *Brain Res* 88, 15-36.

Lothman E.W. and Somjen G.G. (1975) Extracellular potassium activity,

intracellular and extracellular potential responses in the spinal cord. *Journal Of Physiology* 252, 115-36.

Lothman E.W. and Somjen G.G. (1976) Reflex effects and postsynaptic membrane potential changes during epileptiform activity induced by penicillin in decapitate spinal cords. *Electroencephalography And Clinical Neurophysiology* 41, 337-47.

Lücke A., Nagao T., Köhling R., and Avoli M. (1995) Synchronous potentials and elevations in [K+]o in the adult rat entorhinal cortex maintained in vitro. *Neuroscience Letters* 185, 155-8.

McKhann G.M. 2nd, D'Ambrosio R., and Janigro D. (1997) Heterogeneity of astrocyte resting membrane potentials and intercellular coupling revealed by whole-cell and gramicidin-perforated patch recordings from cultured neocortical and hippocampal slice astrocytes. *J Neurosci* 17, 6850-63.

Muhlethaler M., de Curtis M., Walton K., and Llinas R. (1993) The isolated and perfused brain of the guinea-pig in vitro. *Eur J Neurosci* 5, 915-26.

O'Leary J.l. and Goldring S. (1964) d-c potentials of the brain. *Physiol Rev* 44, 91-125.

Ransom B.R. and Goldring S. (1973) Slow depolarization in cells presumed to be glia in cerebral cortex of cat. *J Neurophysiol* 36, 869-78.

Ransom C.B. and Sontheimer H. (1995) Biophysical and pharmacological characterization of inwardly rectifying K+ currents in rat spinal cord astrocytes. *J Neurophysiol* 73, 333-46.

Somjen G.G. (1973) Electrogenesis of sustained potentials. *Progress In Neurobiology* 1, 201-37.

Somjen G.G., Aitken P.G., Giacchino J.L., and McNamara J.O. (1985) Sustained potential shifts and paroxysmal discharges in hippocampal formation. *Journal Of Neurophysiology* 53, 1079-97.

Uva L., Avoli M., and de Curtis M. (2009) Synchronous GABA-receptor-dependent potentials in limbic areas of the in-vitro isolated adult guinea pig brain. *Eur J Neurosci* 29, 911-20.

Uva L., Librizzi L., Marchi N., Noe F., Bongiovanni R., Vezzani A., Janigro D., and de Curtis M. (2008) Acute induction of epileptiform discharges by pilocarpine in the in vitro isolated guinea-pig brain requires enhancement of blood-brain barrier permeability. *Neuroscience* 151, 303-12.

Uva L., Librizzi L., Wendling F., and de Curtis M. (2005) Propagation dynamics of

epileptiform activity acutely induced by bicuculline in the hippocampal-parahippocampal region of the isolated Guinea pig brain. *Epilepsia* 46, 1914-25.

Vanhatalo S., Palva J.M., Holmes M.D., Miller J.W., Voipio J., and Kaila K. (2004) Infraslow oscillations modulate excitability and interictal epileptic activity in the human cortex during sleep. *Proc Natl Acad Sci U S A* 101, 5053-7.

Figure 1 Typical pattern of seizure induced in the temporal lobe of the guinea pig brain after perfusion with bicuculline for 3 minute. In A are shown the three phases identified by the initial deflection with fast activity at 25-30Hz (**a**), the inverting phase after 3sec (**b**) characterized by irregular bursting activity, and then a delayed slow waves with regular bursts and field potential recovery with seizure end. Depth reversal absence (see part B) of the slow components indicates that the origin of this phenomenon is not neuronal, but may be attribute to a distribution of K ions across the EC layers. On the left there is a reconstruction of the elcetrodes positioning in the superficial and deep layers of the cortex. An evoked response after circuit activation showed the typical inversion in field potential response. The interictal spikes (asterisk) maintained the inversion among the layers, but at seizure onset the fast activity and also the slow waves did not showed any depth reversal. (see a, b and c in part B). Also the afterdischarges at seizure endings displayed the same polarity.

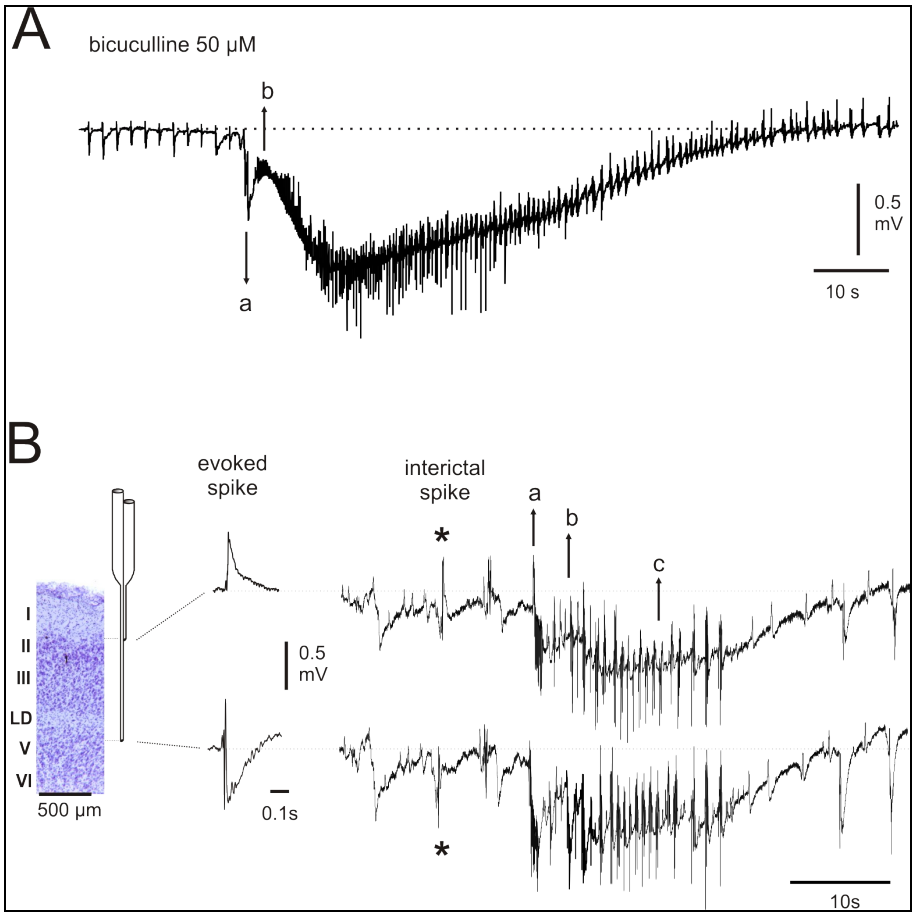
A
bicuculline 50 µM
b
a
0.5
mV
10 s
B
evoked
spike
interictal
spike
a
b
c
*
*
I
II
III
LD
V
VI
500 µm
0.5
mV
0.1s
10s

Figure 2 Symultaneous investigation of field potential slow activity, potassium concentration and pH values in the medial entorhinal cortex (m-EC) of the isolated guinea pig brain. In the upper panel a representative case of slow shift in the field potential, an increase in [K] and the correction operated by the glial cells spatial buffering mechanisms in few seconds after seizure onset. Potassium values are expressed as mM increase from the physiological concentration of 3mM evaluated to be in the tissue. The potassium trace follows the shape of slow potential in the extracellular FP. The pH changes showed a slight basification some instants before the onset of seizure and then a pronounced and persistent acidification. The gray shaded area represents the onset of seizure and the focus of the study, the evluation of themechanisms acting during the first phases of seizure onset and modifying extracellular potassium concentration and pH values. In B there is an enlargement of the gray area, with the three-phasic slow components indicated by **a**, **b** and **c** and arrows. Note that the hump in potassium traces reflects the inversion from phase a to b and then to c; also a change in extracellular activity from an irregular to regular bursting. During this first pteps pH values are still increasing. The arrows indicates the points used to calculate the average amplitude of FP, the [K] mM .

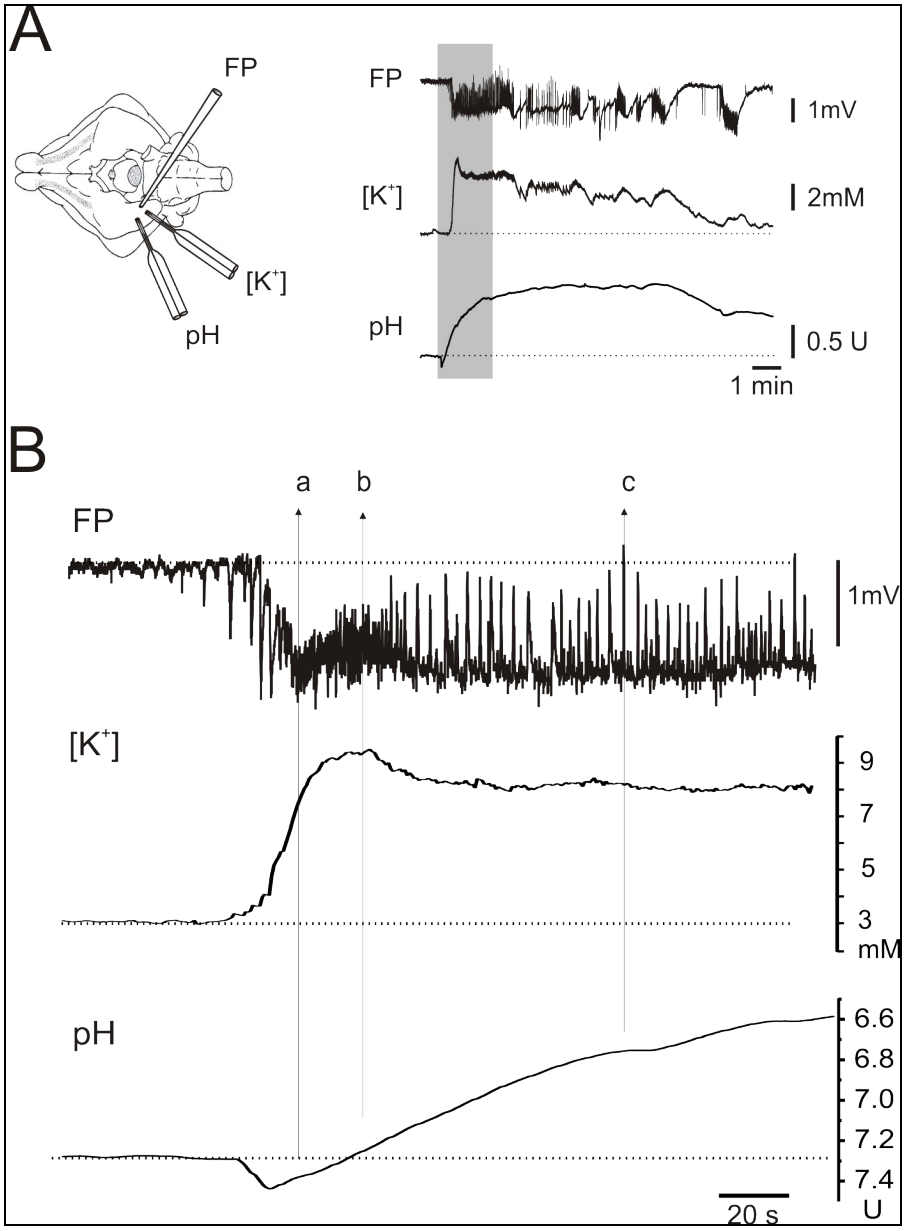
A
FP
[K+]
pH
FP
1mV
[K+]
2mM
pH
0.5 U
1 min
B
a
b
c
FP
1mV
[K+]
9
7
5
3
mM
pH
6.6
6.8
7.0
7.2
7.4
U
20 s

Figure 3. An example of Cesium Chloride action on the field potential. In the right part of panel A an evoked response after LOT stimulation recorded at the site of cesium injection and far from the injecting pipette. The recovery phase after the local mEC activation is slower if the reuptake of K^+ is impaired. Panel B shows the changes in the slow activities during seizure induction with bicuculline in control conditions and after application of local 100mM CsCl. The slow potentials are modified in presence of K-channel blocker (panel C) as measured by the deflection in mV of the fiel potential measured in the three key points (a, b and c) described in the text.

Figure 4 Effect of CsCl on Kir channels of astrocytes. The correcting phase (b) is diminished but not completely abolished by CsCl action versus control condition. Significative reduction of the phase a is attributable both to an impairment of glial buffering action in the short term, that is recovered after phase b and that do non diminish the K values along phase c.

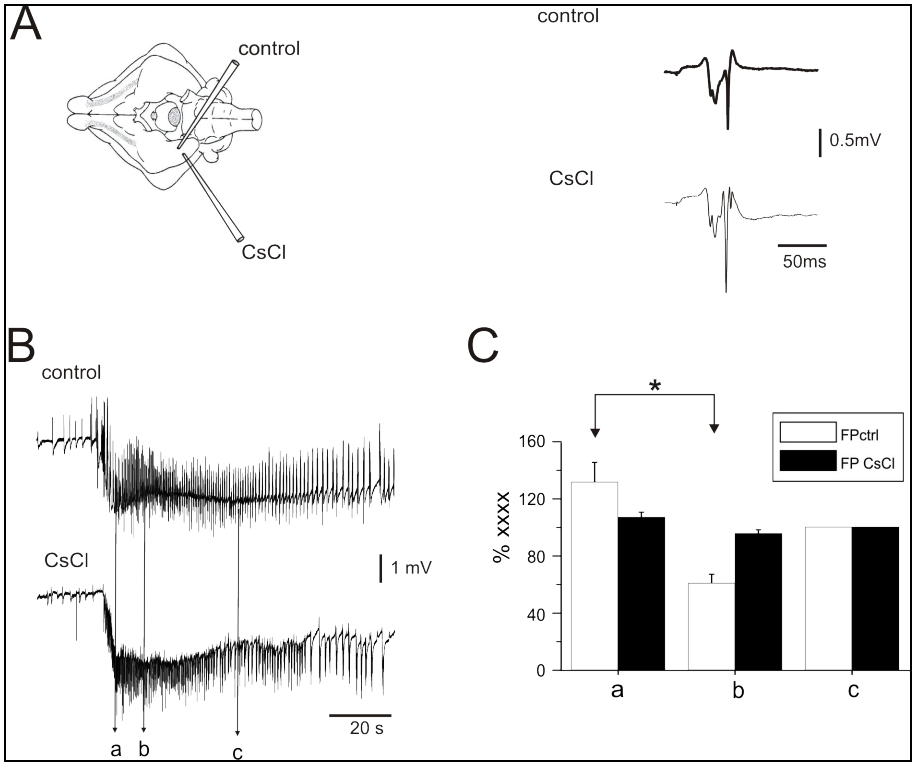
A
control
CsCl
control
0.5mV
CsCl
50ms
B
control
CsCl
1 mV
20 s
a
b
c
C
*
FPctrl
FP CsCl
% xxxx
160
120
80
40
0
a
b
c

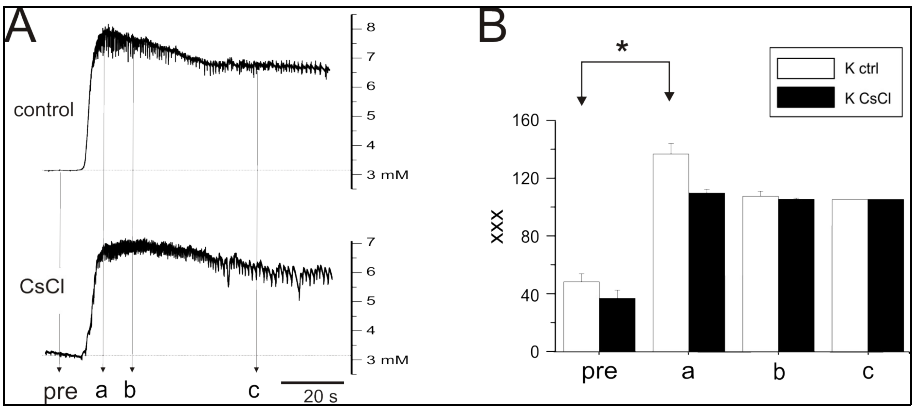
A
control
CsCl
8
7
6
5
4
3 mM
7
6
5
4
3 mM
pre
a
b
c
20 s
B
*
K ctrl
K CsCl
xxx
160
120
80
40
0
pre
a
b
c

Chapter 5

CHANGES IN ACTION POTENTIAL FEATURES MARK DIFFERENT PHASES OF FOCAL SEIZURE DISCHARGES IN THE ENTORHINAL CORTEX OF THE *IN VITRO* ISOLATED GUINEA PIG BRAIN

Federica Trombin, Vadym Gnatkovsky and Marco de Curtis

ABSTRACT

Focal seizures correlate with stereotyped electrophysiological patterns that can be reproduced in animal models. The analysis of the cellular and network changes that subtend these patterns contribute to the understanding of ictogenesis. We analysed seizure-like discharges generated in the entorhinal cortex of the *in vitro* isolated guinea pig brain preparation by 3-minute applications of the $GABA_A$ receptor antagonist, bicuculline. We focused our investigation on the features of action potentials recorded in principal neurons and interneurons recorded intracellularly with sharp electrodes. Ictal events were characterized by a highly reproducible sequence of events, characterized with extracellular electrodes by the initial appearance of fast activity in the beta/gamma range in the field electrode, sequentially followed by irregular spiking and regular bursting that progressively become larger in amplitude and less frequent, until seizure terminated. Analysis of the first derivative of the action potentials ("kinking analysis") was utilized to characterize threshold, amplitude and repolarization features of spikes in the different phases

of the seizure-like discharge. At seizure onset firing ceased in principal neurons but was intense in putative interneurons. During the transition toward the extracellular irregular spiking, action potential firing resumed in principal cells: in layer II-III neurons spikes showed higher threshold, lower peak amplitude and faster repolarization compared to pre-ictal spikes. Spike pairs with action potential features typical of ectopic spikes were observed in 14 out of 17 superficial neurons. Deep layer principal cells and interneurons generated regular spikes in this phase. Within 6,3 ± 1,5 seconds burst firing was observed and become progressively larger and more regular, in parallel to extracellular bursting. Increasingly longer periods of silence were observed between bursts before the ictal discharge terminated. The ectopic spikes in layer II-III neurons correlated with the increases in extracellular potassium observed at seizure onset. Ectopic firing was observed mainly during the plateau phase of potassium increase, while during the rise and falling of the K curve cells fired with regular spiking. The threshold voltage required for spiking was related to the accumulation of extracellular potassium, suggesting a role for ionic dys-equilibrium to originate ectopic spikes from the dendrites of the principal neurons.

INTRODUCTION

The study of seizure generation (ictogenesis) in human and experimental epileptology is one of research priorities recognized by the international epilepsy community [5]. By understanding how seizures initiate and progress, new potential strategies for a possible cure of the cases resistant to current treatments may arise. Focal seizures can be recorded with intracranial electrodes in patients suffering from pharmaco-resistant during pre-surgical studies aimed at defining the boundaries of the epileptogenic region to be surgically removed to cure the epileptic condition. These diagnostic studies demonstrated that focal seizure recorded at the site of generation are often characterized by reproducible patterns that are independent from the localization. One of the most typical focal patterns is characterized by the abrupt fading of the background activity and by the emergence of fast rhythms in the beta/gamma range, often preceded by large-amplitude population spikes [8]. This activity can be followed by an irregular discharge that becomes progressively more synchronous and organizes in bursts of large in amplitude. Focal seizures usually terminate with large amplitude bursts that precede post-ictal depression. A similar progression of events during focal seizures are observed in animal models of focal epilepsy [9,11-13,22] and in acute seizure models *in vivo* and *in vitro* [2,21].

We utilized an acute model of limbic lobe seizures developed on the *in vitro*-isolated guinea pig brain to reproduce the focal seizure pattern observed in humans [7,10,21]. Brief disinhibition of the isolated brain with a 3-minute systemic application of the GABAa receptor antagonist, bicuculline, induced seizures in the hippocampal-parahippocampal regions, characterized in the medial entorhinal cortex (EC) by fast activity at 20-30 Hz at seizure onset, sequentially followed by

irregular firing and rhythmic bursting. This pharmacological procedure does not completely block inhibition, but reduces it by 30-40%. In our model, EC seizures are usually initiated by the of 3-5 large amplitude population spikes, that are sustained by synchronization of inhibitory networks [10]. We demonstrated that the fast activity that initiate the seizure is also generated by inhibitory synchronization mediated by intense firing in putative interneurons, and correlates with a complete interruption of neuronal firing in principal neurons, that resumes within 5-10 seconds after the onset of fast activity [10]. We hypothesize that the recovery of neuronal firing in principal neurons is due to the elevation in extracellular potassium ($[K^+]_o$) that produces two synergic effects: i) it reduces the efficacy of GABAergic inhibition by shifting the reversal potential of the GABAa receptor–mediated chloride current to depolarizing values [19] and ii) it promotes ectopic firing in principal cells. Ectopic firing caused by direct depolarization of axonal membrane by seizure-induced increases in $[K^+]_o$ [15] was demonstrated in the 4-amiopyridine model in hippocampal in vitro slices [3,4].

To verify this hypothesis, we examined the changes in phase plots of action potentials (dV/dt versus voltage; [14] in different populations of neurons during seizure progression by analyzing.

METHODS

The method of the isolated *in vitro* guinea pig brain was extensively described in [6]. Briefly, young adults Hartley guinea-pigs were anesthetized with sodium thiopental (20 mg/kg, i.p.), the heart exposed and perfused with a saline solution (ACSF composition: NaCl 126 mM, KCl 2.3 mM, $NaHCO_3$ 26 mM, $MgSO_4$ 1.3 mM, $CaCl_2$ 2.4 mM, KH_2PO_4 1.2 mM, glucose 15 mM, HEPES 5 mM and 3%

dextran 70.000 oxigenated with a slight acidic pH 7.1 and cold temperature). The brain was carefully dissected out under hypothermic conditions and placed in the recording chamber. A polyethlene (PE60) cannula was inserted in the basilar artery and the brain was perfused with the ACSF solution (pH 7,3 and T 32°C). The surgical procedures were performed at 15°C , for electrophysiology studies the temperature is raised to 32°C (0,2°C/min). The experimental protocol was approved by the Ethical Committee on Animal Care, and all efforts were done to reduce animal sufferance and the number of animal used. The extracellular activity was recorded from the m-EC layer II/III with glass pipettes filled with NaCl 0,9%. Intracellular recordings were performed with sharp electrodes (input resistance 60-120 MΩ) filled with K-acetate 3M and biocytine 2%. The cells were labeled and histochemical revelation with biocytine/avidine system allowed to identify the neuronal type and location in the cortex (images not shown). The evaluation of ion changes in the extracellular matrix required ion-sensitive electrodes. Double barreled glass capillaries with tips of 2-5µm were filled with a ionophore resin (Fluka 60031,Germany) specific for potassium ions in the ion-sensitive capillary and KCl in the reference capillary. The electrodes were calibrated before the experimental measurement with known potassium concentration solutions and the relative voltage increase was referred to a logarithmic increase in [K].

The analogical signals were digitalized with a NI A/D board 64channels (National Instruments, TX), stored on the pc, acquired with the ELPHO® software. Off-line analysis was also performed with specific LABview instruments developed ad hoc by dr. Vadym Gnatkovsky in our lab.

RESULTS

As shown in previous studies, application of 3 minutes bicuculline 50uM induced transiently epileptic seizures in the EC of the isolated brain. The typical pattern consisting of three-phases was observed (Figure 1). An initial low voltage fast activity (25-30Hz) was observed at seizure onset, evidenced also by a deep inflection of the slow components of the extracellular trace (initial slow wave or ISW). A second phase characterized by irregular bursting and an inversion in polarity of the slow component followed this initial phase (also called inverting phase). A third longer phase characterized by bursting activity and a delayed slow wave (or DSW) proceeds until seizure ending. Intracellular recordings were performed from principal neurons of the EC. Intracellular correlate of the **first phase** corresponded to seizure onset characterized by silent phase with IPSP and membrane strong depolarization (see [10]. During the **second phase**, activity with spike doublets and irregular firing occurred. In the **third phase** bursting with afterdischarges was observed (Figure 1). The frequency of AP firing as a function of time, denoted by FAP(t), was calculated by counting the number of spikes over a 500-ms time window sliding by 60-ms step intervals. Joint time-frequency analysis (JTFA) was applied to study the frequency content of the spontaneous extracellular oscillations. JTFA of filtered signal showed a marked increase in firing component among the total frequency content in the signal during the irregular firing phase and during the bursting phase (see Figure 1)

In Figure 2 the type of analysis utilized to characterize the features of APs in different phases of the seizure is illustrated. This analysis, defined as “kinking analysis” [14], is based on the study of the changes

of acceleration in voltage changes against the measured voltage. The changes of voltage (mV on the x axis) in time are calculated as the first derivative expressed in mV/ms (y axis) and are plotted in a graph on the right. With this method it is possible to detect minimal changes in the threshold, in the slope of the membrane voltage during the phases of depolarization, in the maximum voltage peak and in repolarization. These parameters can be easily compared between spikes via a new routine implemented in ELPHO® to automatically perform kinking analysis of APs during the intracellular recording.

A rapid increase (dV) during the depolarizing phase (Figure 2) follows the "all or none rule" of spike generation whenever the threshold is reached. The opening of Na channels is the first step to bring the membrane potential from normal V_{max} values of -65,8+2,6 up to depolarized values of +15,36+2,49 mV, with a slope that is clearly defined by the threshold-dV_{max}-V_{max} curve. The potassium gradient re-polarizes the voltage across the membrane. Spike repolarization is defined by the slope of the V_{max}-dV_{min}–repolarization curve. The slope of this rising and falling phases was calculated as the ratio between the maximum speed of depolarization (called dV max) and the voltage in that time point.

Figure 3 illustrates a typical sequence of changes in firing patterns observed during a seizure recorded in a principal neuron of the superficial layers of the EC. The upper panels illustrate the characteristics of APs before the initiation of the seizure. The second panel from the top shows the characteristics of the AP at the very onset of firing recovery after the fast activity that characterizes the seizure onset. Different parameters of the AP are changed: the threshold, the amplitude and the repolarizing phase. In the following few seconds, in correlation with phase 2 of the seizure, spike

doublettes appear. The first AP of the pair maintain the features described above, while the second AP has much smaller amplitude, duration and threshold (inner circle in the 3rd right panel from the top). In coincidence with the onset of phase 3, characterized by bursting, AP change again and its repolarizing phase is typically slowed. When bursts reinforce, the first AP is followed by a series of smaller amplitude spikes.

Figure 4 illustrates another EC seizure. The time points at which we sampled the APs described in the different panels are marked by the square boxes in the top traces illustrated at slow time scale. As illustrated in the previous figure, the features of AP dramatically change in the 3 seizure phases. In this example a complete post-ictal recovery was demonstrated (bottom right panels).

In order to quantify these changes, correlation analysis was performed on the data set obtained from threshold values, the slope during the depolarization phase, the maximum Voltage and the repolarizing phase. The data obtained from 17 experiments are illustrated in Figure 5 and Table 1. These data demonstrate that in comparison to the pre-ictal period, during phase 2 and during the initial bursting i) the threshold of the spike increases by 10-15 mV, ii) the maximal amplitude of the AP reduces by 10 mV, iii) the AP repolarized with 25-35 mV depolarized values, iv) and the slope of depolarization is decreased. All these parameters recovered during the late bursting phase 3 and when the regular post-seizure firing is resumed. The lower panel in the left part of Figure 5 shows the changes in extracellular potassium during the different phases of the seizure, measured with ion-sensitive extracellular electrodes. As expected, potassium reversibly increases during seizure. The correlation between the potassium changes and the threshold and Vmax values

are illustrated in the 2 graphs in the right part of Figure 5. This correlation is further illustrated for in the plots of Figure 6, where AP depolarizing slope (upper left panel), Vmax (upper right panel), repolarization voltage (lower left panel) and AP threshold (lower right panel) mean values before, during and after seizures a are shown as a function of extracellular potassium concentration.

In conclusion, AP features are modulated and modified in principal neurons of the EC during a seizure event.

DISCUSSION

Based on extracellular recording patterns, EC seizures in our acute limbic model of ictogenesis are characterized by four principal phases: 1) seizure onset promoted by large amplitude interictal spikes followed by fast activity at 20-30 Hz sustained by enhanced inhibitory activity, 2) irregular extracellular spiking characterized by non rhythmic potentials of variable amplitude, superimposed on a slow reverting potential and 3) a late phase characterized by a transition toward burst discharge that become larger in amplitude and more synchronous with time. Large bursts toward the end of the seizure tend to become less frequent and higher in amplitude. The last phase of the seizure is defined by post-ictal depression. Phases 2 and 3 are commonly defined as tonic and clonic, two terms used to describe limb spasms during a grand mal seizure. The use of these definitions to describe seizure patterns recorded from in vitro preparations is erroneous and confusing and should be avoided since, evidently, no tonic and clonic clinical correlates can be generated in slices. Most importantly, human studies with intracranial recordings demonstrated that “tonic” and “clonic” phases are observed during focal seizures

even when the clinical symptoms of the seizures are not characterized by muscular spasms.

Voltage signals from intracellular recordings in principal cells of the superficial and deep layers of the m-EC of the guinea pig brain were analyzed to highlight how the voltage changes in membrane depolarization and repolarization. The method of kinking mathematical analysis [14] on the first derivative of the AP represents the slope of the signal itself versus the absolute value of voltage of the membrane. The AP is plotted as a clock-wise circle in which the breadth represents the maximum Voltage and the height is the maximum and minimum velocity. The five time points/values of the threshold, maximum velocity of depolarization, maximum Voltage, maximum velocity and return potential of repolarization describe the characteristics of the AP.

We demonstrate here that AP features change during the 3 phases of the seizure induced in the EC by brief applications of bicuculline. The perfusion with bicuculline by itself changes some of the AP characteristics, such as threshold, repolarizing potential and the slope of depolarization (difference between spont and pre-seizure values in Figure 5). At reappearance after the fast activity associated with the abolition of firing, AP are characterized by a modest shift in the threshold of activation, that increases during the bursting phase and recovers at the end of the seizure. The maximal voltage amplitude of AP was also reduced, typically in phase 2 and in the first AP of the spike doublettes, and completely recovered during the late bursting phase. Spike repolarization and depolarization slope were also modified maximally during phase 2. Interestingly, these changes paralleled the changes in extracellular potassium, suggesting a possible correlation (causal correlation?) between the two phenomena.

Based on these observations, we can conclude that the AP at the onset of the seizure have some of the features of the ectopic spikes that are generated in regions of the membrane remote to the soma, where presumably intracellular recordings were performed. Ectopic spikes generated either in the axons or in the dendrites are smaller in amplitude, have a depolarized threshold compared to somatic APs.
It is estimated that ectopic spikes can be generated by an excess in potassium ions accumulation around the dendritic arborization of the cells. A depolarizing shift of threshold values may indicate that the generation of the AP is not at the soma. The demonstration that also the process of depolarization is reduced, strongly suggest that this ectopic firing is generated in the dendrites, and it is possibly preceded by a slow spike. The existence of a clear slowing of the time to maximal depolarization of the spike was demonstrated in the second spikes within the doublettes. These probably are non-sodium spikes sustained by dendritic regenerative calcium conductances [1,20]; [17,18]. Also the decrease of the maximum voltage is indicative of the inverting point in which the opening of the K channels repolarizes the voltage transmembrane after an AP. This value is independent of the threshold value or the repolarizing values.

Ectopic spikes were already seen in rat hippocampal slices by Avoli and coworkers [4] and other authors in the '70s [16]. In their experimental protocol administration of 4AP, a blocker of K currents, prevented a correct repolarization leaving the K outside the cells and giving rise to spiking of ectopic origin, because it was seen originating in the axon of the cell and back-propagating to the soma, where it generated a full AP.

In our case the slow ectopic firing was always observed after a regular AP has occurred, during the cellular bursting. This induced the typical spiral shape of the kinking graph, in which a voltage values higher of the one that originated the first spike is necessary and sufficient to start a second spiking and so on for third and fourth spike (see Figure 3 irregular bursting). The V max values was not changed during the ectopic firing generation and at the end of each bursting the membrane potential reverted to rmp values in a short time.

References

1. Amitai Y., Friedman A., Connors B.W., and Gutnick M.J. (1993) Regenerative activity in apical dendrites of pyramidal cells in neocortex. *Cerebral Cortex* 3, 26-38.
2. Avoli M., D'Antuono M., Louvel J., Kohling R., Biagini G., Pumain R., D'Arcangelo G., and Tancredi V. (2002) Network pharmachological mechanisms leading to epileptiform synchronization in the limbic system in vitro. *Progress in Neurobiology* 68, 167-207.
3. Avoli M., Louvel J., Kurcewicz I., Pumain R., and Barbarosie M. (1996) Extracellular free potassium and calcium during synchronous activity induced by 4-aminopyridine in the juvenile rat hippocampus. *Journal Of Physiology* 493 (Pt 3), 707-17.
4. Avoli M., Methot M., and Kawasaki H. (1998) GABA-dependent generation of ectopic action potentials in the rat hippocampus. *Eur J Neurosci* 10, 2714-22.
5. Baulac M. and Pitkanen A. (2008) Research Priorities in Epilepsy for the Next Decade-A Representative View of the European Scientific Community. *Epilepsia*.
6. de Curtis M., Biella G., Buccellati C., and Folco G. (1998) Simultaneous investigation of the neuronal and vascular compartments in the guinea pig brain isolated in vitro. *Brain Research Protocols* 3, 221-8.
7. de Curtis M., Biella G., Forti M., and Panzica F. (1994) Multifocal spontaneous epileptic activity induced by restricted bicuculline ejection in the piriform cortex of the isolated guinea pig brain. *Journal of Neurophysiology* 71, 2463-2475.
8. de Curtis M. and Gnatkovsky V. (2009) Reevaluating the mechanisms of focal ictogenesis: The role of low-voltage fast activity. *Epilepsia*.
9. dos Santos N.F., Arida R.M., Filho E.M., Priel M.R., and Cavalheiro E.A. (2000) Epileptogenesis in immature rats following recurrent status epilepticus. *Brain Res Brain Res Rev* 32, 269-76.
10. Gnatkovsky V., Librizzi L., Trombin F., and de Curtis M. (2008) Fast activity at seizure onset is mediated by inhibitory circuits in the entorhinal cortex in vitro. *Ann Neurol* 64, 674-86.
11. Kadam S.D., White A.M., Staley K.J., and Dudek F.E. (2010) Continuous electroencephalographic monitoring with radio-telemetry in a rat model of perinatal hypoxia-ischemia reveals progressive post-stroke epilepsy. *J Neurosci*

30, 404-15.

12. Kharatishvili I., Nissinen J.P., McIntosh T.K., and Pitkanen A. (2006) A model of posttraumatic epilepsy induced by lateral fluid-percussion brain injury in rats. *Neuroscience* 140, 685-97.
13. Lothman E.W., Collins R.C., and Ferrendelli J.A. (1981) Kainic acid-induced limbic seizures: electrophysiologic studies. *Neurology* 31, 806-12.
14. Naundorf B., Wolf F., and Volgushev M. (2006) Unique features of action potential initiation in cortical neurons. *Nature* 440, 1060-3.
15. Pinault D. (1995) Backpropagation of action potentials generated at ectopic axonal loci: hypothesis that axon terminals integrate local environmental signals. *Brain Res Brain Res Rev* 21, 42-92.
16. Scobey R.P. and Gabor A.J. (1975) Ectopic action-potential generation in epileptogenic cortex. *J Neurophysiol* 38, 383-4.
17. Spruston N., Schiller Y., Stuart G., and Sakmann B. (1995) Activity-dependent action potential invasion and calcium influx into hippocampal CA1 dendrites. *Science* 268, 297-300.
18. Stuart G., Schiller J., and Sakmann B. (1997) Action potential initiation and propagation in rat neocortical pyramidal neurons. *J Physiol* 505 (Pt 3), 617-32.
19. Thompson S.M. and Gahwiler B.H. (1989) Activity-dependent disinhibition. II. Effects of extracellular potassium, furosemide, and membrane potential on ECl- in hippocampal CA3 neurons. *J Neurophysiol* 61, 512-23.
20. Turner R.W., Meyers D.E., Richardson T.L., and Barker J.L. (1991) The site for initiation of action potential discharge over the somatodendritic axis of rat hippocampal CA1 pyramidal neurons. *J Neurosci* 11, 2270-80.
21. Uva L., Librizzi L., Wendling F., and de Curtis M. (2005) Propagation dynamics of epileptiform activity acutely induced by bicuculline in the hippocampal-parahippocampal region of the isolated Guinea pig brain. *Epilepsia* 46, 1914-25.
22. Williams P.A., White A.M., Clark S., Ferraro D.J., Swiercz W., Staley K.J., and Dudek F.E. (2009) Development of spontaneous recurrent seizures after kainate-induced status epilepticus. *J Neurosci* 29, 2103-12.

	Pre-seizure	Phase 2	Phase 3 Burst onset	Phase 3 late bursts
THRESHOLD (mV)	11,82 ± 1,33	21,50 ± 1,75	24,36 ± 1,54	21,85 ± 1,83
DeltaV max (mV/ms)	1,02 ± 0,05	0,88 ± 0,05	0,47 ± 0,04	0,63 ± 0,07
V max (mV)	71,16 ± 2,49	62,24 ± 2,12	63,78 ± 1,88	70,92 ± 2,46
DeltaV min (mV/ms)	-0,41 ± 0,04	-0,23 ± 0,02	-0,18 ± 0,02	-0,24 ± 0,03
Repol (mV)	12,63 ± 1,46	25,98 ± 2,22	31,73 ± 1,72	29,63 ± 2,82
H (mV/ms)	1,42 ± 0,08	0,76 ± 0,08	0,6 ± 0,06	0,87 ± 0,09
L (mV)	57,98 ± 1,84	39,3 ± 2,38	35,69 ± 3,29	43,75 ± 3,40
[K] (mM)	3,10 ± 0,06	7,69 ± 1,71	9,88 ± 1,44	8,18 ± 1,15

Table 1. Standard parameters of voltage threshold and repolarization, maximum velocity of depolarization and repolarization, spike amplitude and sharpness were evaluated during seizure phase progression. The values of potassium concentration were also related to the augmentation of threshold potentials, peak amplitude, slope of depolarization and repolarizing voltage. The values are expressed as mean ± std err.

Figure 1. Joint time-frequency analysis of the extracellular signal clearly shows the appearance of a 25-30Hz frequency band at seizure onset. The fast activity lasts for the first ten seconds after ictal onset and corresponds to the rising phase of potassium concentration. During this phase no cell activity is present, but the membrane potential is slowly depolarized while IPSP in the intracellular trace represents the intense activity of GABAergic interneurons. In the irregular bursting phase no prevalent frequency component can be individuated. Principal neurons start to fire at high frequency but in a disordinated manner, generating the continuous bursting seen on the field potential. Potassium concentration is at its plateau during this phase and slowly is buffered by diffusion thorough the astrocytic syncythium. The regular bursting phase is characterized by recurrent neuronal firing perfectly coincident in the intra- and extra-cellular recordings, that is also represented by the intense activity in the spectrogram graph. Bursting activity involves a range of frequencies from 10 to 60Hz.

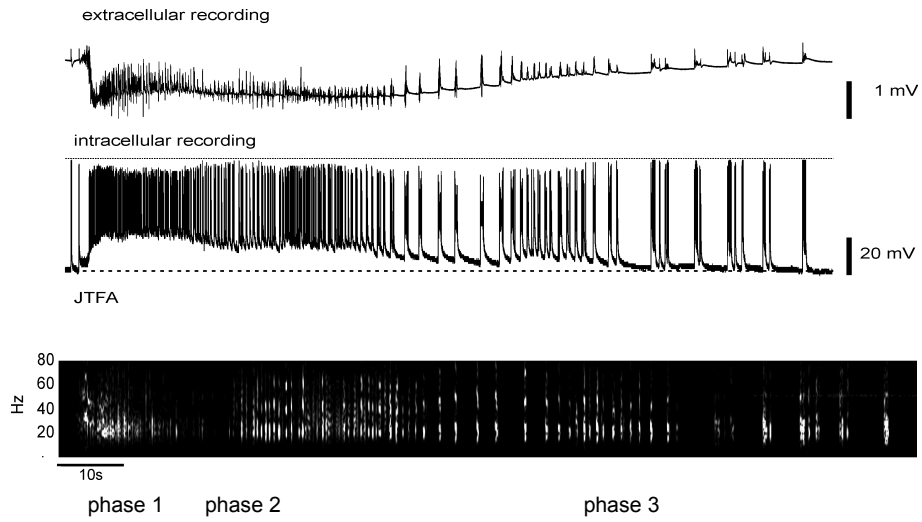
extracellular recording
1 mV
intracellular recording
20 mV
JTFA
80
60
40
20
Hz
10s
phase 1
phase 2
phase 3

Figure 2. Example of kinking analysis performed on one spontaneous spike recorded from a pyramidal neuron in the superficial layer of the m-EC. The first derivative of the voltage values in time (dV/dt) are plotted against the corresponding mV value (right part of figure). The changes in membrane voltage are referred only to their own value of membrane potential and are not dependent on time. This way even small changes in membrane depolarization (or repolarization) are evident. Key points were chosen: membrane voltage threshold, maximum velocity during the depolarization, maximum voltage of spike, minimum velocity and repolarization values. The corresponding values on the spike are indicated by arrows in the left part of figure 2.

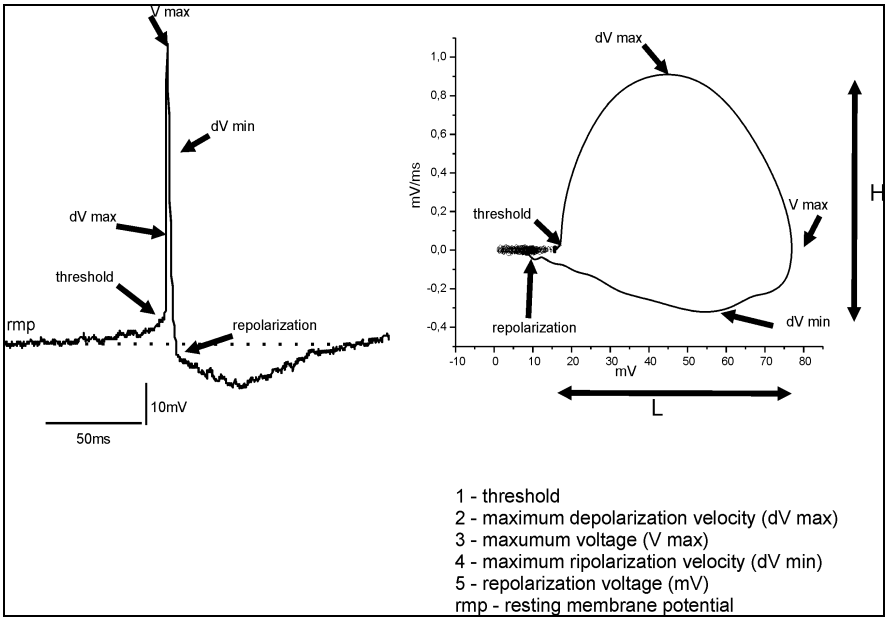
V max
dV min
dV max
threshold
rmp
repolarization
10mV
50ms
dV max
mV/ms
threshold
V max
repolarization
dV min
mV
H
L
1 - threshold
2 - maximum depolarization velocity (dV max)
3 - maxumum voltage (V max)
4 - maximum ripolarization velocity (dV min)
5 - repolarization voltage (mV)
rmp - resting membrane potential

Figure 3 Representative kinking analysis of spike shapes in the subsequent phases of seizure progression. The average of 10 spikes is taken for each graph and the corresponding kinking graph is plotted. The gray line indicates the rmp potential (-65,8 ± 2,6 mV) in basal condition and is maintained through all the graphs. Note that the cell reaches a more depolarized status after seizure onset, and it is represented by the deflection of threshold values to more positive ones. Note that the mV values of membrane repolarization are more positive than threshold values after seizure have started, while the physiolohigal hyperpolarization folowing the repolarizing phase in the spontaneous firing is stil present. On the contrary the maximum voltage of each type of spike do not change across the phases. Spiking during the irregular bursting phase has a slower depolarizing phase that is represented by a more elliptic shape of the kinking graph. In particular doublette spikes has a peculiar feature of a second smaller kink representing the real ectopic spike generated on the long depolarization tail following the first spike. During the bursting there are multiple spikelets innesting on the repolarizing phase of the previous spike, whose kinking graphs returns the particular spiral shape, in which it is evident the distinction in the threshold and repolarizing values of the membrane potential.

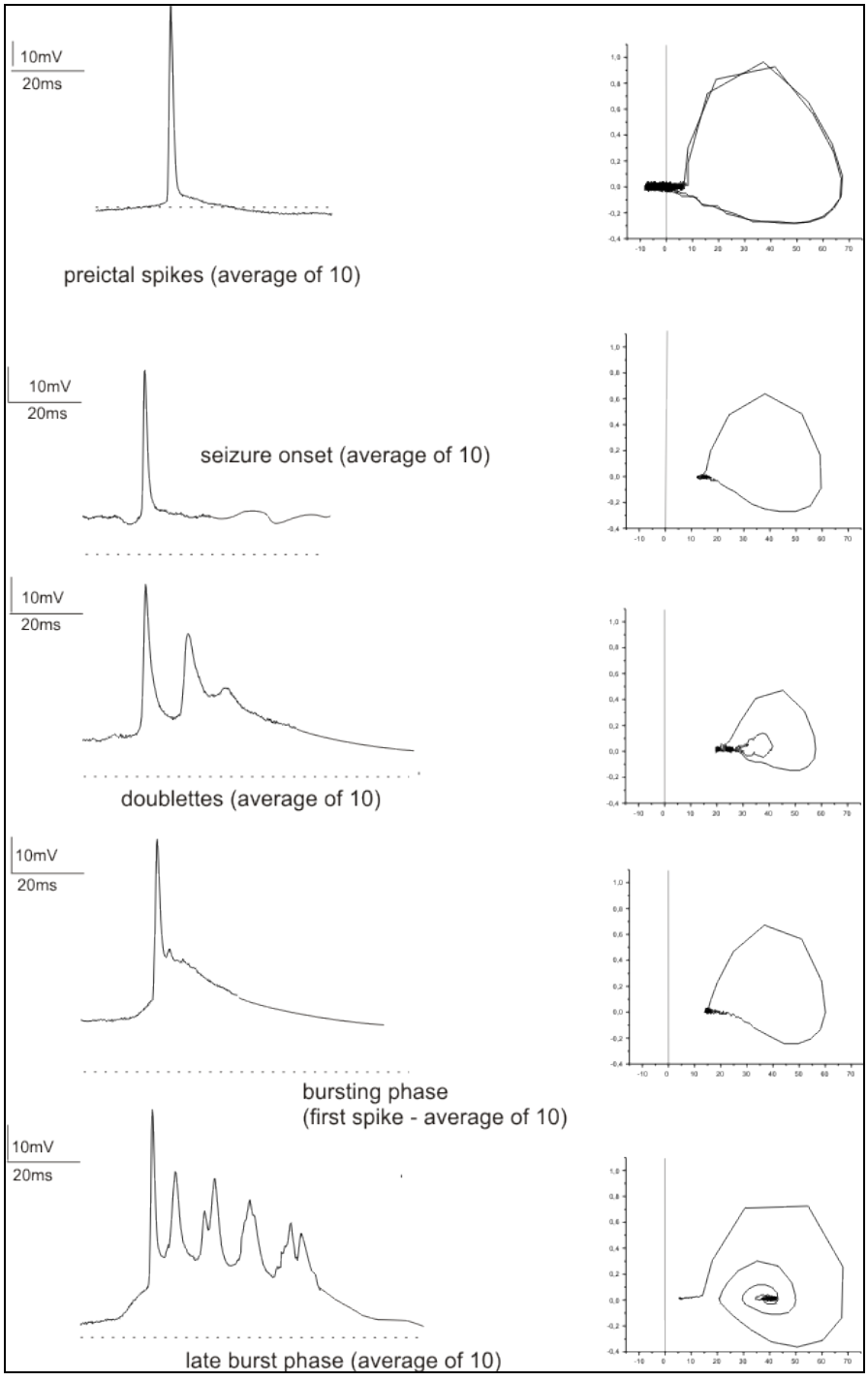
10mV
20ms
preictal spikes (average of 10)
10mV
20ms
seizure onset (average of 10)
10mV
20ms
doublettes (average of 10)
10mV
20ms
bursting phase
(first spike - average of 10)
10mV
20ms
late burst phase (average of 10)

Figure 4. Sequential changes of spikes shape during the progression of seizure. In **a** preictal spontaneous spiking with its kinking graph. Two representative spikes are shown, while each circle in the kinking graph represents one action potential. In **b** a rebound spike with the IPSP typical of the fast activity phase. During this phase spikes maintain the

pre-ictal kinking shape, though the threshold is obviously increased during the depolarizing IPSP phase. When the rmp reaches its plateau, doublettes spikes probably of ectopic origin can be seen. (**c**) The duration of this phase is transient and depends on the ending of fast activity, with a reversal in the field potential initial slow wave. During this phase spikes show a decrease in depolarization slope and smaller amplitudes. The organization of spikes in groups (**d**) precedes the appearance of regular bursts and the termination of seizure with the eventual recovery of spontaneous activity.

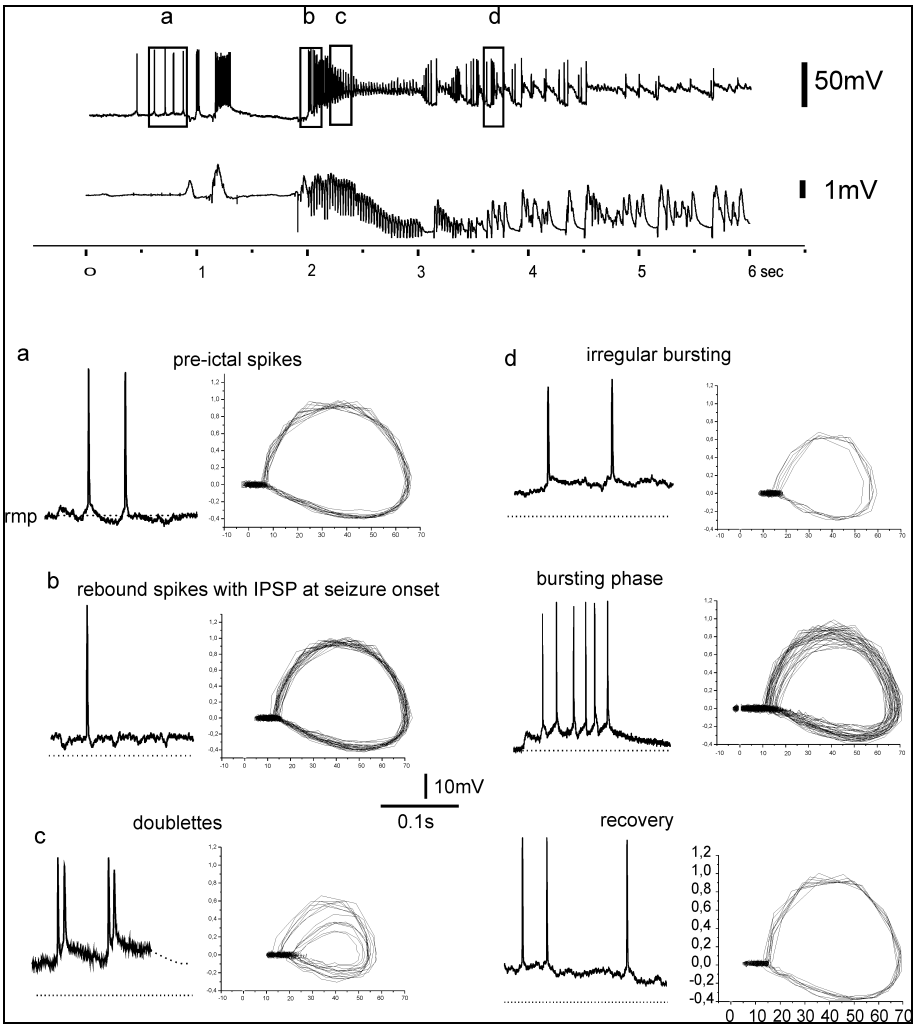
a
b c
d
50mV
1mV
0
1
2
3
4
5
6 sec
a
pre-ictal spikes
rmp
d
irregular bursting
b
rebound spikes with IPSP at seizure onset
bursting phase
10mV
0.1s
c
doublettes
recovery

Figure 5. Changes in threshold values, maximum voltage, repolarization and depolarization velocity (slope) during the described phases of a seizure (left part). The mean values of potassium increase are plotted against the threshold values and the averaged maximum voltages. (right part)

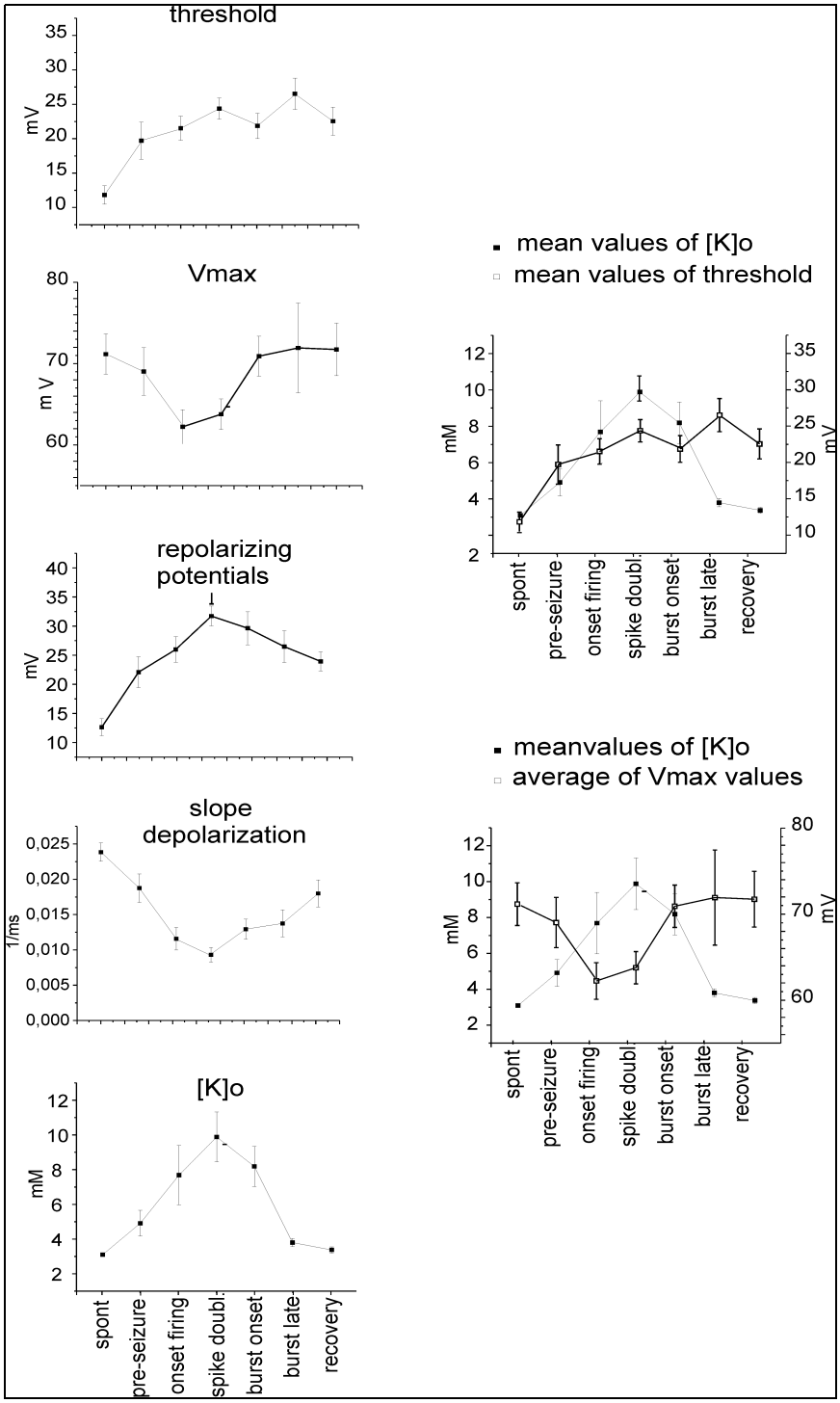
threshold
mV
Vmax
m V
repolarizing
potentials
mV
slope
depolarization
1/ms
[K]o
mM
spont
pre-seizure
onset firing
spike doubl
burst onset
burst late
recovery
mean values of [K]o
mean values of threshold
mM
mV
meanvalues of [K]o
average of Vmax values
mM
mV

Figure 6 Correlation analysis of the extracellular potassium concentration and selected values of threshold, repolarizing membrane potentials, maximum voltage and depolarization slope. Note the positive relation between the threshold values and the [K], and also between the repolarizing values and the [K]. The depolarization slope and the maximum voltage display a negative relation with the extracellular amounts of K.

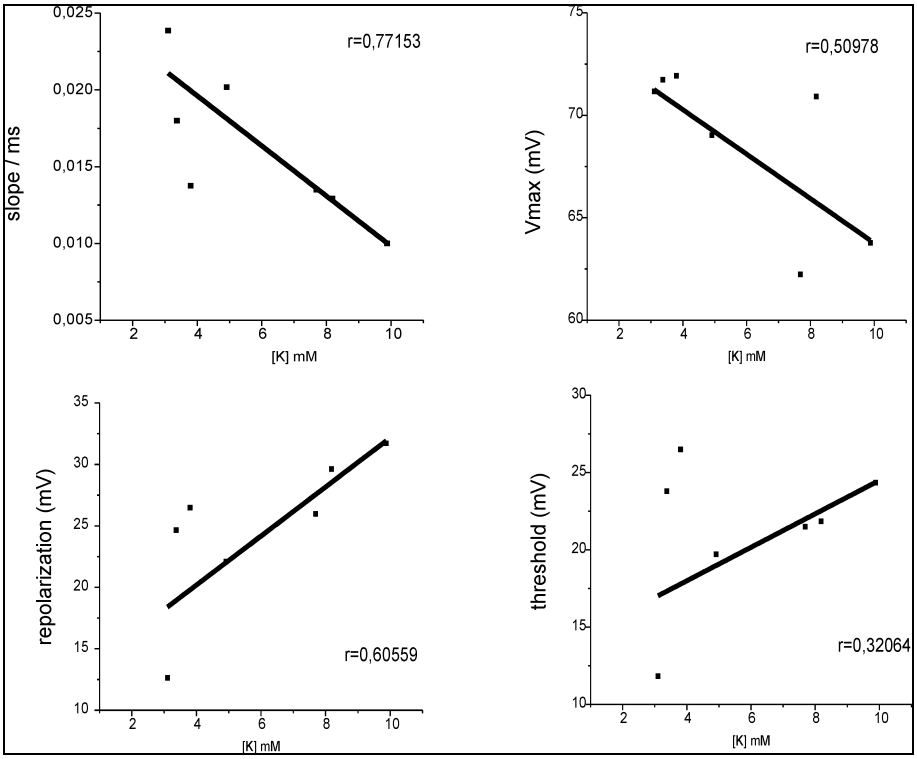
slope / ms
0,025
0,020
0,015
0,010
0,005
r=0,77153
2
4
6
8
10
[K] mM
Vmax (mV)
75
70
65
60
r=0,50978
[K] mM
repolarization (mV)
35
30
25
20
15
10
r=0,60559
[K] mM
threshold (mV)
30
25
20
15
10
r=0,32064
[K] mM

Chapter 6

Conclusions and Future Perspective

The model of the in vitro isolated guinea pig brain is optimal to study of limbic structure alterations such as temporal lobe epilepsy. Recordings from the piriform cortex and the lateral entorhinal cortex (l-EC) revealed these are leading structures in the development of interictal rhythmic spiking. The hippocampus and the parahippocampal region (the medial entorhinal cortex) are the site of ictal spikes generation. Low involvement of peri-rhinal cortex (PRC) hs been demonstrated.

The PC-EC-HIPP-EC loop activation has been extensively studied in this preparation in conditions of both normal excitability and hyperexcitability. Field potential recordings, laminar profile analysis and intracelluar investigation of principal neurons in the superficial and deep layer and interneurons of m-EC, delineate a complex scenario that involves also the contribution of glial compartment to epileptiform discharges.

The perfusion of bicuculline for 3 minutes through the arterial system of the isolated brain induces a partial and transient disinhibition of the circuitry in the temporal lobe. The GABAergic interneuronal system is paradoxically over-activated and very high firing rates interneuron activity is seen in the superficial layers of the EC. This can be seen as a low voltage fast activity in the field potential and is followed by a critical increase in extracellular potassium values, due to the sudden cellular activation. The transition from an interictal to ictal spiking

pathway has been investigated by means of multichannel silicon probes placed in the m-EC of the guinea pig brain.
These observations showed impressive similarities with the human depth electrode recordings performed in patients undergoing epilepsy surgery. Intracranial stereo EEG recordings revealed a fast activity just at time of seizure onset, superimposed on a slow depolarizing shift. Field potential recordings in the corresponding areas of the guinea pig brain featured the same characteristics with a typical 25-30Hz activity at seizure onset and a three-phasic slow component that resembles the human situation. The study of slow potentials in DC-potentials showed a relation between the depth of the field potential deflection and the $[K]_o$ changes. Modulation of ions spatial buffering by local injection of drugs that act on potassium inward rectifying channels (Kir) for example CsCl, or inhibiting the Na/K-ATPase with ouabaine lead to an increase of the amount of extracellular K.
These potassium changes could act on neurons, inducing phenomena of ectopic firing at dendritic sites. This hypothesis was evaluated in the study of spike shapes. Kinking analysis on different spiking types and on different neuronal populations revealed a stereotyped AP changes that are consistent with the generation of ectopic spikes. These AP are characterized by a slower depolarization, a higher threshold value and smaller amplitude (mV) and are possibly generated in the dendrites. The appearance of ectopic spiking is strictly related to the extracellular values of K^+.

Further studies of the cellular mechanisms and network abnormalities that regulate seizures onset and their maintenance will clarify the role of each cellular category in the complicated interplay between neurons, glia and interneurons. The explanation of network

connections and functionalities will be relevant for the understanding of ictogenesis in the temporal lobe of the guinea pig first, but most important in the human focal seizures of the temporal lobe. Experiments aiming at clarify the exact role of glial spatial buffering during the first seconds of seizure onset are in progress.

The thesis work should recollect all the learning, efforts and progresses of three years. It is not as simple as it can look like (or maybe as I thought at the beginning) to put together and write them down. For this reason there are some people who greatly helped me to set down and conclude this work. First of all I really want to thank MdC for his patience and constancy in following me up for all the time and in particular during this last period. I really felt much more as a daughter than a student. VG has been my daddy in the lab and everything I have learned I owe it to him. His essential teaching always left me (sometimes too much) freedom of action but made me think about what I was doing. I am not a kind of ordinate and precise person for sure, but I am learning from LU the magical art of making it simpler by writing down the "pros and cons" list or the "to do" list. It is still a long way for me to go but I am making it out... Many thanks to LL, too. If you want to get together with her there's no other way: you love her or hate her (it's a Sicilian prerogative), but you can always trust on her. I'd like to thank CP even if we didn't work together directly, but we had beautiful dinners at her home and had a great time together. All my respect to AC an outstanding example of commitment to science and attachment to his job: thank you for every single spot of reality you gave me. I want to thank also LR, VM, GM and MC for having supported me in this intense period and many thanks to EC, PS, BT and GB, the lively next-door neighbors. Because of my poor capacity to concentrate I asked political asylum to IZ who always welcomed my presence in her lab and gave me a desk,too. (I know, it is as rectangular as mine with four legs and a chair to sit down...) Last but not least, GC and GLB my two rat-mates in my PhD years: we really have been freely moving students in an electrophysiology lab. But most of all they are friends and I want them to know I really love the things we do together.